

DEVELOPMENT OF A DOT-BLOT ENZYME-LINKED IMMUNOSORBENT
ASSAY TO DETECT AVIAN BORNAVIRUS ANTIBODIES

A Dissertation

by

PAULINA ESCANDON

Submitted to the Office of Graduate and Professional Studies of
Texas A&M University
in partial fulfillment of the requirements for the degree of

DOCTOR OF PHILOSOPHY

Chair of Committee,	Jeffery M.B. Musser
Committee Members,	Ian R. Tizard
	J. Jill Heatley
	Luc R. Berghman
Head of Department,	Ramesh Vemulapalli

May 2020

Major Subject: Biomedical Sciences

Copyright 2020 Paulina Escandon

ABSTRACT

Avian bornavirus (ABV) is the causal agent of a progressive fatal avian neurologic syndrome referred to as Parrot bornavirus syndrome, a complex of clinical problems that can include enteric ganglioneuritis and encephalitis, or neurological deficits. The purpose of this dissertation is to develop a dot-blot enzyme-linked immunosorbent assay (ELISA) with good sensitivity and specificity and a run-time of ≤ 30 minutes, which could be utilized as a rapid patient-side diagnostic assay. The first objective in optimizing the dot-blot ELISA was to investigate the effect of species-specific secondary antibody in the test performance. Secondly, conditions for the dot-blot ELISA were adjusted to optimize test performance. This included investigating target antigen (recombinant nucleoprotein) concentration, sample dilution and type, and incubation times. Thirdly, the performance of the dot-blot ELISA was evaluated against the western blot, the gold standard for serologic testing of avian bornavirus. Finally, this research generated the first report of gross pathology, histopathological lesions, and viral tissue distribution in Monk parakeets following experimental inoculation with PaBV-2. The research concluded that dot-blot ELISA test characteristics were optimized using an anti-macaw IgY secondary antibody, 0.3 μg of target antigen and two 5-minute incubations and a sample of whole blood or plasma diluted 1:60. The assay had a sensitivity and specificity of 100 and 96% testing a sample population of PaBV-2 infected Monk parakeets at 3 weeks post-inoculation.

DEDICATION

I dedicate this dissertation to the one person that gave me all the fundamental values which lead me to where I am now, my Mother. She always did everything in her power to show me that I could do anything if I set my mind on it. Her moral principles on dedication and hard work have been bestowed by her and have become the major part of my core values. She showed me that success is never given but earned with every helping hand, listening ear and attentive smile. She is the strongest, kindest and most caring person I know. My goal in life is to become at least a fraction of the person she is. Te quiero mucho.

Gracias, Mami <3

ACKNOWLEDGEMENTS

I am thankful for all the people that have help me evolve into the PhD candidate, I am today. My time at Texas A&M University has been filled of amazing life changing experiences and it couldn't have happened without the help from my friends, family, boyfriend and colleagues, Thank you. Debra Turner is the most supportive and caring person throughout my time at the Schubot Exotic Bird Health Center. Dr. Guo's brilliant mind and kindness, help me troubleshoot any research setbacks that occurred throughout the course of this research. I am grateful for the mentorship and support of my committee chair and committee members, Dr. Ian Tizard, Dr. J. Jill Heatley, and Dr. Luc R. Berghman, Dr. Jeffrey M.B. Musser. Finally, thanks to my loving boyfriend, Javier Delgado for being supportive, caring and patient throughout my 10 years in university.

CONTRIBUTORS AND FUNDING SOURCES

Contributors

This research was supervised by a dissertation committee consisting of Dr. Jeffrey M.B. Musser and Dr. Ian Tizard professors from the Department of Veterinary Pathobiology, Dr. J. Jill Heatley professor from the Department of Small Animal Clinical Sciences and Dr. Luc R. Berghman professor from the Department of Poultry Science.

Viral inoculant and *E.coli* for the production of recombinant N-protein were provided by Dr. Guo. The RT-PCR data was processed and analyzed with assistance of master's student Zoe G. Kolkhorst. Histopathology was processed and analyzed by Texas A&M Veterinary Medical Diagnostic Laboratory. The Western blot and dot-blot ELISA membranes were digitized by Tim Stephenson a medical photographer from the College of Veterinary Medicine. General assistance was provided by Debra Turner, without whom research and the aviary would cease. All other research conducted for the dissertation was completed by the PhD graduate student independently.

Funding Sources

Graduate student studies was supported by the Graduate Diversity Excellence Fellowship from Texas A&M University. The dissertation research was supported by the Schubot Exotic Bird Health Center of the College of Veterinary Medicine and Biomedical Sciences at Texas A&M University, Dr. Sarah A. Hamer, Dr. Ian Tizard, Dr. and Dr. Jeffrey M.B. Musser.

NOMENCLATURE

2° Antibody	Secondary antibody
ABBV	Aquatic bird bornavirus
ABV	Avian bornavirus
AG	Avian ganglioneuritis
BCS	Body condition score
BoDV	Borna disease virus
cDNA	Complementary deoxyribonucleic acid
CnBV	Canary bornavirus
DNA	Deoxyribonucleic acid
E. coli	Escherichia coli
EsBV-1	Estrildid finch bornavirus 1
ELISA	Enzyme-linked immunosorbent assay
FBS	Fetal bovine serum
FeLV	Feline leukemia virus
FFU	Focus forming units
GI	Gastrointestinal
H&E	haematoxylin and eosin
IFA	Immunofluorescent antibody
IPTG	Isopropyl β -D-1-thiogalactopyranoside
mRNA	Messenger ribonucleic acid

MuBV-1	Munia bornavirus 1
MW	Molecular weight
NC	Nitrocellulose
N-Protein	Nucleoprotein
PaBV	Parrot bornavirus
PaBVs	Parrot bornavirus syndrome
PBS	Phosphate-buffered saline
PCR	Polymerase chain reaction
PCV	Packed cell volume
PDD	Proventricular dilatation disease
PVDF	Polyvinylidene difluoride
qRT-PCR	Quantitative reverse transcriptase-polymerase chain reaction
RNA	Ribonucleic acid
RT-PCR	Reverse transcription polymerase chain reaction
VSBV-1	Variiegated squirrel bornavirus 1
WaBV	Waterbird Bornavirus

TABLE OF CONTENTS

	Page
ABSTRACT.....	ii
DEDICATION.....	iii
ACKNOWLEDGEMENTS.....	iv
CONTRIBUTORE AND FUNDING SOURCES.....	v
NOMENCLATURE.....	vi
TABLE OF CONTENTS.....	viii
LISTS OF FIGURES.....	xii
LIST OF TABLES.....	xv
 1. INTRODUCTION AND REVIEW OF LITERATURE.....	 1
1.1. Avian bornavirus.....	1
1.1.1. History of avian bornavirus.....	1
1.1.2. Pathogenesis of ABV.....	2
1.1.3. ABV and the immune system.....	4
1.2. Parrot bornavirus syndrome.....	5
1.3. ABV diagnostic assays.....	6
1.3.1. Immunoassays.....	6
1.3.1.1. Whole blood in immunoassays.....	8
1.3.1.2. Secondary antibodies for the detection of Avian IgY	10
1.4. Conclusion.....	12
1.5. Reference.....	12
 2. COMPARISON OF FOUR ANTI-AVIAN IGY SECONDARY ANTIBODIES USED IN WESTERN BLOT AND DOT-BLOT ELISA TO DETECT AVIAN BORNAVIRUS ANTIBODIES IN FOUR DIFFERENT BIRD SPECIES.....	 23
2.1. Introduction.....	23
2.2. Materials and methods.....	25
2.2.1. Anti-IgY secondary antibodies.....	25

2.2.2. Sample collection.....	25
2.2.3. Recombinant nucleoprotein expression and purification.....	26
2.2.4. Western blot.....	28
2.2.5. Dot-blot enzyme-linked immunosorbent assays.....	29
2.2.6. Semi-quantitative signal intensity of dot-blot ELISA.....	29
2.2.7. Statistical analysis.....	30
2.3. Results.....	30
2.3.1. Western blot.....	30
2.3.2. Dot-blot ELISA.....	33
2.3.2.1. Semi-quantification of dot-blot ELISA.....	35
2.4. Discussion.....	40
2.5. Conclusion.....	44
2.6. References.....	45
3. DEVELOPMENT OF A DOT-BLOT ENZYME IMMUNOSORBENT ASSAY TO DETECT AVIAN BORNAVIRUS IMMUNOGLOBULINS.....	50
3.1. Introduction	50
3.2. Materials and methods.....	52
3.2.1. Sample collection.....	52
3.2.2. Recombinant nucleoprotein expression and purification.....	52
3.2.3. Western blot.....	54
3.2.4. Dot-blot enzyme-linked immunosorbent assays.....	55
3.2.5. Semi-quantitative signal intensity of dot-blot ELISA.....	57
3.2.6. Statistical analysis.....	57
3.3. Results.....	58
3.3.1. Purity of recombinant N-protein and <i>E. coli</i> protein using SDS- PAGE.....	58
3.3.2. Western blot.....	59
3.3.2.1. Seropositive and seronegative status.....	59
3.3.2.2. Purified recombinant N-protein and <i>E. coli</i> protein.....	60
3.3.3. Dot-blot ELISA.....	61
3.3.3.1. Study 1: Serial dilution of recombinant N-protein amounts per dot with three different plasma dilutions used for dot- blot ELISA at an incubation time of 10-minutes.....	61
3.3.3.2. Study 2: Three different plasma dilutions and three different recombinant N-protein amounts per dot used for dot-blot ELISA at incubation times of 10-and 5-minutes.....	65
3.3.3.3. Study 3: Three different plasma dilutions and three different recombinant N-protein amounts per dot used for dot-blot ELISA at an incubation times of 5-and 2-minutes	68
3.3.3.4. Study 4: Whole blood.....	71
3.4. Discussion.....	74
3.5. Conclusion.....	79

3.6. References.....	79
4. PROOF OF CONCEPT FOR A DOT-BLOT ENZYME IMMUNOSORBENT ASSAY TO DETECT AVIAN BORNAVIRUS IMMUNOGLOBULINS.....	85
4.1. Introduction.....	85
4.2. Materials and methods.....	86
4.2.1. Animal and sample collection.....	86
4.2.2. Recombinant nucleoprotein expression and purification	87
4.2.3. Recombinant nucleoprotein vaccination.....	88
4.2.4. Parrot bornavirus-2 inoculation.....	89
4.2.5. Western blot.....	90
4.2.6. Dot-blot enzyme-linked immunosorbent assay.....	91
4.2.7. Digital images.....	93
4.2.8. Statistical analysis.....	93
4.3. Results.....	94
4.3.1. Western blot	94
4.3.2. Dot-blot ELISA scoring	96
4.3.3. Dot-Blot ELISA performance.....	98
4.4. Discussion.....	102
4.5. Conclusion.....	104
4.6. References.....	104
5. CONCLUSIONS ON INOCULATION OF VACCINATED AND UNVACCINATED MONK PARAKEETS (<i>Myiopsitta monachus</i>) WITH PARROT BORNAVIRUS-2.....	109
5.1. Introduction.....	109
5.2. Materials and methods.....	110
5.2.1. Animals.....	110
5.2.2. Recombinant nucleoprotein expression and purification	111
5.2.3. Recombinant nucleoprotein vaccination	112
5.2.4. Parrot bornavirus-2 inoculation.....	113
5.2.5. Necropsy.....	113
5.2.6. Western blot.....	114
5.2.7. Histology.....	115
5.2.8. RT-PCR.....	115
5.2.9. Digital images.....	116
5.2.10. Statistical analysis.....	116
5.3. Results.....	117
5.3.1. Clinical and gross observations.....	117
5.3.2. RT-PCR.....	117
5.3.3. Western blot.....	121
5.3.4. Histology.....	122

5.4. Discussion.....	126
5.5. Conclusion.....	127
5.6. References.....	128
APPENDIX A CHAPTER 3 DIGITAL IMAGES.....	133
APPENDIX B CHAPTER 4 DIGITAL IMAGES AND ROCS.....	137

LIST OF FIGURES

		Page
Figure 1.1.	Diagrammatic representation of the four different types of ELISAs.....	9
Figure 2.1.	Representative membranes of western blot results using anti-macaw, anti-bird, anti-duck, and anti-chicken IgY secondary antibody on ABV antibody positive and negative plasma from Blue and gold macaw (<i>Ara ararauna</i>), Cockatiel (<i>Nymphicus hollandicus</i>), and Mallard (<i>Anas platyrhynchos</i>).....	32
Figure 2.2.	Representative membranes of dot-blot ELISA results using anti-macaw, anti-bird, anti-duck, and anti-chicken IgY secondary antibody on ABV antibody positive and negative plasma from Blue and gold macaw (<i>Ara ararauna</i>), Cockatiel (<i>Nymphicus hollandicus</i>), Monk Parakeet (<i>Myiopsitta monachus</i>), and Mallard (<i>Anas platyrhynchos</i>).....	34
Figure 2.3.	Digital image analysis of dot-blot ELISA used to generate the signal intensity value.....	37
Figure 3.1.	Stained SDS-PAGE gel fractions of recombinant N-protein purification and <i>E. coli</i> used for expression.....	58
Figure 3.2.	Representative membranes of western blot results using A. negative and B. positive plasma.....	59
Figure 3.3.	Representative membranes of western blot results using recombinant N-protein and <i>E. coli</i> protein with negative and positive plasma.	60
Figure 3.4.	Digital image analysis of dot-blot ELISA used to generate the signal intensity value.....	62
Figure 3.5.	Representative membranes of dot-blot ELISA which used ten-fold serial dilutions of recombinant N-protein, 1.4, 0.14, 0.014, 0.0014 and 0.00014 µg per dot, testing 1:100, 1:60, and 1:30 plasma dilutions and incubated for 10-minutes.....	63

Figure 3.6.	Mean (\pm Std) signal intensities of dot-blot ELISA which used ten-fold serial dilutions of recombinant N-protein, 1.4, 0.14, 0.014, 0.0014 and 0.00014 μ g per dot, testing 1:100, 1:60, and 1:30 plasma dilutions and incubated for 10-minutes.....	64
Figure 3.7.	Representative membranes of dot-blot ELISA which used 0.15, 0.3, and 0.6 μ g of recombinant N-protein per dot, testing 1:100, 1:60, and 1:30 plasma dilutions, and incubation times of 5- and 10-minutes.....	66
Figure 3.8.	Mean (\pm Std) signal intensities of dot-blot ELISA which used 0.15, 0.3, and 0.6 μ g of recombinant N-protein per dot, testing 1:100, 1:60, and 1:30 plasma dilutions, and incubation times of 5- and 10-minutes.....	67
Figure 3.9.	Representative membranes of dot-blot ELISA which used 0.3, and 0.6 μ g of recombinant N-protein per dot, testing 1:60, 1:30, and 1:20 plasma dilutions, and incubation times of 2- and 5-minutes....	69
Figure 3.10.	Mean (\pm Std) signal intensities of dot-blot ELISA which used 0.3, and 0.6 μ g of recombinant N-protein per dot, testing 1:60, 1:30, and 1:20 plasma dilutions, and incubation times of 2- and 5-minutes.	70
Figure 3.11.	Representative membranes of dot-blot ELISA which used 0.3 μ g of recombinant N-protein per dot, testing 1:60 plasma dilution, 1:100, 1:60, and 1:30 whole blood dilutions, and incubated for 5-minutes.....	72
Figure 3.12.	Mean (\pm Std) signal intensities dot-blot ELISA which used 0.3 μ g of recombinant N-protein per dot, testing 1:60 plasma dilution, 1:100, 1:60, and 1:30 whole blood dilutions, and incubated for 5-minutes.....	73
Figure 4.1.	Dot-blot ELISA reference membranes scored zero to four.....	92
Figure 4.2.	ROC curves composed of results for the four separate scenarios....	100
Figure 4.3.	Dot diagram of the known-positive and -negative samples displayed on two vertical axes.....	101
Figure 5.1.	Mild dilation and discoloration of proventriculus in unvaccinated Monk parakeet (<i>Myiopsitta monachus</i>) inoculated with PaBV-2.....	119

Figure 5.2.	Western blot membranes detecting PaBV-2 antibodies from unvaccinated and vaccinated Monk parakeets (<i>Myiopsitta monachus</i>) inoculated with PaBV-2.....	121
Figure 5.3.	Lymphocytic and plasmacytic infiltration of the proventriculus of an unvaccinated Monk parakeet (<i>Myiopsitta monachus</i>) at 400x....	123
Figure 5.4.	Lymphocytic and plasmacytic infiltration of the ventriculus of an unvaccinated Monk parakeet (<i>Myiopsitta monachus</i>) at 400x.....	123
Figure 5.5.	Lymphocytic and plasmacytic infiltration of the adrenal glands of an unvaccinated Monk parakeet (<i>Myiopsitta monachus</i>) at 100x....	124
Figure 5.6.	Lymphocytic and plasmacytic infiltration of the liver of an unvaccinated Monk parakeet (<i>Myiopsitta monachus</i>) at 400x.....	124
Figure 5.7.	Lymphocytic and plasmacytic infiltration of the brain of an unvaccinated Monk parakeet (<i>Myiopsitta monachus</i>) at 400x.....	125
Figure 5.8.	Lymphocytic and plasmacytic infiltration of the crop of an unvaccinated Monk parakeet (<i>Myiopsitta monachus</i>) at 200x.....	125

LIST OF TABLES

		Page
Table 1.1.	Bornaviridae species, genotypes and animals infected.....	3
Table 2.1.	Signal intensities obtained when testing ABV antibody positive and negative plasma from Blue and gold macaw (<i>Ara ararauna</i>), Cockatiel (<i>Nymphicus hollandicus</i>), Monk Parakeet (<i>Myiopsitta monachus</i>), and Mallard (<i>Anas platyrhynchos</i>) with a dot-blot ELISA using anti-macaw, anti-bird, anti-duck, and anti-chicken IgY secondary antibody.....	49
Table 3.1.	Recombinant N-protein amounts per dot, plasma dilutions, whole blood dilutions, and incubation times for each of the dot-blot ELISA studies	56
Table 4.1.	Western blot results for the detection of viral antibodies from control, vaccinated, vaccinated/ PaBV-2 inoculated, and PaBV-2 inoculated Monk parakeets (<i>Myiopsitta monachus</i>).....	95
Table 4.2.	Dot-blot ELISA membrane scorings of control, vaccinated, vaccinated/ PaBV-2 inoculated, and PaBV-2 inoculated Monk parakeets (<i>Myiopsitta monachus</i>).....	97
Table 4.3	Sensitivity, specificity, 95% confidence intervals, accuracy and AUC for the dot-blot ELISA results with four separate scenarios.....	99
Table 5.1.	Body condition score, weight and necropsy finding of vaccinated and unvaccinated Monk parakeets (<i>Myiopsitta monachus</i>) inoculated with PaBV-2.....	118
Table 5.2.	RT-PCR results of the tissue and cloacal swabs from unvaccinated and vaccinated Monk parakeets (<i>Myiopsitta monachus</i>) inoculated with PaBV-2.....	120
Table 5.3.	Histopathology findings within the gastrointestinal tract, brain and nerves tissues from unvaccinated and vaccinated Monk parakeets (<i>Myiopsitta monachus</i>) inoculated with PaBV-2	122

1. INTRODUCTION AND LITERATURE REVIEW

When reviewing the history and literature of both avian bornavirus (ABV) and proventricular dilatation disease (PDD) nomenclature continue to evolve. For clarity in this dissertation, all literature focuses on ABV and parrot bornavirus syndrome (PaBVs) as the syndrome associated with ABV infection instead of PDD, unless noted as otherwise.

1.1. Avian bornavirus

1.1.1. History of avian bornavirus

In 2008, ABV was first determined as the causative agent of parrot bornavirus syndrome, a neurological and gastrointestinal inflammation secondary to ABV infection affecting parrots.¹⁻² Avian bornavirus was identified in naturally occurring cases of clinical PaBVs but not in non-symptomatic/apparently healthy birds by using next-generation sequencing technology and basic local alignment search tool.¹⁻² The correlation of ABV and PaBVs was proven via Koch's postulates by isolating ABV from the brains of birds with confirmed PaBVs and using the homogenate to experimentally induce PaBVs in both conures and cockatiels.³⁻⁴

Avian bornavirus is an enveloped, non-segmented, negative-sense single-stranded RNA virus, in the family Bornaviridae, order Mononegavirales. Mammalian 1 bornavirus was the only identified member in the family Bornaviridae, prior to the discovery of ABV. The family Bornaviridae currently comprises eight virus species, of which five species infect birds (Table 1.1).⁵⁻¹⁸ Avian bornavirus-Mall,¹⁹ Gaboon viper

virus 1 and PaBV-6 remain unclassified at species level.⁵ The restructuring of the Bornaviridae has increased the knowledge of individual viral species but the term ABV is still commonly used to identify all avian species within this family. Since the discovery of ABV, viral identification and distribution has grown worldwide, to include United States, Brazil, Japan, South Africa, Australia, Italy, Denmark, Spain, United Kingdom, Canada, Germany, Austria, and Thailand.^{5-8,12,20-23}

1.1.2. Pathogenesis of ABV

The natural mode of ABV transmission through which ABV infects birds is still not completely understood. The main means of transmission is believed to be a horizontal transmission of the virus via urofecal-oral and/or respiratory routes; virus has been isolated from urine, feces, cloacal swabs, choanal swabs and skin.²⁴⁻²⁷ Rubbenstroth et al. analyzed the phylogenetic sequences of PaBV-2, PaBV-4 and ABBV-1 in captive and free-ranging birds to identify horizontal transmission.²⁵ Results showed that viral sequences were identical or genetically closely in parallel to various different avian species, suggesting that interspecies transmission of ABV is frequent.²⁵ Intriguingly, uninfected cagemates of birds infected with ABV and sentinel birds can remain uninfected over prolonged periods of contact.^{22,28,29} Thus, the exact nature of horizontal transmission is not fully clear.

Table 1.1. Bornaviridae species, genotypes and animals infected.

Species	Genotypes	Animals infected	References
Psittaciform 1 bornavirus	Parrot bornavirus (PaBV) 1,2,3,4,7,8	Psittacines including: Salmon-crested cockatoo (<i>Cacatua moluccensis</i>), Macaws (<i>Ara macao</i> , <i>Ara sp.</i>), Cockatiels, African grey parrots, Amazon parrots, Conures	Philadelpho et al., 2014 Last et al., 2014 Sassa et al., 2015 Rubbenstroth et al., 2012 Kuhn et al., 2015
Psittaciform 2 bornavirus	Parrot bornavirus (PaBV-5)	Psittacines including: Palm cockatoo (<i>Probosciger aterrimus</i>)	Guo et al., 2015A Kuhn et al., 2015
Passeriform 1 bornavirus	Canary bornavirus (CnBV) 1,2,3	Canary (<i>Serinus canaria</i>)	Weissenbock et al., 2009 Kuhn et al., 2015
Passeriform 2 bornavirus	Munia bornavirus 1 (MuBV-1) estrildid finch bornavirus 1 (EsBV-1)	Munia finches (<i>Lonchura punctulata</i>) Estrildid finches (Estrildidae)	Kuhn et al., 2015 Rubbenstroth et al., 2014
Waterbird 1 bornavirus	Aquatic bird bornavirus 1 (ABBV-1)	Canada geese (<i>Branta canadensis</i>) Herring Gulls (<i>Larus argentatus</i>) Ring-billed Gulls (<i>Larus delawarensis</i>) Laughing Gulls (<i>Leucophaeus atricilla</i>) Emu (<i>Dromaius novaehollandiae</i>)	Delnatte et al., 2011 Guo et al., 2015B Kuhn et al., 2015 Nielsen et al., 2018
Elapid 1 bornavirus	Loveridge garter snake Bornavirus (LGSV-1)	Loveridge garter snakes (<i>Elapsoidea loveridgei</i>)	Stenglein et al., 2014 Kuhn et al., 2015
Mammalian 1 bornavirus	Borna disease virus (BoDV) 1,2	Horses (<i>Equus caballus</i>) Sheep Bicolored shrew Cats	Kuhn et al., 2015 Tizard et al., 2016
Mammalian 2 bornavirus	Variegated squirrel bornavirus 1 (VSBV-1)	Squirrels subfamilies: Sciurinae and Callosciurinae	Schlottau et al., 2017 Kuhn et al., 2015

Vertical transmission has also been suggested as a means of transmission. Avian bornavirus is seen in juvenile psittacines in breeding aviaries.^{30,31} Avian bornavirus infected parents can produce ABV mRNA positive embryos found dead-in-shell.³¹⁻³³ Avian bornavirus mRNA has also been identified in nonviable eggs.^{31,32}

Experimental routes of transmission, such as intramuscular, intravenous, oral, intranasal and intraocular have been successful in producing infection, and histopathological changes associated with clinical PaBVs.^{3,34-37} Natural transmission may be through a variety of means, the literature is ambiguous on this point. But, ABV infection is opportunistic and depends on multiple situational factors such as age, species, immunostatus, exposure dose, viral shedding, and viral load.³⁴

An ABV infected bird may not display clinical PaBVs, despite lifelong infection. These asymptomatic birds are still infectious and can be a source of exposure to other birds.^{4,21} Asymptomatic birds, after years of infection and viral shedding, can eliminate the virus. In naturally infected cockatiels, cloacal swabs were routinely positive for RT-PCR 5 years, spontaneously become RT-PCR negative. Upon necropsy, no gross lesion of PaBVs, histopathological changes, nor PaBV genetic material were found.³⁸

1.1.3. ABV and the immune system

Avian bornavirus can spread throughout an infected bird's body by evading the bird's immune system. The virus reproduces in a non-cytopathic manner in the cell nucleus.³⁹ ABV evades the activation of the innate immune system by inhibiting the production of type I interferons, a strategy used by the Bornaviridae family.³⁹ Understanding of the pathogenesis mechanism through which ABV causes lesions

associated with PaBVs remains limited. At some point, ABV may, based on unknown mechanisms, fail to evade the innate immune system and trigger an inflammatory response that damages the nervous system. Virus is easily isolated from damaged nerves of birds with PaBVs.⁴⁰

An autoimmune response, similar to Guillain-Barre syndrome in humans, is also suggested as the underlying cause of PaBVs. Inflammation of nerve ganglia by anti-ganglioside antibodies corresponds to neurological dysfunction and clinical signs of PaBVs.⁴¹ Anti-ganglioside antibodies are identified in the sera of PaBVs birds and reproduction of PaBVs has been successful via inoculation of purified ganglioside into healthy cockatiels.⁴² However, this theory remains controversial as inoculation of Monk parakeets (*Myiopsitta monachus*) with PaBV brain gangliosides fails to induce clinical symptoms of PaBVs.⁴³

1.2. Parrot bornavirus syndrome

Parrot bornavirus syndrome diagnosis relies on clinical presentation, histopathological lesions, or viral antigen or mRNA detection, with more than one diagnostic test being positive providing greater probability in identifying clinically and subclinically infected birds.^{27,36,44,45} Histopathology findings consistent with ABV lesions include lymphoplasmacytic meningoencephalomyelitis and ganglioneuritis in the central, peripheral and/or autonomic nervous system.^{27,36,44,45} Clinical signs of PaBVs vary and likely depend on the avian species and lesion distribution of the viral infection. Clinical signs usually involve the nervous and gastrointestinal (GI) systems. Neurologic signs include inability to perch, general weakness, ataxia, seizures and blindness.^{41,46,47}

Gastrointestinal system signs include delayed crop emptying, regurgitation, dilatation of one or several parts of the GI tract and impaired GI system transit caused by nerve damage in the enteric nervous system.^{41,46,47} Ultimately these lesions cause dysfunction leading to starvation and/or death.

1.3. ABV diagnostic assays

Avian bornavirus is known as a neurotropic virus but can affect an extensive range of tissues and cell types.⁴⁸ Tissue distribution of ABV in an infected bird can be wide; ABV antigens and mRNA have been detected in the brain, eye, spinal cord, heart, gastrointestinal system, adrenal glands, and kidneys by reverse transcriptase polymerase chain reaction (RT-PCR) and immunohistochemistry assays.^{2,27,44,48-53} Feather calami, feces/urine, choanal swab and cloacal swab, are less invasive samples for RT-PCR,^{27,44,48-51,54,55} however results can vary due to the intermittent viral shedding.²⁴⁻²⁶ Quantitative reverse transcriptase-polymerase chain reaction (qRT-PCR) quantifies the viral load and is highly sensitive.

Western blot, immunofluorescence assay, and enzyme-linked immunosorbent assays (ELISA) detect antibodies.⁵²⁻⁵⁸ Immunologic testing comparing ABV specific antigens found that the viral nucleoprotein is immunodominant and the preferred antigen for use in microtiter plate ELISA⁵⁴ and in immunofluorescence assays.⁵⁹

1.3.1. Immunoassays

Immunoassay function is based on specific binding of an antibody and an antigen of interest for diagnosis of exposure to a pathogenic organism. Immunoassays are reliable diagnostic assays that can process large numbers of samples with high

sensitivity and specificity. The immunoassay's specificity and sensitivity are due to antibodies' highly specific and strong binding properties which will bind only to the three-dimensional structure of a target antigen or analyte.⁶⁰ The simplest form of immunoassay is the immunometric design, which consists of immobilizing the antibody or antigen to a solid surface, allowing the capture of the analyte of interest from the sample,⁶¹ and then exposing the antibody or antigen bound to the target analyte to a labeled secondary antibody that will generate a measurable and/or visual signal.

A subgroup of immunometric assays are enzyme-linked immunosorbent assays (ELISAs). There are four different types of ELISAs; direct, indirect, sandwich, and competitive (Figure 1.1.). The process is similar with any type of ELISA: fixing either the analyte or antibody and detecting the conjugate with an enzyme catalyst. Detection is accomplished by assessing the conjugated enzyme activity via incubation with a substrate to produce a measurable product. The most crucial element of the detection strategy is a highly specific antibody-antigen interaction. Depending on the enzyme/substrate reaction, a generation of color, fluorescence, or luminescent product can be visualized with the naked eye or electrical equipment such as a spectrophotometer (Wild 2013). In indirect ELISAs, an antigen is bound to a solid surface. The sample is added and if antibodies to the target analyte are present, the antibody complex with the antigen. Then an antibody conjugated to an enzyme (2° anti-IgY antibody) will bind to the antibody of the antigen-antibody complex. In direct ELISA, an antigen (target analyte) is detected by an antibody directly conjugated to an enzyme. In sandwich ELISA, two antibodies are required, each bind to different, non-overlapping epitopes of

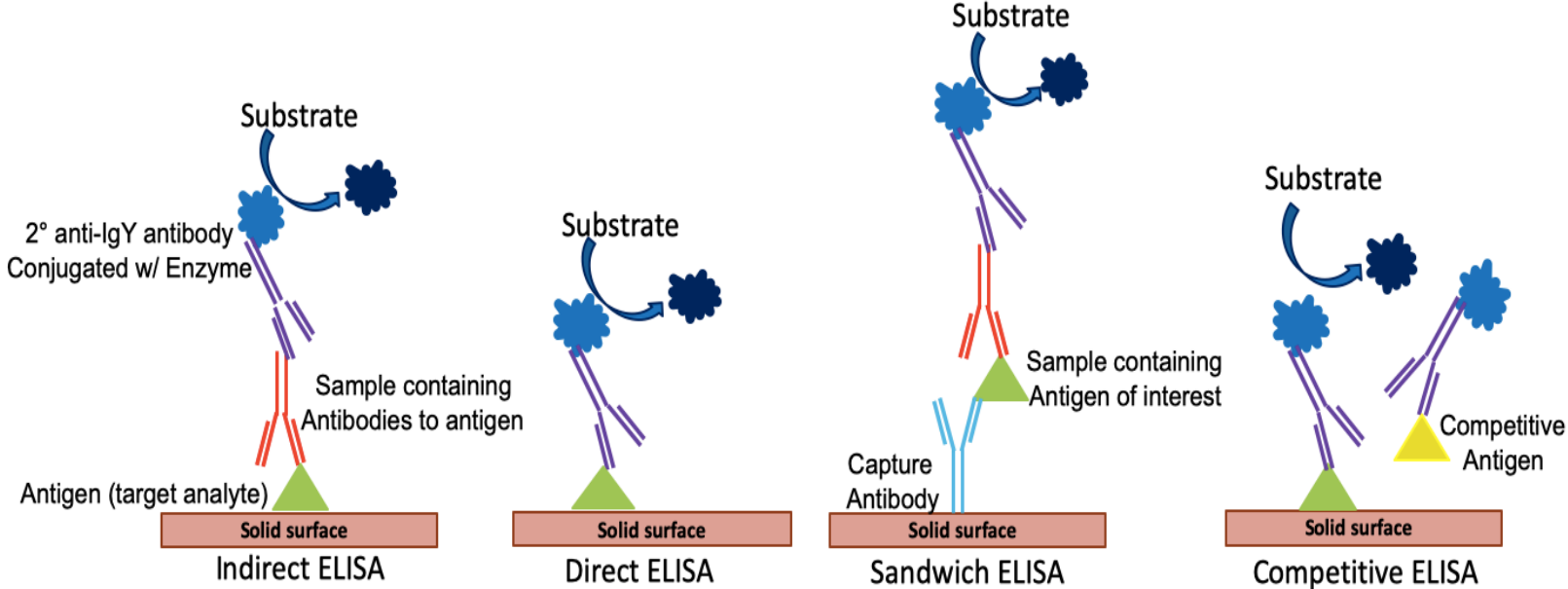
the antigen of interest and is detected by an antibody directly conjugated to an enzyme. In competitive ELISA, a known amount of enzyme conjugated competitive antigen is used to determine the amount of target analyte of interest by determining the binding ratio of enzyme conjugated competitive antigen versus the target analyte of interest.

Enzyme-linked immunosorbent assays can be run in laboratory setting or as a patient-side assay also known as lateral flow immunoassay. Lateral flow immunoassay operates as either a sandwich or competitive immunoassay, provides results within minutes, is economic, and used as diagnostics for home or clinic testing. A home pregnancy test for humans and a heartworm test for dogs are the two most common known lateral flow immunoassays.

1.3.1.1. Whole blood in immunoassays

Laboratory-run ELISAs take up to several hours to complete, require trained personnel and commonly test serum or plasma samples, rarely is whole blood the test sample. Patient-side ELISAs are preferred diagnostic immunoassay due to rapidity in obtaining results and to convenience of use. To streamline the procedure for further speed and convenience, whole blood is used in lieu of serum or plasma samples, as the use of whole blood removes a sample processing step. However, whole blood potentially could alter results and even cause false positives or false negatives to occur.

Figure 1.1. Diagrammatic representation of the four different types of ELISAs.



In general, immunoassays are unaffected by hemolysis and analytical interference is rare.^{62,63} But, the use of whole blood in ELISAs is discouraged.⁶⁴ As an example, the use of whole blood in ELISA testing for Feline leukemia virus results in more false-positive reactions than the use of serum.^{65,66} These false positive results are attributed to inadequate washing steps.^{65,67} Thus, controversy exists on use of whole blood and whether increased washing steps could reduce interference and false positive results.

1.3.1.2. Secondary antibodies for the detection of Avian IgY

Secondary antibodies are used for the indirect detection of a target to which a specific primary antibody (the antibody in the sample) is first bound (bound to the target analyte). The secondary antibody must have specificity and a strong affinity for the epitopes on the antibody species being used. Secondary antibodies are generated by immunizing a host animal (usually rabbit, goat, chicken and guinea pig) which is a different species from a target animal species that is being tested with the assay. The two types of secondary antibodies are monoclonal and polyclonal antibodies. Monoclonal antibodies are the product of a single B-cell clone which are specific to one immunogen, but less likely to work for multiple applications. Polyclonal antibodies are the product of a pool of immunoglobulins from a target species. For example, immunization of a goat with purified macaw IgY will generate goat IgG anti-macaw IgY antibodies that will bind macaw IgY as well as any other molecules sharing the same conserved domains. Polyclonal antibodies can vary from batch to batch and generate background because of

the mixture of specificities; however, they have a high avidity, are inexpensive and can be used for multiple applications.

There is no known secondary antibody commercially available that can select antibodies across all bird species. Anti-chicken IgY secondary antibodies have been used to detect antibodies in some wild avian species.^{68,69} However, the efficacy of using anti-chicken IgY secondary antibody to detect across all avian species remains unknown.

Anti-bird IgY secondary antibody has been used to recognize multiple avian species. Anti-bird IgY secondary antibody is produced in goats immunized with immunoglobulins from the White-crowned sparrow, Ringed turtle dove, domestic chicken, and Muscovy duck.^a This secondary antibody has been used in immunoassays for the detection of arboviruses,⁷⁰ flaviviruses,⁷¹ alpha-viruses,⁷² poxviruses,⁷³ and ABV.^{36,52-54,56,58} The advantage of an anti-bird IgY secondary antibody is the greater range of species that can be tested. This anti-bird IgY secondary antibody has been used in serologic tests for the detection of antibodies in psittacines, even though the immunogen used to stimulate this secondary antibody lacked antibodies from psittaciformes. Anti-passerine IgY secondary antibody produces better results than the anti-bird IgY secondary antibody or the anti-chicken IgY secondary antibody for serologic assays of passerine birds.⁷⁴ This suggests that species-specific secondary antibodies may provide more appropriate results in immunologic assays than commercially available mixed species anti-bird secondary antibody.

1.4. Conclusion

A rapid high quality diagnostic test is sorely needed since ABV was discovered to be the causative agent of PaBVs. With the exception of clinical signs and imaging which are generally non-specific, no diagnostic tests are available for clinical use as a rapid patient-side test. The goal is to develop a dot-blot ELISA that has the potential to detect ABV exposure within minutes to assist veterinarians in making appropriate data based decisions on management, therapeutics, prevention and biosecurity practices.

^a Product insert Bird IgG-heavy and light chain Antibody, Bethyl Laboratories

1.5. References

1. Kistler AL, Gancz A, Clubb S, et al. Recovery of divergent avian bornaviruses from cases of proventricular dilatation disease: identification of a candidate etiologic agent. *Virology*. 2008;5:88–102.
2. Honkavuori KS, Shivaprasad HL, Williams BL, et al. Novel bornavirus in psittacine birds with proventricular dilatation disease. *Emerg Infect Dis*. 2008;14(12):1883–1886.
3. Gancz AY, Kistler AL, Greninger AL, et al., Experimental induction of proventricular dilatation disease in cockatiels (*Nymphicus hollandicus*) inoculated with brain homogenates containing avian bornavirus 4. *J Virol*. 2009;6:100.
4. Gray P, Hoppes S, Suchodolski P, et al. Use of avian bornavirus isolated to induce proventricular dilatation disease in conures. *Emerg Infect Dis*. 2010;16(3):473–479.

5. Kuhn JH, Dürrwald R, Bào Y, et al. Taxonomic reorganization of the family Bornaviridae. *Arch Virol.* 2015;160(2):621–632.
6. Philadelpho NA, Rubbenstroth D, Guimaraes MB, Ferreira AJP, et al. Survey of Bornaviruses in pet psittacines in Brazil reveals a novel parrot bornavirus. *Vet Microbiol.* 2014;174(3-4):584–590.
7. Last RD, Weissenböck H, Nedorost N, Shivaprasad HL. Avian bornavirus genotype 4 recovered from naturally infected psittacine birds with proventricular dilatation disease in South Africa. *J S Afr Vet Assoc.* 2012;83(1):938.
8. Sassa Y, Nghia Bui V, Saitoh K, et al. Parrot bornavirus-2 and -4 RNA detected in wild bird samples in Japan are phylogenetically adjacent to those found in pet birds in Japan. *Virus Genes.* 2015;51(2):234–243.
9. Rubbenstroth D, Rinder M, Kaspers B, Staeheli P. Efficient isolation of avian bornaviruses (ABV) from naturally infected psittacine birds and identification of a new ABV genotype from a salmon-crested cockatoo (*Cacatua moluccensis*). *Vet Microbiol.* 2012;161(1-2):36–42.
10. Guo J, Tizard I. The genome sequence of parrot bornavirus 5. *Virus Genes.* 2015;51(3):430–433.
11. Weissenböck H, Sekulin K, Bakonyi T, Hogler S, Nowotny N. Novel avian bornavirus in a nonpsittacine species (Canary; *Serinus canaria*) with enteric ganglioneuritis and encephalitis. *J Virol.* 2009;83:11367–11371.

12. Rubbenstroth D, Schmidt V, Rinder M, et al. Discovery of a new avian bornavirus genotype in estrildid finches (*Estrildidae*) in Germany. *Vet Microbiol.* 2014;168(2-4):318–323.
13. Delnatte P, Berkvens C, Kummrow M, Smith DA, Campbell D, Crawshaw G, Ojkic D, DeLay J. New genotype of avian bornavirus in wild geese and trumpeter swans in Canada. *Vet Rec.* 2011;169:108.
14. Guo J, Tizard I, Baroch J, Shivaprasad HL, Payne SL. Avian Bornaviruses in North American Gulls. *J Wild Dis.* 2015;51(3):754–758.
15. Nielsen AMW, Ojkic D, Dutton CJ, Smith DA. Aquatic bird bornavirus 1 infection in a captive emu (*Dromaius novaehollandiae*): presumed natural transmission from free-ranging wild waterfowl. *Avian Pathol.* 2018;47(1):58-62.
16. Stenglein MD, Sanders C, Kistler AL, et al. Genome sequence of a bornavirus recovered from an African garter snake (*Elapsoidea loveridgei*). *Gen Anno.* 2014;2(5):e0077914.
17. Tizard I, Ball J, Stoica G, Payne S. The pathogenesis of bornaviral diseases in mammals. *Anim Health Res Rev.* 2016;17(2):92-109.
18. Schlottau K, Jenckel M, Van Den Brand J, et al. Variegated Squirrel Bornavirus 1 in Squirrels, Germany and the Netherlands. *Emerg Infect Dis.*, 2017;23(3):477–481.
19. Guo J, Shivaprasad HL, Rech RR, et al. Characterization of new genotype of avian bornavirus from wild ducks. *Virol J.* 2014;11:197.

20. Weissenböck H, Bakonyi T, Sekulin K, et al. Avian bornaviruses in psittacine birds from Europe and Australia with proventricular dilatation disease. *Emerg Infect Dis.* 2009; 15(9):1453–1459.
21. Encinas-Nagel N, Enderlein D, Piepenbring A, et al. Avian bornavirus in free-ranging psittacine birds, Brazil. *Emerg Infect Dis.* 2014;20(12):2103–2106.
22. Heffels-Redmann U, Enderlein D, Herzog S, et al. Occurrence of avian bornavirus infection in captive psittacines in various European countries and its association to proventricular dilatation disease. *Avian Pathol.* 2011;40(4):419–426.
23. Sa-Arda P, Rinder M, Sanyathitiseeree P, et al. First detection and characterization of Psittaciniform bornaviruses in naturally infected and diseased birds in Thailand. *Vet Microbiol.* 2019;230:62-71.
24. Kistler AL, Smith JM, Alexander L, et al. Analysis of naturally occurring avian bornavirus infection and transmission during an outbreak of proventricular dilatation disease among captive psittacine birds. *J Virol.* 2010;84(4):2176–2179.
25. Rubbenstroth D, Schmidt V, Rinder M, et al. Phylogenetic analysis supports horizontal transmission as a driving force of the spread of avian bornavirus. *PLoS One.* 2016;11(8):e0160936.
26. Heatley JJ, Villalobos AR. Avian bornavirus in the urine of infected birds. *Vet Med Res Rep.* 2012;3:19–23.
27. Leal de Araujo J, Rech RR, Heatley JJ, et al. From nerves to brain to gastrointestinal tract: A time-based study of parrot bornavirus 2 (PaBV-2)

- pathogenesis in cockatiels (*Nymphicus hollandicus*). *PLoS One*. 2017;12(11):e0187797.
28. Rubbenstroth D, Brosinski K, Rinder M, et al. No contact transmission of avian bornavirus in experimental infected cockatiels. (*Nymphicus hollandicus*) and domestic canaries (*Serinus canaria forma domestica*). *Vet Microbiol*. 2014;172(1-2):146–156.
29. Heffels-Redmann U, Enderlein D, Herzog S, et al. Follow-up investigation on different courses of natural avian bornavirus infections in Psittacines. *Avian Dis*. 2012;56(6):153–159.
30. Delnatte P, Nagy E, Ojkic D, Crawshaw G, Smith DA. Investigation into the possibility of vertical transmission of avian bornavirus in free-ranging Canada geese (*Branta canadensis*). *Avian Pathol*. 2014;43(4):301–304.
31. Kerski A, de Kloet AH, de Kloet SR. Vertical transmission of avian bornavirus in Psittaciformes: avian bornavirus RNA and anti-avian bornavirus antibodies in eggs, embryos, and hatchlings obtained from infected sun conures (*Aratinga solstitialis*). *Avian Dis*. 2012;56(3):471–478.
32. Monaco E, Hoppes S, Guo J, Tizard I. The detection of avian bornavirus within psittacine eggs. *J Avian Med Surg*. 2012;26(3):144–148.
33. Lierz M, Piepenbring A, Herden D, et al. Vertical transmission of avian bornavirus in psittacines. *Emerg Infect Dis*. 2011;17(12):2390–2391.
34. Heckmann J, Enderlein D, Piepenbring AK, et al. Investigation of different infection routes of parrot bornavirus in cockatiels. *Avian Dis*. 2017;61(1):90–95.

35. Mirhosseini N, Gray PL, Hoppes S, et al. Proventricular dilatation disease in cockatiels (*Nymphicus hollandicus*) after infection with a genotype 2 avian bornavirus. *J Avian Med Surg*. 2011;25(3):199–204.
36. Piepenbring AK, Enderlein D, Herzog S, et al. Pathogenesis of avian bornavirus in experimentally infected Cockatiels. *Emerg Infect Dis*. 2012;18(2):234–241.
37. Piepenbring AK, Enderlein D, Herzog S, et al. Parrot bornavirus (PaBV)-2 isolate cause different disease patterns in cockatiels than PaBV-4. *Avian Pathol*. 2016;45(2):156–168.
38. Murray O, Turner D, Streeter K, et al. Apparent resolution of parrot bornavirus infection in cockatiels (*Nymphicus hollandicus*). *Vet Med Res Rep*. 2017;8:31–36.
39. Reuter A, Ackermann A, Kothlow S, et al. Avian bornaviruses escape recognition by the innate immune system. *Viruses*. 2010;2(4):927–938.
40. Payne SL, Delnatte P, Guo JH, et al. Birds and bornavirus. *Anim Health Res Rev*. 2012;13:145–156.
41. Rossi G, Dahlhausen RD, Galosi L, Orosz SE. Avian ganglioneuritis in clinical practice. *Vet Clin: Exot Anim Pract*. 2018;21(1):33–67.
42. Rossi G, Enderlein D, Herzog S, et al. Comparison of anti-ganglioside antibodies and anti-ABV in psittacines. *Proc 11th Eur AAV Conf Madrid (Spain)*. 2011;187-189.
43. Leal de Araujo J, Tizard I, Guo J, et al. Are anti-ganglioside antibodies associated with proventricular dilatation disease in birds? *PeerJ*. 2017;5:e3144.

44. Raghav R, Taylor M, DeLay J, et al. Avian bornavirus is present in many tissues of psittacine birds with histopathologic evidence of proventricular dilatation disease. *J Vet Diagn Invest.* 2010;22(4):495–508.
45. Payne S, Shivaprasad HL, Mirhosseini N, et al. Unusual and severe lesions of proventricular dilatation disease in cockatiels (*Nymphicus hollandicus*) acting as healthy carriers of avian bornavirus (ABV) and subsequently infected with a virulent strain of ABV. *Avian Pathol* 2011;40(1):15–22.
46. Hoppes S, Gray PL, Payne S, Shivaprasad HL, Tizard I. The isolation, pathogenesis, diagnosis, transmission, and control of avian bornavirus and proventricular dilatation disease. *Vet Clin North Am Exot Anim Pract.* 2010;13(3):495–508.
47. Hoppes S, Tizard I, Shivaprasad HL. Avian Bornavirus and proventricular dilatation disease: diagnostics, pathology, prevalence, and control. *Vet Clin Exot Anim.* 2013;16(2):339–355.
48. Rinder M, Ackermann A, Kempf H, et al. Broad tissue and cell tropism of avian bornavirus in parrots with proventricular dilatation disease. *J Virol.* 2009;83(11):755–756.
49. Rubbenstroth D, Rinder M, Stein M, et al. Avian bornaviruses are widely distributed in canary birds (*Serinus canaria* f. domestica). *Vet Microbiol.* 2013;165(3-4):287–295.

50. Delnatte P, Mak M, Ojkic D, et al. Detection of avian bornavirus in multiple tissues of infected psittacine birds using real-time reverse transcription polymerase chain reaction. *J Vet Diagn Invest.* 2014;26(2):266–271.
51. Weissenbock H, Fragner K, Nerdorost N, et al. Localization of avian bornavirus RNA by in situ hybridization in tissues of psittacine birds with proventricular dilatation disease. *Vet Microbiol.* 2010;145(1-2):9–16.
52. Fluck A, Enderlein D, Piepenbring A, et al. Correlation of avian bornavirus-specific antibodies and viral ribonucleic acid shedding with neurological signs and feather-damaging behavior in psittacine birds. *Vet Rec.* 2019;184(15):476–482.
53. de Kloet SR, Dorrestein GM. Presence of avian bornavirus RNA and anti-avian bornavirus antibodies in apparently healthy macaws. *Avian Dis.* 2009;53(4):568–573.
54. de Kloet AH, Kerski A, de Kloet SR. Diagnosis of avian bornavirus infection in psittaciformes by serum antibody detection and reverse transcription polymerase chain reaction assay using feather calami. *J Vet Diagn Invest.* 2011;23(3):421–429.
55. Delnatte P, Nagy E, Ojkic D, et al. Avian bornavirus in free-ranging waterfowl: prevalence of antibodies and cloacal shedding of viral RNA. *J Wildl Dis.* 2014;50(3):512–523.

56. Herzog S, Enderlein D, Heffels-Redmann U, et al. Indirect immunofluorescence assay for *Intra Vitam* diagnosis of avian bornavirus infected in psittacine birds. *J Clin Microbiol.* 2010;48(6):2282–2284.
57. Villanueva I, Grey P, Mirhosseini N, et al. The diagnosis of proventricular dilatation disease: Use of a Western blot assay to detect antibodies against avian Borna virus. *Vet Microbiol.* 2010;143(2-4):196–201.
58. Lierz M, Hafez HM, Honkavuori KS, et al. Anatomical distribution of avian bornavirus in parrots, its occurrence in clinically healthy birds and ABV-antibody detection. *Avian Pathol.* 2009;38(6):491–496.
59. Zimmermann V, Rinder M, Kaspers B, et al. Impact of antigenic diversity on laboratory diagnosis of avian bornavirus infections in birds. *J Vet Diagn Invest.* 2014;26(6):769–777.
60. Wild D. The Immunoassay Handbook: Theory and Applications of Ligand Binding, ELISA and Related Techniques. *Elsevier Science Technol.* 2013. ProQuest. Ebook Central.
<http://ebookcentral.proquest.com/lib/tamumebooks/detail.action?docID=1117226>
61. Jiang H, Weng X, Li D. Microfluidic whole-blood immunoassays. *Microfluid Nanofluid.* 2011;10:941–964.
62. Dimeski G. Interference testing. *Clin Biochem Rev.* 2008;29 Suppl 1:S43-49.
63. Jones G. Handling common laboratory interferences. *Clin Biochem Rev.* 2002;23:105–11.

64. Hartmann K, Werner RM, Egberink H, et al. Comparison of six in-house tests for the rapid diagnosis of feline immunodeficiency and feline leukemia virus infections. *Vet Rec.* 2001;149(11):317–320.
65. Hawks DM, Legendre AM, Rohrbach BW. Comparison of four test kits for feline leukemia virus antigen. *J Am Vet Med Assoc.* 1991;199(10):1373–1377.
66. Sand C, Englert T, Egberink H, et al. Evaluation of a new in-clinic test system to detect feline immunodeficiency virus and feline leukemia virus infection. *Vet Clin Path.* 2010;39(2):210–214.
67. Pedersen NC, Madewell BR. Immunodiagnosis of feline leukemia virus infection. In: Kirk RW, ed. *Current veterinary therapy IX*. Philadelphia: WB Saunders Co. 1986;448-452.
68. Martínez J, Tomas G, Merino S, et al. Detection of serum immunoglobulins in wild birds by direct ELISA: a methodological study to validate the technique in different species using anti-chicken antibodies. *Funct Ecol.* 2003;17:700–706.
69. Cray C, Villar D. Cross-reactivity of anti-chicken IgY antibody with immunoglobulins of exotic avian species. *Vet Clin Path.* 2008;37(3):328–331.
70. Chiles RE, Reisen WK. A new enzyme immunoassay to detect antibodies to arboviruses in the blood of wild birds. *J Vector Ecol.* 1998;23(2):123–135.
71. Hofmeister EK, Dusek RJ, Fassbinder-Orth C, et al. Susceptibility and antibody response of vesper sparrows (*Pooecetes gramineus*) to West Nile virus: a potential amplification host in sage-brush grassland habitat. *J Wildl Dis.* 2016;52(2):345–353.

72. Fassbinder-Orth CA, Barak VA, Brown CR. Immune response of a native and an invasive bird to Buggy Creek virus (*Togaviridae: Alphavirus*) and its arthropod vector, the swallow bug (*Oeciacus vicarious*). *PLoS One*. 2013;8:e58045.
73. Ellison KS, Hofmeister EK, Ribic CA, et al. Relatively high prevalence of pox-like lesions in Henslow's sparrows (*Ammodrammus henslowii*) among nine species of migratory grassland passerines in Wisconsin. *J Wildl Dis*. 2013;50(4):810–816.
74. Fassbinder-Orth CA, Wilcoxon TE, Tran T, et al. Immunoglobulin detection in wild birds: effectiveness of three secondary anti-avian IgY antibodies in direct ELISA in 41 avian species. *Methods Ecol Evol*. 2016;7(10):1174–1181.

2. COMPARISON OF FOUR ANTI-AVIAN IGY SECONDARY ANTIBODIES USED IN WESTERN BLOT AND DOT-BLOT ELISA TO DETECT AVIAN BORNAVIRUS ANTIBODIES IN FOUR DIFFERENT BIRD SPECIES*

2.1. Introduction

In 2008, avian bornavirus (ABV) was discovered to be the causative agent of Parrot bornavirus syndrome (PaBVs), formerly known as macaw wasting disease, proventricular dilatation disease or PDD, enteric ganglioneuritis and encephalitis, and avian ganglioneuritis.¹⁻³ Since then, multiple ABV genotypes have been recognized in over 80 different species such as psittaciformes, passeriformes, and waterfowls.⁴ Diagnosis of PaBVs includes clinical signs and radiological changes, detection of viral antigen, viral RNA or ABV antibodies, gross pathology, and histopathology.⁵⁻⁸ Sampling for histopathology and tissue immunoassays, especially of nervous tissues, is not practical in living birds, thus these tests are more commonly used in post-mortem diagnosis. Reverse transcriptase polymerase chain reaction (RT-PCR) can utilize less invasive samples such as feather follicles, feces/urine, and cloacal swabs,^{5,7,9-13} however sensitivity will vary due to intermittent viral shedding.¹³⁻¹⁵

*Reprinted with permission from “Comparison Of Four Anti-Avian IgY Secondary Antibodies Used In Western Blot And Dot-Blot ELISA To Detect Avian Bornavirus Antibodies In Four Different Bird Species.” by Escandon P., Heatley J.J., Berghman L.R., Tizard I., Musser J.M.B. *Veterinary Medicine: Research and Reports* 2019;10:141-150, Copyright 2019 by Dove Medical Press Limited.

Immunologic testing comparing ABV specific antigens found that the viral nucleoprotein is immunodominant and hence the best antigen to use in a microtiter plate ELISA and in fluorescent antibody assays.^{9,16} A mixed anti-avian species IgY secondary antibody is often used in ABV serologic tests.^{8,9,17-20} The anti-bird IgY secondary antibody, produced in goats using immunoglobulins from the White-crowned sparrow, Ringed turtle dove, domestic chicken, and Muscovy duck, has been used in other ELISAs for the detection of arboviruses, flaviviruses, alpha-viruses, poxviruses.²¹⁻²⁴ The advantage of an anti-bird secondary antibody is the range of species that can be tested. This anti-bird secondary antibody has been used in serologic tests for the detection of antibodies in psittacine birds, even though the immunogen used to stimulate this secondary antibody did not contain antibodies from psittaciformes. Anti-passerine IgY secondary antibody produces better results than the anti-bird IgY secondary antibody or the anti-chicken IgY secondary antibody for serologic assays on passerine birds.²⁵ This suggests that species-specific secondary antibodies may provide more sensitive results in immunologic assays than commercially available mixed species anti-bird secondary antibody. In assays that employ short antigen-antibody incubation times, such as dot-blot or lateral flow ELISAs, a species-specific secondary antibody may be more useful when testing psittacine birds. Additionally due to the large variety of avian species susceptible to ABV infection, a low affinity of the secondary antibody could result in erroneous test results. The goal of this study was to evaluate the specificity of different avian secondary antibodies used in western blot and dot-blot ELISA to detect ABV antibodies in the

plasma of Blue and gold macaw (*Ara ararauna*), Cockatiel (*Nymphicus hollandicus*), Monk parakeet (*Myiopsitta monachus*), and Mallard (*Anas platyrhynchos*).

2.2. Materials and methods

2.2.1. Anti-IgY secondary antibodies

Polyclonal IgG rabbit anti-chicken IgY-H+L (anti-chicken IgY secondary antibody), conjugated with alkaline phosphatase, 0.1 mg/mL (Sigma-Aldrich A9171) was obtained from Sigma-Aldrich, Inc. (St. Louis, MO, USA). Polyclonal IgG goat anti-duck IgY-H+L (anti-duck IgY secondary antibody), conjugated with alkaline phosphatase, 0.1 mg/mL (Kirkegaard & Perry LB 261-06) was obtained from Kirkegaard & Perry Laboratories, Inc (Gaithersburg, MD, USA). Polyclonal IgG goat anti-macaw IgY-H+L (anti-macaw IgY secondary antibody), conjugated with alkaline phosphatase, 1.0 mg/mL (Bethyl A140-116AP) and polyclonal IgG goat anti-bird IgY-H+L (anti-bird IgY secondary antibody), conjugated with alkaline phosphatase, 1.0 mg/mL (Bethyl A140-110F) were obtained from Bethyl Laboratories, Inc (Montgomery, TX, USA).

2.2.2. Sample Collection

The experimental protocol was reviewed and approved by the Texas A&M University Bio-safety and Animal Use Committees (IACUC 2016-0274, 2014-0010, 2016-0054 and 2017-0217), which, complies with the guidelines included in the National Research Council of the National Academies' publication Guide for the Care and Use of Laboratory Animals, 8th edition. Blood samples equivalent to 1% body weight were collected by jugular venipuncture. Blood was collected into lithium heparin

tubes and stored at 4°C prior to centrifugation (5,000 x g, 10 minutes). Plasma was collected and stored at -20°C prior to analysis. Two Blue and gold macaws, one Cockatiel, one Monk parakeet and two Mallards were sampled. Blue and gold macaw blood samples were collected from one bird naturally infected with ABV that routinely tested positive for ABV mRNA by RT-PCR in its urofeces and from one bird that was not known to be exposed to ABV and routinely tested negative by RT-PCR. Cockatiel and Monk parakeet blood samples were collected prior to and following experimental infection; the birds were tested routinely by RT-PCR. The Mallard samples were collected from an experimentally infected, RT-PCR positive Mallard and from a non-infected, RT-PCR negative Mallard.

2.2.3. Recombinant nucleoprotein expression and purification

Recombinant nucleoprotein (N-protein), purified from *E. coli*, was produced following the method of Hameed et al (2018).²⁶ Briefly, the procedure was as follows. Total RNA was extracted from frozen brain tissue of a Yellow-collared macaw (*Primolius auricollis*) infected with PaBV-4 using Qiagen RNeasy Mini kit (Qiagen, Hilden, Germany). The RNA was used to generate cDNA using reverse transcription kits (High Capacity Reverse Transcription Kit, Applied Biosystems, Foster City, CA, USA) and random hexamers. Subsequent PCR was performed to amplify the N-protein gene with primers Forward 5'-CATG CAT ATG CCA CCC AAG AGA CAA AGA AGC-3' and Reverse 5'-GTAC CTC GAG GTT TGC GAA TCC GGT TAC ACC-3'. The resulting PCR products were cloned, sequenced, and inserted into pET21a vector to generate a His-tagged fusion protein for expression in *Escherichia coli* (Rosetta, Sigma-

Aldrich, St. Louis, MO, USA). Recombinant *E. coli* was incubated for 12 hrs in Luria broth fortified with ampicillin; the culture was continuously mixed at 150 rpm at room temperature. Recombinant *E. coli* was transferred to fresh media of Luria broth, ampicillin, and Isopropyl β -D-1-thiogalactopyranoside to induce protein expression and incubated for 6 hours, while being continuously stirred at 200 rpm at room temperature. The solution was centrifuged at 3500 x g for 30 mins and the supernatant was removed. The bacterial pellet was resuspended in 40 mL of phosphate-buffered saline (PBS) and sonicated for 3 sets of 8 mins to lyse the bacteria. The sonicated solution was then centrifuged at 12,000 x g for 20 mins at 4°C. The supernatant was loaded on a Qiagen Ni-NTA Agarose column, which had been pre-conditioned with 10 mL of binding buffer (20mM sodium phosphate, 300mM NaCl, pH 7.4, 10 mM imidazole); the Qiagen Ni-NTA Agarose column has a high affinity for His-tagged proteins. Ten milliliters of wash buffer (20mM sodium phosphate, 300mM NaCl, pH 7.4, 20mM imidazole) was loaded on the column and allowed gravity flow. The column was then eluted by gravity flow with 10 mL of elution buffer (20mM sodium phosphate, 300mM NaCl, pH 7.4, 200 mM imidazole) and the elutant was collected in 1mL fractions. The purity of each protein fraction was determined by sodium dodecyl sulfate polyacrylamide gel (SDS-PAGE) electrophoresis. Fractions containing the N-protein were combined and an Amico Ultra 15 mL centrifugal filter was used to concentrate the N-protein in 1 mL PBS. Finally, the protein concentration was measured using BCA™ Protein Assay Kit (Thermo Scientific™ PIERCE™, Waltham, MA. USA).

2.2.4. Western blot

Western blot assays were performed according to Guo et al (2014),²⁷ with the following modifications. Recombinant N-protein was separated using SDS-PAGE and the protein was electrophoretically transferred to a polyvinylidene difluoride (PVDF) membrane. The PVDF membrane was incubated in 5% dried skim milk/0.05%Tween/0.02M PBS overnight at room temperature. The membrane was then incubated for 2 hrs with plasma that had been diluted 1:200 with 3 mL of 2% dried skim milk/0.02M PBS /0.05%Tween, and followed with three 15 min washes of PBS/0.05% Tween. The membrane was then incubated for 1 hr with one of the four conjugated secondary antibodies. The anti-macaw and anti-bird IgY secondary antibodies, which had initial concentrations of 1.0 mg/mL, were diluted 1:50,000 with 3 mL of 2% dried skim milk/PBS/0.05% Tween; the anti-chicken and anti-duck IgY secondary antibodies, which had initial concentrations of 0.1 mg/mL, were diluted 1:5,000 with 3 mL of 2% dried skim milk/PBS/0.05% Tween. This was followed by three 15 min washes with PBS/0.05%Tween. The membrane was then incubated for approximately 5 mins, or until color change was observed, in a 5-bromo-4-chloro-3-indolyl phosphate (BCIP)/nitro blue tetrazolium (NBT) solution (SigmaFast BCIP/NBT substrate tablet, Sigma Aldrich, St. Louis, MO. USA) dissolved in 10 mL ultra-pure water. Finally, the membrane was rinsed with ultra-pure water.

2.2.5. Dot-blot enzyme-linked immunosorbent assays

Dot-blot ELISAs were performed according to Guo et al (2014),²⁷ with the following modifications. Briefly, 2.0 µl of a 0.15 mg/ml recombinant N-protein solution was dotted onto a nitrocellulose (NC) membrane strip and incubated in 5% skim dried milk/ 0.05% Tween/0.02M PBS overnight at room temperature. The membrane strip was incubated for 5 mins with plasma diluted 1:60 with 3 mL 2% dried skim milk/0.02M PBS/0.05% Tween solution, followed by three 1 min rinses with 3 mL of PBS/0.05%Tween. The membrane was incubated for five minutes in 3 mL of one of the diluted secondary antibodies, followed by three 1 min rinses with 3 mL of PBS/0.05%Tween. The membrane was then incubated for 5 mins in a solution containing SigmaFast BCIP/NBT substrate tablet dissolved in 10 mL ultra-pure water. Finally, the membrane was rinsed with ultra-pure water.

2.2.6. Semi-quantitative signal intensity of dot-blot ELISA

Membranes were scanned using an Epson Expression 100000 XL flatbed scanner with 300 dpi resolution. The scan was saved in a digital format as a .jpeg image. An image analysis software program (ImageJ, National Institutes of Health; <https://imagej.nih.gov/ij/>) was used to obtain semi-quantitative intensity values of the dot-blot ELISA signals. Digitally formatted images were converted into 2-bit grey-scale by selecting Image, Type, 32-bit. Image brightness and contrast was adjusted by selecting Image, Adjust, Brightness/Contrast, Auto, Apply. An area of interest was delineated over individual signal dots using the rectangular selection tool, then selecting Analyse, Gel, Select First Lane. This delineated rectangular area was dragged to each of

the other signal dots and then selecting Analysis, Gel, Select Next Lane. Use of a consistent delineated area provided equally sized areas of interest for analysis. A graphical depiction of dot signal intensity for each dot selected was acquired by selecting Analysis, Gel, Plot Lanes. The area representing the dot signal intensity was delineated using the straight line tool from the bar menu. After all dot areas were delineated, the wand tool from the bar menu was used to highlight these areas, which generated a signal intensity value. For each dot, three dot signal intensity values were independently generated with Image J and a mean dot signal intensity value was reported.

2.2.7. Statistical analysis

Dot signal intensities were analyzed using Two Way Analysis of Variance (ANOVA) with the Holm-Sidak method for pairwise multiple comparisons. A $P \leq 0.05$ was considered statistically significant. SigmaPlot version 10.0.1 was used for performing all statistical analyses (Systat Software, Inc., San Jose, CA).

2.3. Results

2.3.1 Western blot

Western blot membranes using the different secondary antibodies with each of the bird species sampled are shown in Figure 2.1. The N-protein signal was located at approximately 38-41 kDa. A strong signal was detected for ABV antibodies in positive Blue and gold macaw plasma when using anti-macaw IgY secondary antibody. Negative Blue and gold macaw plasma resulted in no signal. A strong signal was detected for ABV antibodies in positive Cockatiel plasma when using anti-macaw IgY secondary antibody and no signal was seen in negative Cockatiel plasma. No signal was detected in

either ABV positive nor negative Mallard plasma when using anti-macaw IgY secondary antibody.

A strong signal was detected for ABV antibodies in positive Cockatiel, Blue and gold macaw, Cockatiel, and Mallard plasma when using the anti-bird IgY secondary antibody. No signal was detected in any of the negative plasma.

A weak signal was detected for ABV antibodies in positive Blue and gold macaw plasma when using anti-duck IgY secondary antibody, however this signal was similar to that detected in the negative Blue and gold macaw, positive and negative Cockatiel, and negative Mallard plasma. A strong signal was detected for ABV antibodies in positive Mallard plasma when using anti-duck IgY secondary antibody.

A weak signal was detected when anti-chicken IgY secondary antibody was used with positive and negative Blue and gold macaw, positive and negative Cockatiel, and negative Mallard plasma. A strong signal was detected for ABV antibodies in positive Mallard plasma when using anti-chicken IgY secondary antibody.

Figure 2.1. Representative membranes of western blot results using anti-macaw, anti-bird, anti-duck, and anti-chicken IgY secondary antibody on ABV antibody positive and negative plasma from Blue and gold macaw (*Ara ararauna*), Cockatiel (*Nymphicus hollandicus*), and Mallard (*Anas platyrhynchos*). **Notes:** The N-protein signal was located at approximately 38-41 kDa. Adapted with permission from “Comparison Of Four Anti-Avian IgY Secondary Antibodies Used In Western Blot And Dot-Blot ELISA To Detect Avian Bornavirus Antibodies In Four Different Bird Species.” by Escandon P., Heatley J.J., Berghman L.R., Tizard I., Musser J.M.B. *Veterinary Medicine: Research and Reports* 2019;10:141-150, Copyright 2019 by Dove Medical Press Limited.

	Anti-macaw IgY 2° Ab	Anti-bird IgY 2° Ab	Anti-duck IgY 2° Ab	Anti-chicken IgY 2° Ab
Positive Blue and gold macaw plasma	MW 82 57 41 27 20 15 	MW 82 57 41 27 20 15 	MW 82 57 41 27 20 15 	MW 82 57 41 27 20 15
Negative Blue and gold macaw plasma				
Positive Cockatiel plasma				
Negative Cockatiel plasma				
Positive Mallard plasma				
Negative Mallard plasma				

2.3.2. Dot-blot ELISA

Dot-blot ELISA results using the different secondary antibodies with each of the bird species sampled are shown in Figure 2.2. When anti-macaw IgY secondary antibody was used, a strong signal was detected for ABV antibodies with positive Blue and gold macaw and positive Cockatiel plasma, while a good signal was detected with positive Monk parakeet plasma. No signal was seen with positive Mallard plasma and negative plasma from Blue and gold macaw, Cockatiel, Monk parakeet and Mallard. A minimally visible signal was observed for ABV antibodies in positive Mallard plasma when using anti-macaw IgY secondary antibody.

When anti-bird IgY secondary antibody was used, a weak signal was detected for ABV antibodies with positive Blue and gold macaw, Cockatiel, and Monk parakeet plasma. A good signal was detected for ABV antibodies with positive Mallard plasma when using anti-bird IgY secondary antibody. No signal was detected in any of the negative plasma samples when using anti-bird secondary antibody.

No signal was detected for ABV antibodies in positive and negative Blue and gold macaw, Cockatiel and Monk parakeet plasma when using anti-duck secondary antibody. A strong signal was detected in positive Mallard plasma when using anti-duck IgY secondary antibody. Negative Mallard plasma resulted in no signal using anti-duck IgY secondary antibody.

A weak signal was detected when anti-chicken IgY secondary antibody was used with positive Blue and gold macaw, positive Cockatiel, and positive Mallard plasma. No

signal was detected for ABV antibodies with negative plasma nor with positive Monk parakeet plasma when using anti-chicken IgY secondary antibody.

Figure 2.2. Representative membranes of dot-blot ELISA results using anti-macaw, anti-bird, anti-duck, and anti-chicken IgY secondary antibody on ABV antibody positive and negative plasma from Blue and gold macaw (*Ara ararauna*), Cockatiel (*Nymphicus hollandicus*), Monk Parakeet (*Myiopsitta monachus*), and Mallard (*Anas platyrhynchos*). Adapted with permission from “Comparison Of Four Anti-Avian IgY Secondary Antibodies Used In Western Blot And Dot-Blot ELISA To Detect Avian Bornavirus Antibodies In Four Different Bird Species.” by Escandon P., Heatley J.J., Berghman L.R., Tizard I., Musser J.M.B. *Veterinary Medicine: Research and Reports* 2019;10:141-150, Copyright 2019 by Dove Medical Press Limited.

	Anti-macaw IgY 2° Ab	Anti-bird IgY 2° Ab	Anti-duck IgY 2° Ab	Anti-chicken IgY 2° Ab
Positive Blue and gold macaw plasma				
Negative Blue and gold macaw plasma				
Positive Cockatiel plasma				
Negative Cockatiel plasma				
Positive Monk Parakeet plasma				
Negative Monk Parakeet plasma				
Positive Mallard plasma				
Negative Mallard plasma				

2.3.2.1 Semi-quantification of dot-blot ELISA

A representation of the dot-blot ELISA signals, the ImageJ graphic results, and the signal intensity values generated for the dot are shown in Figure 2.3. Signal intensities of the dot-blot ELISA using different secondary antibodies within each bird species sampled are shown in Table 2.1. For Blue and gold macaw plasma samples, the mean signal intensity of 19,461 obtained for the positive Blue and gold macaw plasma tested using anti-macaw IgY secondary antibody was significantly greater ($P < 0.05$) than the signal intensity obtained when using any of the other three secondary antibodies. The signal intensity of the dots obtained for positive Blue and gold macaw plasma was significantly greater ($P < 0.05$) than that obtained for negative Blue and gold macaw plasma when using anti-macaw IgY secondary antibody. The signal intensity values obtained for the positive Blue and gold macaw samples did not differ significantly from the negative Blue and gold macaw samples when anti-bird, anti-chicken, or anti-duck IgY secondary antibodies were used.

For Cockatiel samples, the mean signal intensity of 21,032 was obtained for positive Cockatiel plasma tested using the anti-macaw IgY secondary antibody was significantly greater ($P < 0.05$) than the signal intensity obtained when using any of the other three secondary antibodies. The signal intensity of the positive plasma dots obtained for positive Cockatiel plasma was significantly greater ($P < 0.05$) than that obtained for negative Cockatiel plasma when using anti-macaw or anti-bird IgY secondary antibody. The signal intensity values did not significantly differ between the

positive and negative samples when anti-chicken or anti-duck IgY secondary antibodies were used.

For Monk parakeet samples, the mean signal intensity of 17,785 obtained for the positive plasma tested using anti-macaw IgY secondary antibody was significantly greater ($P < 0.05$) than the signal intensity when the other three secondary antibodies were used. The signal intensity of the positive plasma was significantly greater ($P < 0.05$) than that of the negative plasma when using anti-macaw or anti-bird IgY secondary antibody. The signal intensity values did not differ significantly between the positive and negative samples when anti-chicken or anti-duck IgY secondary antibodies were used.

For Mallard samples, the mean dot signal intensity obtained using positive Mallard plasma was significantly different ($P < 0.05$) between all the secondary antibodies; the anti-duck IgY secondary antibody generated the greatest signal intensity value of 18,098, while the anti-macaw IgY secondary antibody generated the least signal intensity value of 561. The signal intensity of the positive plasma dot was significantly greater ($P < 0.05$) than that of the negative plasma dot when using anti-bird, anti-chicken, and anti-duck IgY secondary antibodies. The signal intensity value did not differ significantly between the positive and negative samples, 561 and 297, respectively, when using anti-macaw IgY secondary antibodies.

Mean dot signal intensity obtained using the negative plasma samples did not differ significantly within each bird species.

Figure 2.3. Digital image analysis of dot-blot ELISA used to generate the signal intensity value. Adapted with permission from “Comparison Of Four Anti-Avian IgY Secondary Antibodies Used In Western Blot And Dot-Blot ELISA To Detect Avian Bornavirus Antibodies In Four Different Bird Species.” by Escandon P., Heatley J.J., Berghman L.R., Tizard I., Musser J.M.B. *Veterinary Medicine: Research and Reports* 2019;10:141-150, Copyright 2019 by Dove Medical Press Limited.

Notes: The dot-blot ELISA with the delineated area of interest highlighted in the red rectangle, the graphic display, and the signal intensity value are displayed using samples from A) Blue and gold macaw (*Ara ararauna*), B) Cockatiel (*Nymphicus hollandicus*), C) Monk parakeet (*Myiopsitta monachus*), and D) Mallard (*Anas platyrhynchos*).

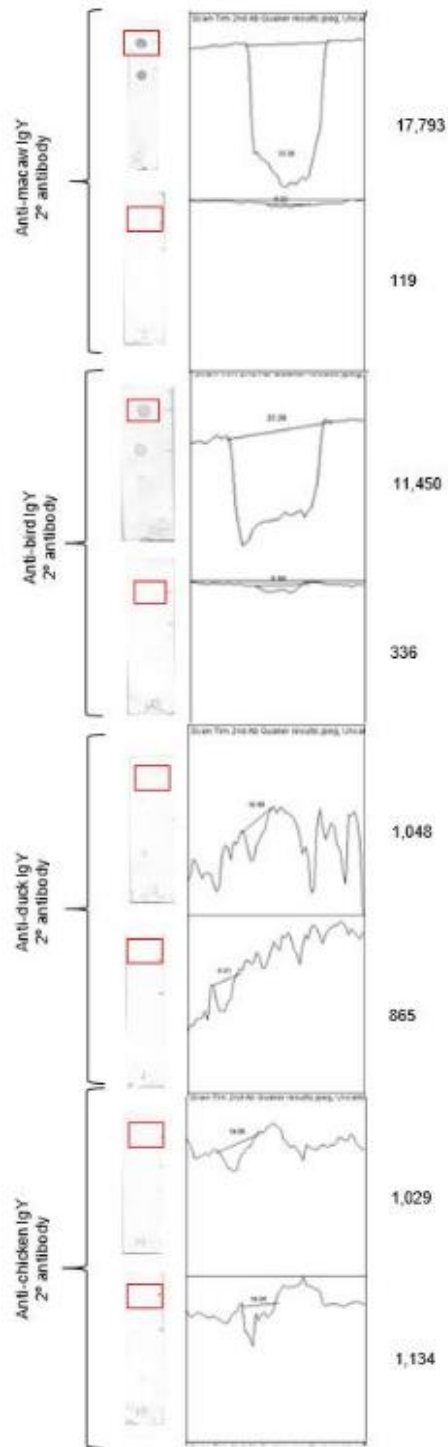
A) Blue and gold macaw samples

B) Cockatiel samples



Figure 2.3. Continued.

C) Monk parakeet samples



D) Mallard samples

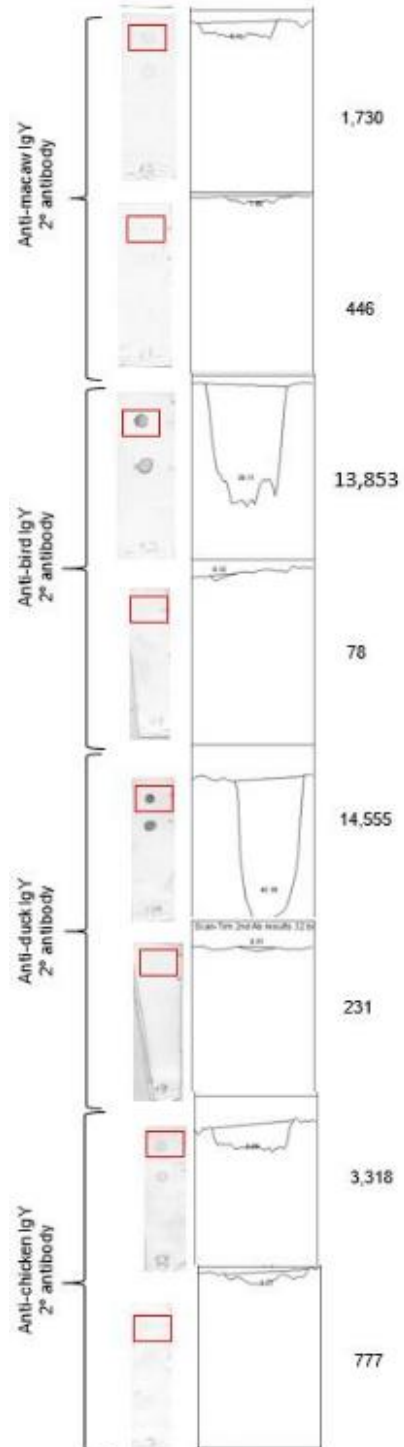


Table 2.1. Signal intensities obtained when testing ABV antibody positive and negative plasma from Blue and gold macaw (*Ara ararauna*), Cockatiel (*Nymphicus hollandicus*), Monk Parakeet (*Myiopsitta monachus*), and Mallard (*Anas platyrhynchos*) with a dot-blot ELISA using anti-macaw, anti-bird, anti-duck, and anti-chicken IgY secondary antibody. Adapted with permission from “Comparison Of Four Anti-Avian IgY Secondary Antibodies Used In Western Blot And Dot-Blot ELISA To Detect Avian Bornavirus Antibodies In Four Different Bird Species.” by Escandon P., Heatley J.J., Berghman L.R., Tizard I., Musser J.M.B. *Veterinary Medicine: Research and Reports* 2019;10:141-150, Copyright 2019 by Dove Medical Press Limited.

Bird species	2° antibody	N	Signal Intensity Mean	
			Positive sample	Negative sample
Blue and gold macaw				
	anti-macaw	6	19461 ^a (±1338)	318* (±135)
	anti-bird	6	2549 ^b (±462)	1080 (±786)
	anti-duck	6	92 ^c (±40)	148 (±76)
	anti-chicken	6	415 ^c (±148)	152 (±52)
Cockatiel				
	anti-macaw	6	21032 ^a (±1218)	221* (±116)
	anti-bird	6	3690 ^b (±459)	109* (±18)
	anti-duck	6	180 ^c (±54)	127 (±63)
	anti-chicken	6	435 ^c (±251)	94 (±43)
Monk parakeet				
	anti-macaw	6	17785 ^a (±830)	805* (±176)
	anti-bird	6	15522 ^b (±1032)	703* (±136)
	anti-duck	6	1389 ^c (±355)	739 (±267)
	anti-chicken	6	736 ^c (±88)	1328 (±381)
Mallard				
	anti-macaw	6	561 ^a (±333)	297 (±87)
	anti-bird	6	12724 ^b (±2459)	814* (±514)
	anti-duck	6	18098 ^c (±2102)	146* (±51)
	anti-chicken	6	5751 ^d (±714)	846* (±393)

Notes: Signal intensity data are presented as the mean (±SEM). ^{a,b,c,d} Different superscript letters within each bird species sampled indicate a significant difference ($P<0.05$) between secondary antibody values. *Negative sample value is significantly different ($P<0.05$) from the corresponding positive sample value of the same secondary antibody. The negative values within each bird species sampled were not significantly different

2.4. Discussion

In serologic testing of birds, variations in the specificity of the secondary antibody used can generate erroneous results. Our study demonstrated species specificity of secondary antibodies to bird IgY in Western blot and dot-blot ELISA. Our results suggest that rapid, patient-side serologic assays for ABV antibodies in psittacines, such as the dot-blot ELISA, should employ anti-IgY secondary antibody against a similar psittacine species. In this study, the use of anti-macaw IgY secondary antibody in the dot-blot ELISA for testing antibody-positive Blue and gold macaw plasma generated appreciably better visible signals with consistently higher signal intensity than the use of anti-bird, anti-duck, or anti-chicken IgY secondary antibodies (Figure 2.2.; Table 2.1.). Though some studies have used anti-chicken secondary antibody in serologic assays in wild birds,^{28,29} our results were in agreement with a study that found the use of anti-passerine IgY secondary antibody in a microplate ELISA performed better than anti-chicken and anti-bird secondary antibodies when testing passerines.²⁵ In fact, we found that the use of anti-macaw IgY secondary antibody, in both the Western blot and the dot-blot ELISAs, showed strong species specificity for psittacines.

Conversely, the use of anti-macaw IgY secondary antibody showed no difference between positive and negative Mallard plasma in either of immunological assays (Figure 2.1. and 2.2.; Table 2.1.). Due to the diversity of avian species that can be infected with ABV, specificity of the secondary antibody to the antiglobulin species being tested is critically important and must be considered in the development of ABV assays and in ABV research.

Western blot and immunofluorescence assays are considered gold standards in serologic testing for ABV. N-protein is the immunodominant antigen,^{9,27} thus a recombinant N-protein was utilized as the antigen of interest in our assays. The use of the Western blot in our study was two-fold: 1) to verify the seropositive / seronegative status of the plasma samples and 2) to evaluate the use of the different secondary antibodies as compared to the dot-blot ELISA. Anti-macaw and anti-bird IgY secondary antibodies produced strong reactions at 38-41 kDa, but additional bands were seen at 17, 27, and 30 kDa. These bands likely represent degraded N-protein to which the secondary antibodies were able to bind.

The use of anti-bird IgY secondary antibody in the Western blot worked well for Blue and gold macaw, Cockatiel, and Mallard plasmas, a result similar to that obtained in other studies using anti-bird IgY secondary antibody to detect ABV exposure.^{9,11,20} However using the anti-bird IgY secondary antibody in the dot-blot ELISA, the Blue and gold macaw and Cockatiel samples had poor positive responses while the Mallard samples were strongly positive. Monk parakeet plasma was not assayed by Western blotting due to the limited plasma volume available. The dissimilar results obtained using anti-bird IgY secondary antibody in the Western blot and the dot-blot ELISAs may have been due to multiple factors, including; antigen-antibody reactions, the species used to generate the anti-bird antibody and the different procedural methods of the assays. Many factors influence antigen-antibody reactions, such as pH, temperature, antibody and antigen concentration, and incubation time.³⁰ In this study, the Western blot procedure allowed for a longer duration of incubation for the antigen-antibody reactions

between plasma IgY and the recombinant N-protein and between the anti-IgY secondary antibody and the plasma IgY. The commercially available anti-bird IgY secondary antibody was manufactured using White-crowned sparrow, Ringed turtle dove, domestic chicken, and Muscovy duck IgY and has been reported to react with dove, duck, sparrow, chicken, turkey, emu, ostrich, quail, macaw and cockatiel antiglobulins (Product insert, Bird IgG-heavy and light chain Antibody, Bethyl Laboratories).

This ability of anti-bird IgY secondary antibody to react with the antiglobulins of many bird species makes it a useful secondary antibody for assays that utilize long incubation periods; the anti-bird IgY secondary antibody has been used in ABV testing using, Western blot analysis, microplate ELISA, and indirect immunofluorescence assays.^{8,9,17-19} In our Western blots, strong signals were obtained using the anti-bird IgY secondary antibody with the positive samples from Blue and gold macaw, Cockatiel, and Mallard (Figure 2.1.), however when used in our dot-blot ELISA, the use of anti-bird IgY secondary antibody produced weak signals with Blue and gold macaw and Cockatiel positive plasma (Figure 2.2.). The polyclonal nature of the anti-bird IgY antibodies make it an ideal secondary antibody for immunodiagnostic assays due to its ability to recognize multiple epitopes on the target antiglobulin and on the different species antiglobulins. However, the varying affinities of the polyclonal IgY antibodies can cause differences in the signal strength obtained from assays with long or short incubation times, such as seen between the Western blot and dot-blot ELISA, respectively, in our study. In the dot-blot ELISA, mainly high affinity secondary antibodies, which bind quickly and with a greater stability than lower affinity secondary

antibodies, produce the signal. Additionally, the polyclonal nature of the anti-bird IgY secondary antibody produced a higher avidity in the dot-blot ELISAs for Monk parakeet and Mallard antiglobulins, as observed by the stronger dot visibility and signal intensity, than the avidity for Blue and gold macaw and Cockatiel antiglobulins (Figure 2.2.). Exactly what factors were involved and how they differed was beyond the scope of this project, but the issue of reaction incubation time and its effect on avidity should be explored further if a dot-blot ELISA is to be optimized as a rapid, patient-side diagnostic assay.

Background noise in all tests must also be considered. In this study, a faint signal was observed in the negative samples of Blue and gold macaw and Cockatiel samples when the anti-duck and anti-chicken IgY secondary antibodies were used in the Western blot and dot-blot ELISAs; the signals of the corresponding negative samples were visibly similar to those of the positive samples (Figure 2.1. and 2.2.). However, when analyzing the signal intensities of the dot-blot ELISA, there was no significant difference between the signal intensity of the negative and positive Blue and gold macaw or Cockatiel samples when anti-duck or anti-chicken IgY secondary antibody was used (Table 2.1.). This background signal may have been due to cross-reactions with antibodies to *E.coli* antigens in the samples. Antibodies against *E. coli* are found in human serum and can cause background noise in serologic assays that use recombinant proteins.³¹⁻³² Similar studies in birds show non-specific signals due to *E. coli* antibodies in plasma samples and to recombinant *E. coli* antigens in serologic tests.^{33,34} Affinity purification of the His-tagged recombinant N-protein with the Ni-NTA Agarose column

may not have removed all *E. coli* antigens from the recombinant *E. coli*/N-protein solution. *E. coli* proteins can have some histidine conformation or during the generation of the recombinant N-protein, some His-tagged *E. coli* proteins may have been generated with the insertion of the pET21a vector into the *E. coli*. Thus, some *E. coli* antigens may have been present in the PVDF membranes and the NC membrane strips of the Western blot and dot-blot ELISAs, respectively, and able to react with antibodies in the sample. To reduce non-specific signals and background noise in the assays, procedures that will absorb or neutralize *E. coli* antibodies in plasma samples or that will increase the purity of the recombinant N-protein antigen need to be investigated. However even without these additional procedures, the dot-blot ELISA readily discriminated between ABV antibody positive and negative samples (Figure 2), especially in species most prone to natural infection. This suggests the possibility of developing a rapid, patient-side assay that will detect ABV antibodies in psittacine birds.

2.5. Conclusion

Our study shows that species-specific anti-IgY secondary antibodies provided more accurate results in serologic assays than the use of commercially available anti-chicken and anti-bird IgY secondary antibodies. Due to the large variety of avian species susceptible to ABV infection, the specificity of the secondary antibody must be considered when developing or performing serologic assays, such as dot-blot ELISA and Western blot.

2.6. References

1. Kistler AL, Gancz A, Clubb S, et al. Recovery of divergent avian bornaviruses from cases of proventricular dilatation disease: Identification of a candidate etiologic agent. *Virology*. 2008;5:88–102.
2. Honkavuori KS, Shivaprasad HL, Williams BL, et al. Novel borna virus in psittacine birds with proventricular dilatation disease. *Emerg Infect Dis*. 2008;14:1883–1886.
3. Gray P, Hoppes S, Suchodolski P, et al. Use of avian bornavirus isolated to induce proventricular dilatation disease in conures. *Emerg Infect Dis*. 2010;16:473–479.
4. Kuhn JH, Dürrwald R, Bào Y, et al., Taxonomic reorganization of the family Bornaviridae. *Arch Virol*. 2015;160:621–632.
5. Raghav R, Taylor M, DeLay J, et al. Avian bornavirus is present in many tissues of psittacine birds with histopathologic evidence of proventricular dilatation disease. *J Vet Diagn Invest*. 2010;22:495–508.
6. Payne S, Shivaprasad HL, Mirhosseini N, et al. Unusual and severe lesions of proventricular dilatation disease in cockatiels (*Nymphicus hollandicus*) acting as healthy carriers of avian bornavirus (ABV) and subsequently infected with a virulent strain of ABV. *Avian Pathol*. 2011;40:15–22.
7. Leal de Araujo J, Rech RR, Heatley JJ, et al. From nerves to brain to gastrointestinal tract: A time-based study of parrot bornavirus 2 (PaBV-2)

- pathogenesis in cockatiels (*Nymphicus hollandicus*). *PLoS One*. 2017;12:e0187797.
8. Piepenbring AK, Enderlein D, Herzog S, et al. Pathogenesis of avian bornavirus in experimentally infected Cockatiels. *Emerg Infect Dis*. 2012;18:234–241.
 9. de Kloet AH, Kerski A, de Kloet SR. Diagnosis of avian bornavirus infection in psittaciformes by serum antibody detection and reverse transcription polymerase chain reaction assay using feather calami. *J Vet Diagn Invest*. 2011;23:421–429.
 10. Rubbenstroth D, Rinder M, Stein M, et al. Avian bornaviruses are widely distributed in canary birds (*Serinus canaria* f. domestica). *Vet Microbiol*. 2013;165:287–295.
 11. Delnatte P, Mak M, Ojkic D, et al. Detection of avian bornavirus in multiple tissues of infected psittacine birds using real-time reverse transcription polymerase chain reaction. *J Vet Diagn Invest*. 2014;26:266–271.
 12. Reuter A, Ackermann A, Kothlow S, et al. Avian bornaviruses escape recognition by the innate immune system. *Viruses*. 2010;2:927–938.
 13. Heatley JJ, Villalobos AR. Avian bornavirus in the urine of infected birds. *Vet Med Res Rep*. 2012;3:19–23.
 14. Kistler AL, Smith JM, Alexander L, et al. Analysis of naturally occurring avian bornavirus infection and transmission during an outbreak of proventricular dilatation disease among captive psittacine birds. *J Virol*. 2010;84:2176–2179.

15. Rubbenstroth D, Schmidt V, Rinder M, et al. Phylogenetic analysis supports horizontal transmission as a driving force of the spread of avian bornavirus. *PLoS One*. 2016;11:e0160936
16. Zimmermann V, Rinder M, Kaspers B, et al. Impact of antigenic diversity on laboratory diagnosis of avian bornavirus infections in birds. *J Vet Diagn Invest*. 2014;26:769–777.
17. Lierz M, Hafez HM, Honkavuori KS, et al. Anatomical distribution of avian bornavirus in parrots, its occurrence in clinically healthy birds and ABV-antibody detection. *Avian Pathol*. 2009;38:491–496.
18. de Kloet SR, Dorrestein GM. Presence of avian bornavirus RNA and anti-avian bornavirus antibodies in apparently healthy macaws. *Avian Dis*. 2009;53:568–573.
19. Herzog S, Enderlein D, Heffels-Redmann U, et al. Indirect immunofluorescence assay for *Intra Vitam* diagnosis of avian bornavirus infected in psittacine birds. *J Clin Microbiol*. 2010;48:2282-2284.
20. Fluck A, Enderlein D, Piepenbring A, et al. Correlation of avian bornavirus-specific antibodies and viral ribonucleic acid shedding with neurological signs and feather-damaging behavior in psittacine birds. *Vet Rec*. 2019;184:476–482.
21. Chiles RE, Reisen WK. A new enzyme immunoassay to detect antibodies to arboviruses in the blood of wild birds. *J Vector Ecol*. 1998;23:123–135.
22. Hofmeister EK, Dusek RJ, Fassbinder-Orth C, et al. Susceptibility and antibody response of vesper sparrows (*Pooecetes gramineus*) to West Nile virus: a

- potential amplification host in sage-brush grassland habitat. *J Wildl Dis.* 2016;52:345–353.
23. Fassbinder-Orth CA, Barak VA, Brown CR. Immune response of a native and an invasive bird to Buggy Creek virus (*Togaviridae: Alphavirus*) and its arthropod vector, the swallow bug (*Oeciacus vicarius*). *PLos One.* 2013;8:e58045.
24. Ellison KS, Hofmeister EK, Ribic CA, et al. Relatively high prevalence of pox-like lesions in Henslow's sparrows (*Ammodrammus henslowii*) among nine species of migratory grassland passerines in Wisconsin. *J Wildl Dis.* 2013;50:810–816.
25. Fassbinder-Orth CA, Wilcoxon TE, Tran T, et al. Immunoglobulin detection in wild birds: effectiveness of three secondary anti-avian IgY antibodies in direct ELISA in 41 avian species. *Methods Ecol Evol.* 2016;7:1174–1181.
26. Hameed SS, Guo J, Tizard I, et al. Studies on immunity and immunopathogenesis of parrot bornaviral disease in cockatiels. *Virology.* 2018;515:81-91.
27. Guo J, Payne S, Zhang S, et al. Avian bornaviruses: diagnosis, isolation, and genotyping. *Curr Protoc Microbiol.* 2014;34:15i.1.11.11–15i.11.33.
28. Martínez J, Tomas G, Merino S, et al. Detection of serum immunoglobulins in wild birds by direct ELISA: a methodological study to validate the technique in different species using anti-chicken antibodies. *Funct Ecol.* 2003;17:700–706.
29. Cray C, Villar D. Cross-reactivity of anti-chicken IgY antibody with immunoglobulins of exotic avian species. *Vet Clin Path.* 2008;37:328–331.

30. Reverberi R, Reverberi L. Factors affecting the antigen-antibody reaction. *J Blood Transfus.* 2007;5:227–240.
31. Yip CW, Hon CC, Zeng F, et al. Naturally occurring anti-*Escherichia coli* protein antibodies in the sera of healthy humans cause analytical interference in a recombinant nucleocapsid protein-based enzyme-linked immunosorbent assay for serodiagnosis of severe acute respiratory syndrome. *Clin Vaccine Immunol.* 2007;14:99–101.
32. Hernandez P, Heimann M, Riera C, et al. Highly effective serodiagnosis for Chagas' disease. *Clin Vaccine Immunol.* 2010;17:1598–1604.
33. Hadifar F, Ignjatovic J, Tarigan S, et al. Multimeric recombinant M2e protein-based ELISA: A significant improvement in differentiating avian influenza infected chickens from vaccinated ones. *PLoS One.* 2014;9:e108420.
34. Zhao S, Jin M, Li H, et al. Detection of antibodies to the nonstructural protein (NS1) of avian influenza viruses allows distinction between vaccinated and infected chickens. *Avian Dis.* 2005;49:488–493.

3. DEVELOPMENT OF A DOT-BLOT ENZYME IMMUNOSORBENT ASSAY TO DETECT AVIAN BORNAVIRUS IMMUNOGLOBULINS

3.1. Introduction

Avian bornavirus (ABV) is the causative agent of Parrot bornavirus syndrome (PaBVs), a devastating disease of psittacine populations.¹⁻³ Avian bornavirus is a neurotropic virus but can affect an extensive range of tissues and cell types.⁴ Avian bornavirus antigens and mRNA have been detected in the brain, eye, spinal cord, heart, gastrointestinal system, adrenal glands, and kidneys by reverse transcriptase polymerase chain reaction (RT-PCR) and immunohistochemistry assays.^{2,4-10} The reverse transcriptase polymerase chain reaction can utilize less invasive samples such as feather follicles, feces/urine, and cloacal swab,^{4-8,11-13} but results can vary due to the intermittent viral shedding.¹⁴⁻¹⁶ RT-PCR detects and measures viral RNA, while immunohistochemistry, immunofluorescence, and immunocytochemistry are routinely used to visualize virus distribution and amount within a tissue or cell culture sample.¹⁷

To identify bird exposure, western blot, indirect immunofluorescence assay, and enzyme-linked immunosorbent assays (ELISA) have been used to detect ABV antibodies, with the nucleoprotein (N-protein) being immunodominant and most frequently used as the target analyte in the assay.^{9-11,13,17-21} These serology assays are primarily laboratory-based assays that use serum or plasma as the test sample.

In ELISAs, an enzyme is conjugated to the labeled antibody. Depending on the enzyme/substrate reaction, a generation of color, fluorescence, or luminescent product

can be visualized with the naked eye or electrical equipment such as spectrophotometer.²² The process is similar for any type of ELISA: fixing either an analyte or antibody on the test matrix and detecting the conjugate with an enzyme catalyst. Laboratory-controlled ELISAs take up to several hours to complete, require trained personnel and commonly test serum or plasma samples, rarely is whole blood the test sample. Patient-side ELISAs are preferred diagnostic immunoassay due to rapidity in obtaining results and to convenience of use. To streamline the procedure for further rapidity and convenience, many practitioners would rather use whole blood in lieu of serum or plasma samples, as the use of whole blood would remove the sample processing step. However, whole blood potentially could alter results and even cause false positives or false negatives to occur.

Demand has increased for avian bornavirus diagnostics that have high sensitivity, high specificity, minimal processing time, and a rapid turn-around time for results, all of which can be achieved with the dot-blot ELISA. The purpose of this study was to develop and optimize a dot-blot ELISA for the detection of ABV antibodies that can be run with a small sample volume and quickly provide accurate results.

3.2. Materials and methods

3.2.1. Sample Collection

The experimental protocol was reviewed and approved by the Texas A&M University Bio-safety and Animal Use Committees (IACUC 2017-0217), which complies with guidelines included in the National Research Council of the National Academies' publication *Guide for the Care and Use of Laboratory Animals*, 8th edition. Two Blue and gold macaws (*Ara ararauna*) were used for sample collection: one macaw was naturally infected and routinely ABV positive by RT-PCR on fecal swabs, while the other bird was not known to be exposed to ABV and routinely RT-PCR negative. Blood samples equivalent to 1% body weight were collected by jugular venipuncture. For studies 1, 2, and 3, whole blood was collected into lithium heparin tubes, stored at 4°C until centrifuged at 5,000 x g for 10 minutes. Plasma was collected and stored at -20°C prior to analysis. For study 4, whole blood was collected into lithium heparin tubes, divided into two samples, and stored at 4°C. One set of samples was centrifuged at 5,000 x g, for 10-minutes and the plasma collected. Matched plasma and whole blood samples were stored at 24°C until analyzed, which occurred within 30-minutes of plasma collection.

3.2.2. Recombinant nucleoprotein expression and purification

Recombinant nucleoprotein (N-protein), purified from *E. coli*, was produced following the method of Hameed et al (2018).²³ Briefly, the procedure was as follows. Total RNA was extracted from frozen brain tissue of a Yellow-collared macaw (*Primolius auricollis*) infected with PaBV-4 using Qiagen RNeasy Mini kit (Qiagen,

Hilden, Germany). The RNA was used to generate cDNA using reverse transcription kits (High Capacity Reverse Transcription Kit, Applied Biosystems, Foster City, CA, USA) and random hexamers. Subsequent PCR was performed to amplify the N-protein gene with primers Forward 5'-CATG CAT ATG CCA CCC AAG AGA CAA AGA AGC-3' and Reverse 5'-GTAC CTC GAG GTT TGC GAA TCC GGT TAC ACC-3'. The resulting PCR products were cloned, sequenced, and inserted into pET21a vector to generate a His-tagged fusion protein for expression in *E. coli* (Rosetta, Sigma-Aldrich, St. Louis, MO, USA). Recombinant *E. coli* was incubated for 12 hours in Luria broth fortified with ampicillin; the culture was continuously mixed at 150 rpm at room temperature. Recombinant *E. coli* was transferred to fresh media of Luria broth, ampicillin, and Isopropyl β -D-1-thiogalactopyranoside to induce protein expression and incubated for 6 hours, while being continuously stirred at 200 rpm at room temperature.

Following the final incubation of the recombinant *E. coli*, the broth solution was centrifuged at 3500 x g for 30-minutes and the supernatant was removed. The bacterial pellet was resuspended in 40 mL of phosphate-buffered saline (PBS) and sonicated for 3 sets of 8 minutes to lyse the bacteria. The sonicated solution was then centrifuged at 12,000 x g for 20 minutes at 4°C. The supernatant was loaded on a Qiagen Ni-NTA Agarose column (Qiagen, Hilden, Germany), which had been pre-conditioned with 10 mL of binding buffer (20mM sodium phosphate, 300mM NaCl, pH 7.4, 10mM imidazole); the Ni-NTA Agarose column has a high affinity for His-tagged proteins. Ten milliliter of wash buffer (20mM sodium phosphate, 300mM NaCl, pH 7.4, 20mM imidazole) was loaded on the column and allowed gravity flow. The column was then

eluted by gravity flow with 10 mL of elution buffer (20mM sodium phosphate, 300mM NaCl, pH 7.4, 200 mM imidazole) and the elutant was collected in 1.0 mL fractions. The purity of each protein fraction was determined by sodium dodecyl sulfate polyacrylamide gel (SDS-PAGE) electrophoresis. Fractions containing the recombinant N-protein were combined and an Amicon Ultra 15 mL centrifugal filter (MilliporeSigma, Burlington, MA, USA) was used to concentrate the recombinant N-protein in 1.0 mL PBS. Finally, the protein concentration was measured using BCA™ Protein Assay Kit (Thermo Scientific™ PIERCE™, Waltham, MA. USA). Just prior to being used in a dot-blot ELISA or Western blot, the stock recombinant N-protein solution (0.7 mg/mL) was diluted with PBS.

A sham solution without recombinant N-protein was produced by utilizing the aforementioned process, but without cloning the N-protein gene into the *E. coli*.

3.2.3. Western blot

Western blot assays were performed according to Guo (2014),²¹ with the following modifications. Briefly, 0.1 mg/mL of recombinant N-protein solution or *E. coli* protein without recombinant N-protein was mixed at a 1:1 ratio with gel loading buffer and boiled in a water bath for 3-minutes. Then 15 µL of the boiled sample was loaded into each SDS-PAGE gel well, separated using SDS-PAGE and electrophoretically transferred to a polyvinylidene difluoride (PVDF) membrane. The PVDF membrane was incubated in 5% dried skim milk/0.05%Tween/0.02M PBS overnight at room temperature. All incubations and rinses performed were done at 4°C and on a rocking platform. The membrane was then incubated for 2-hours with macaw

plasma that had been diluted 1:200 with 3.0 mL of 2% dried skim milk/0.05% Tween/0.02M PBS, and followed with three 15-minute rinses of 0.05% Tween/0.02M PBS. The membrane was then incubated for 1-hour with 3.0 mL with a 1:50,000 dilution of 1.0 mg/ml polyclonal IgG goat anti-macaw IgY-H+L conjugated with alkaline phosphatase (anti-macaw IgY secondary antibody) (Bethyl A140-116AP, Bethyl Laboratories, Inc., Montgomery, TX, USA) and 2% dried skim milk/PBS/0.05% Tween, followed by three 15-minute rinses with 0.05% Tween/0.02M PBS. The membrane was then incubated for approximately 5-minutes, or until color change was observed, in a 5-bromo-4-chloro-3-indolyl phosphate (BCIP)/nitro blue tetrazolium (NBT) solution (SigmaFast BCIP/NBT substrate tablet, Sigma Aldrich, St. Louis, MO, USA) dissolved in 10 mL ultra-pure water. Finally, the membrane was rinsed with ultra-pure water.

3.2.4. Dot-blot enzyme-linked immunosorbent assays

Recombinant N-protein amounts per dot, plasma dilutions, whole blood dilutions, and incubation times for each of the dot-blot ELISA studies are shown in Table. 3.1. The nitrocellulose (NC) membrane strip was blotted with 2.0 μ L of recombinant N-protein solution and allowed to air dry for 5-minutes. The stock recombinant N-protein solution was diluted with PBS so that the required antigen amount on the NC membrane strip in each study would be delivered in 2.0 μ L. After air drying for 5-minutes, the NC membrane strip was incubated in 5% dried skim milk/0.05% Tween/0.02M PBS overnight for 12 hours. In studies 2, 3, & 4, two separate areas on each NC membrane strip were blotted so that there were two blots with the same

recombinant N-protein amount per strip; study 1 had only one blot. The NC membrane strip was incubated for a specified time in 3.0 mL of the plasma or whole blood diluted with 2% dried skim milk/0.02M PBS/0.05% Tween solution; incubation time and dilution factor of plasma or whole blood are specified for each study in Table

3.1. Incubation was followed by three 1-minute rinses with 3.0 mL of PBS/0.05%Tween. The membrane was then incubated at specified times, see Table 3.1, with 3.0 mL of a 1:50,000 dilution of anti-macaw IgY secondary antibody and 2% dried skim milk/0.05%Tween/0.02M PBS; this was followed by three 1-minute rinses with 3.0 mL of 0.05%Tween/ 0.02M PBS. The membrane was then incubated for 5-minutes in a solution containing SigmaFast BCIP/NBT substrate tablet dissolved in 10 mL ultra-pure water. Finally, the membrane was rinsed with ultra-pure water.

All incubations and rinses were at 4°C and done on a rocking platform. Three independent NC membrane strips were tested for all dot-blot ELISAs studies.

Table 3.1. Recombinant N-protein amounts per dot, plasma dilutions, whole blood dilutions, and incubation times for each of the dot-blot ELISA studies.

Notes: N/A means not applicable to the particular study.

	Study 1	Study 2	Study 3	Study 4
Recombinant N-protein (µg) per dot	1.4 0.14 0.014 0.0014 0.00014	0.6 0.3 0.15	0.6 0.3	0.3
Plasma dilution	1:100 1:60 1:30	1:100 1:60 1:30	1:60 1:30 1:20	1:60
Whole blood dilution	N/A	N/A	N/A	1:100 1:60 1:30
Incubation time (min)	10	10 & 5	5 & 2	5

3.2.5. Semi-quantitative signal intensity of dot-blot ELISA

Membranes were scanned using an Epson Expression 100000 XL flatbed scanner with 300 dpi resolution. The scan was saved in a digital format as a .jpeg image.

An image analysis software program (ImageJ, National Institutes of Health; <https://imagej.nih.gov/ij/>) was used to obtain semi-quantitative intensity values of the dot-blot ELISA signals. Digitally formatted images were converted into 2-bit grey-scale by selecting Image, Type, 32-bit. Image brightness and contrast were adjusted by selecting Image, Adjust, Brightness/Contrast, Auto, Apply. An area of interest was delineated over individual signal dots using the rectangular selection tool, then selecting Analyze, Gel, Select First Lane. This delineated rectangular area was dragged to each of the other signal dots and then Analysis, Gel, Select Next Lane were selected. Use of a consistent delineated area provided equally sized areas of interest for analysis. A graphical depiction of dot-signal intensity for each dot selected was acquired by selecting Analysis, Gel, Plot Lanes. The area representing the dot-signal intensity was delineated using the straight line tool from the bar menu. After all dot areas were delineated, the wand tool from the bar menu was used to highlight these areas, which generated a signal intensity value.

3.2.6. Statistical analysis

Dot-signal intensities were analyzed using Two Way Analysis of Variance (ANOVA) with the Holm-Sidak method for pairwise multiple comparisons. A $P \leq 0.05$ was considered statistically significant. SigmaPlot version 10.0.1 was used for performing all statistical analyses (Systat Software, Inc., San Jose, CA).

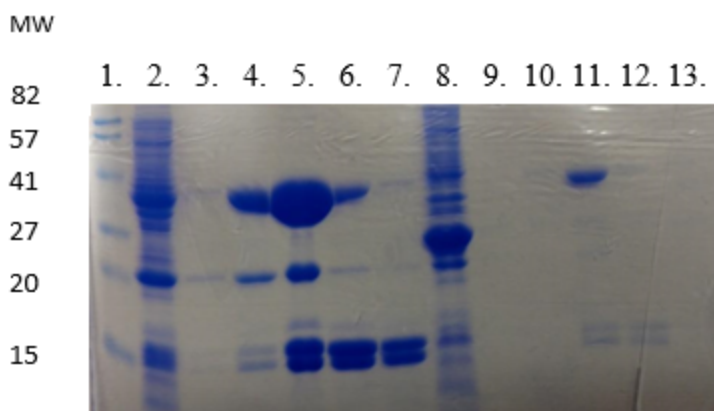
3.3. Results

3.3.1 Purity of recombinant N-protein and *E. coli* protein using SDS-PAGE

Each protein fraction separated by molecular weight using SDS-PAGE electrophoresis is shown in Figure 3.1. A fraction of *E.coli* protein was found after purification. (Figure 3.1, lane 11.). The purified *E.coli* without the recombinant N-protein had an *E. coli* protein that had the same molecular weight (MW) of approximately 38-40kDa than the recombinant N-protein (Figure 3.1, lane 11), similar to the MW of the recombinant N-protein (Figure 3.1, lane 5).

Figure 3.1. Stained SDS-PAGE gel fractions of recombinant N-protein purification and *E. coli* used for expression.

Notes: Recombinant N-protein MW is approximately 38-40kDa.



Left to Right

1. Ladder
2. Recombinant N-Protein: Post-sonicated/ Pre-Column
3. Recombinant N-protein: fraction 1
4. Recombinant N-protein: fraction 2
5. Recombinant N-protein: fraction 3
6. Recombinant N-protein: fraction 4
7. Recombinant N-protein: fraction 5
8. *E. coli* protein: Post-sonicated/ Pre-Column
9. *E. coli* protein: fraction 1
10. *E. coli* protein: fraction 2
11. *E. coli* protein: fraction 3
12. *E. coli* protein: fraction 4
13. *E. coli* protein: fraction 5

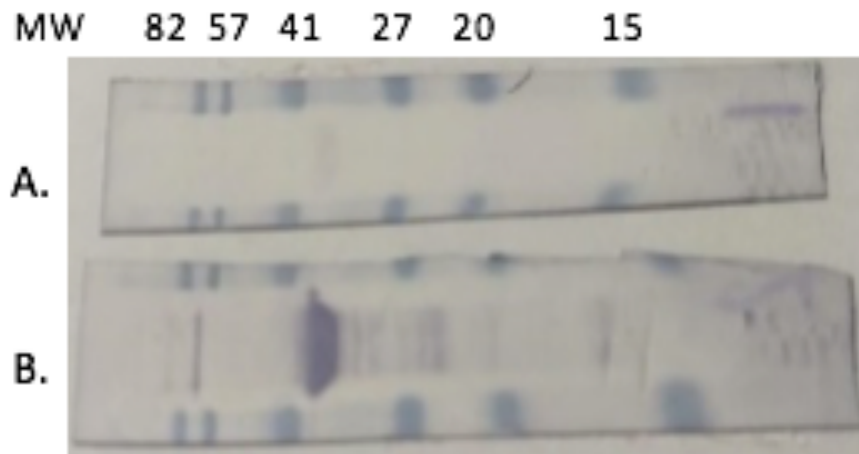
3.3.2. Western blot

3.3.2.1. Seropositive and seronegative status

Western blot membranes with positive and negative plasma samples are shown in Figure 3.2. Western blot assays using plasma from ABV positive Macaw showed a strong signal with a 38–40 kDa protein (Figure 3.2B). A minor to no signal was seen at this molecular weight in ABV negative Macaw plasma (Figure 3.2A).

Figure 3.2. Representative membranes of western blot results using A. negative and B. positive plasma.

Notes: Visual signal at 38–40kDa is for the recombinant N-protein.

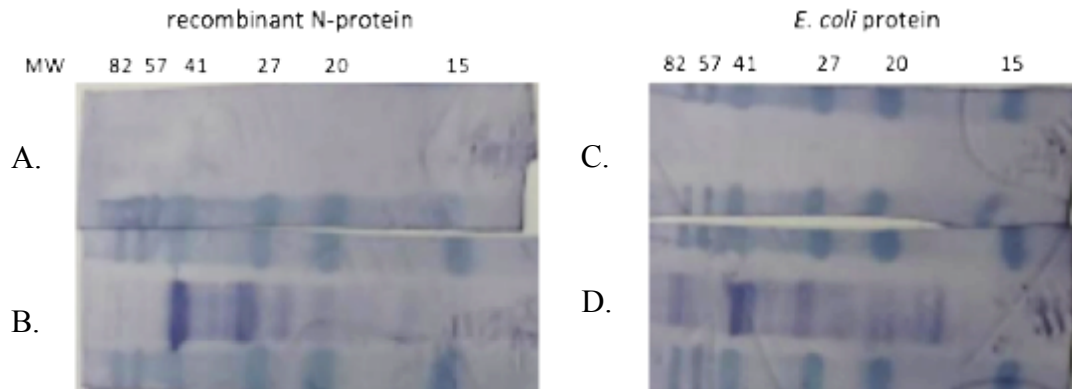


3.3.2.2. Purified recombinant N-protein and *E. coli* protein

A strong signal was detected for ABV N-protein antibodies when using recombinant N-protein in positive plasma (Figure 3.3B), while negative plasma showed slight to no signal (Figure 3.3A). Similarly, a strong signal was detected for *E. coli* antibodies in positive plasma when using *E. coli* protein (Figure 3.3D), but negative plasma resulted in a slight to no signal in the same test (Figure 3.3C).

Figure 3.3. Representative membranes of western blot results using recombinant N-protein with A. negative and B. positive plasma and *E. coli* protein with C. negative and D. positive plasma.

Notes: Recombinant N-protein MW is approximately 38-40kDa.



3.3.3. Dot-blot ELISA

Three sets of independent NC membrane strips were tested for all dot-blot ELISA studies. Digital images of all NC membranes strips for all dot-blot ELISA studies are found in APPENDIX A.

3.3.3.1. Study 1: Serial dilution of recombinant N-protein amounts per dot with three different plasma dilutions used for dot-blot ELISA at an incubation time of 10-minutes

A representation of the dot-blot ELISA signals, the ImageJ graphic results, and the signal intensity values generated for the dot reaction are shown in Figure 3.4. For each dot, three dot-signal intensity values were independently generated with Image J and a mean (\pm Std) dot-signal intensity value was reported.

Dot-blot ELISAs, which used ten-fold serial dilutions of recombinant N-protein and testing 1:100, 1:60, and 1:30 plasma dilutions are shown in Figure 3.5. No signal was detected for ABV antibodies in any of the negative plasma dilutions regardless of recombinant N-protein amounts of the ELISA.

In the positive plasma, no signal was detected for ABV antibodies at either 0.0014 μ g or 0.00014 μ g N-protein per dot. A minimally visible signal was observed with 0.014 μ g N-protein per dot. In both 1.4 μ g and 0.14 μ g N-protein per dot, a strong signal was detected.

Signal intensities derived from the reaction on the dot-blot ELISA differed significantly (Figure 3.6.). For positive plasma, the signal intensity values increased significantly ($P < 0.05$) as recombinant N-protein amount increased; there was no

significant difference between the two lowest amounts of recombinant N-protein. For positive plasma samples, there was no significant difference in the signal intensity within the recombinant N-protein amounts across plasma dilutions. For negative samples, the signal intensity of 1:100 and 1:60 dilutions assayed with 1.4 μg recombinant N-protein per dot were significantly greater ($P < 0.05$) than the signal intensity with the lower recombinant N-protein amounts.

Figure 3.4. Digital image analysis of dot-blot ELISA used to generate the signal intensity value. **Notes:** The delineated area of interest is highlighted in the red rectangle. The signal intensity values are graphically displayed using samples from study 1, with positive macaw plasma diluted to 1:100 and recombinant N-protein amounts of A. 1.4, B. 0.14, C. 0.014, D. 0.0014 and E. 0.00014 μg per dot.

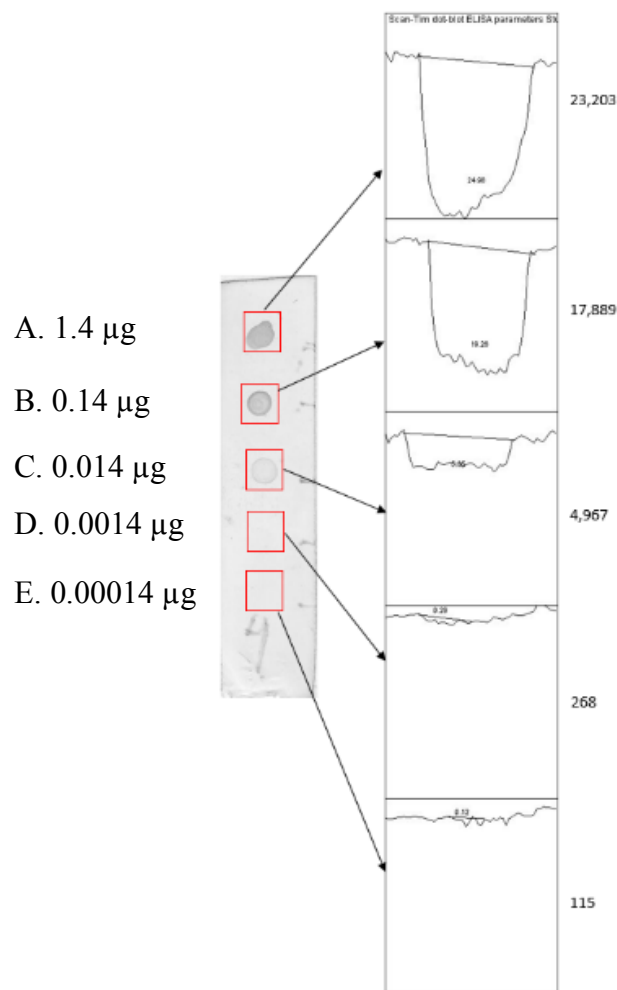


Figure 3.5. Representative membranes of dot-blot ELISA which used ten-fold serial dilutions of recombinant N-protein, 1.4, 0.14, 0.014, 0.0014 and 0.00014 μg per dot, testing 1:100, 1:60, and 1:30 plasma dilutions and incubated for 10-minutes.

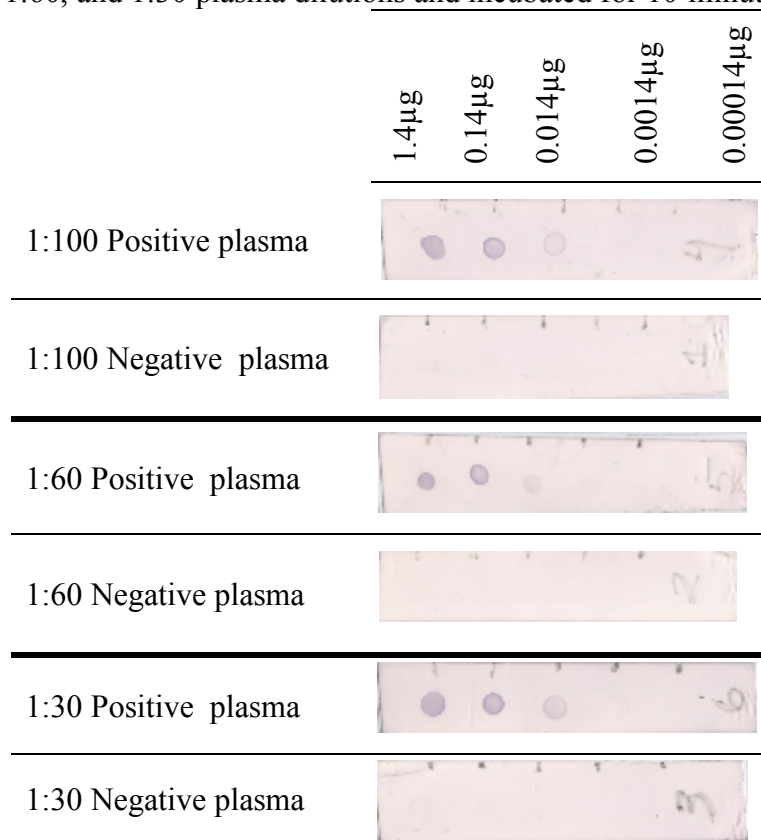
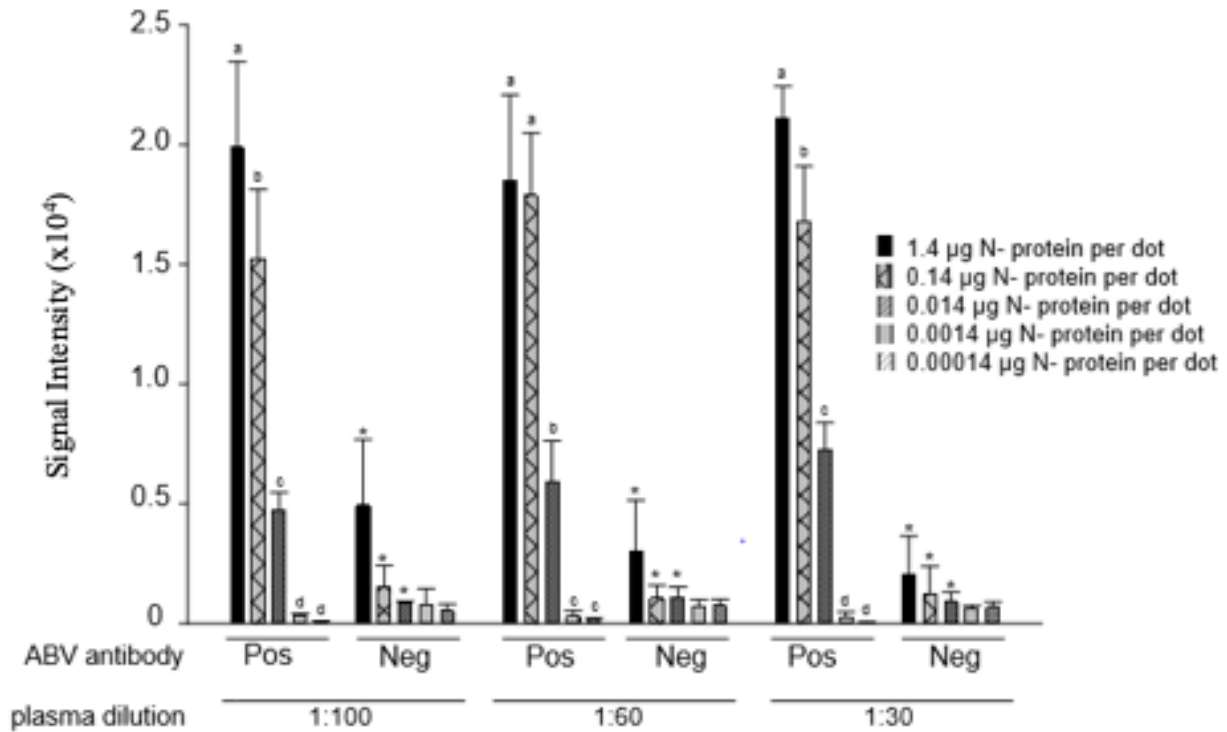


Figure 3.6. Mean (\pm Std) signal intensities of dot-blot ELISA which used ten-fold serial dilutions of recombinant N-protein, 1.4, 0.14, 0.014, 0.0014 and 0.00014 μ g per dot, testing 1:100, 1:60, and 1:30 plasma dilutions and incubated for 10-minutes.

Notes: Different superscript letter within plasma dilution group indicates significant difference ($P < 0.05$) between recombinant N-protein amounts.

An asterisk (*) indicates significant difference ($P < 0.05$) between positive and negative samples within the same plasma dilutions.



3.3.3.2. Study 2: Three different plasma dilutions and three different recombinant N-protein amounts per dot used for dot-blot ELISA at incubation times of 10-and 5-minutes

Dot-blot ELISAs, which tested 1:100, 1:60 and 1:30 plasma dilutions, used 0.15, 0.3 and 0.6 µg of recombinant N-protein per dot, and incubation times of 5- and 10-minutes are shown in Figure 3.7. Testing positive samples, a strong signal was detected for ABV antibodies with all plasma dilutions, at all recombinant N-protein amounts and at both incubation times. No signal was detected for ABV antibodies in negative plasma regardless of sample dilutions, recombinant N-protein amounts, or incubation time.

Signal intensities of the dot-blot ELISA, which tested 1:100, 1:60 and 1:30 plasma dilutions, used 0.15, 0.3 and 0.6 µg of recombinant N-protein per dot, and incubation times of 5- and 10-minutes are shown in Figure 3.8. For ELISAs incubated for 10 minutes, signal intensity for positive plasma did not significantly differ ($P < 0.05$) using 0.6 or 0.3 µg recombinant N-protein per dot within or between plasma dilutions. Signal intensity was significantly less ($P < 0.05$) with the use of 0.15 µg recombinant N-protein per dot within plasma dilutions.

Signal intensity of the plasma samples, regardless of plasma dilution, was significantly greater ($P < 0.05$) for all recombinant N-protein amounts when a 10-minutes compared to 5-minutes incubation was used.

For ELISAs incubated for 5 minutes, signal intensity did not significantly differ for the positive plasma dilutions between recombinant N-protein amounts.

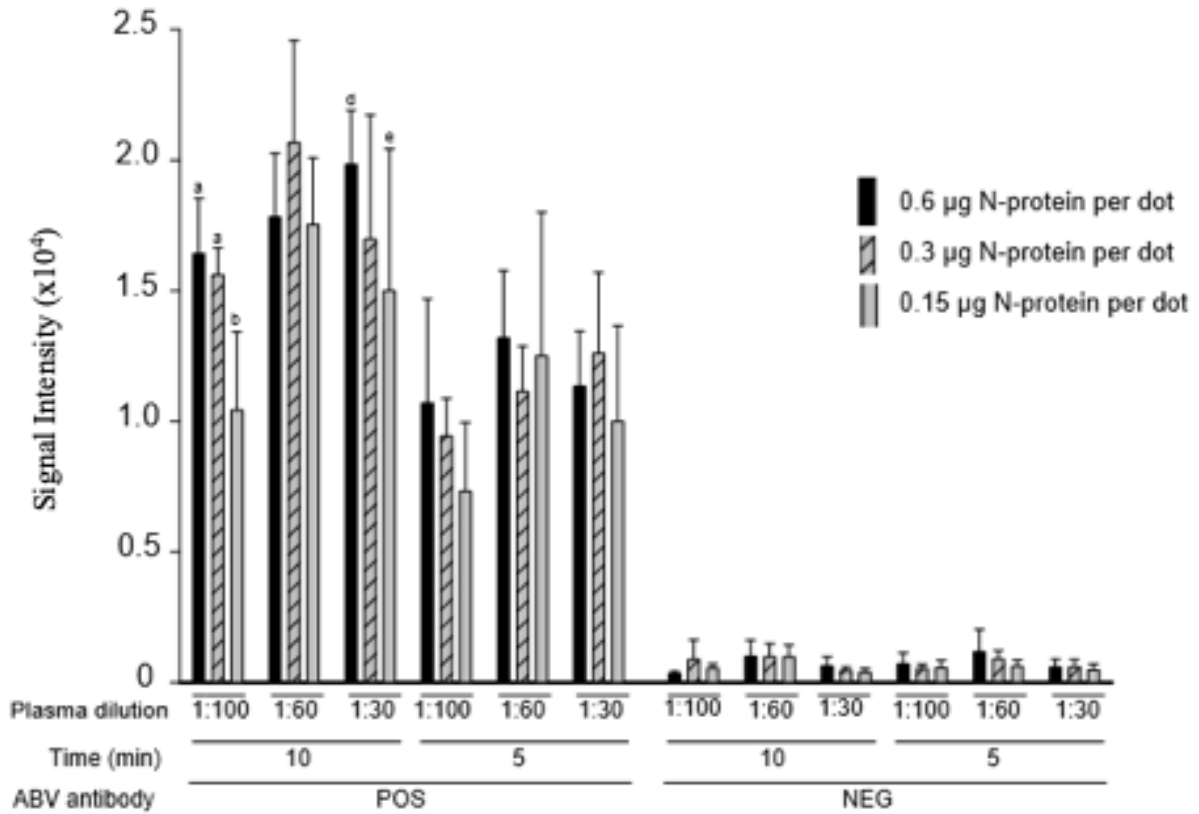
For the negative samples, signal intensity did not significantly differ between plasma dilutions, recombinant N-protein amounts, nor incubation times. There was a significant difference ($P < 0.05$) between all positive and negative paired samples.

Figure 3.7. Representative membranes of dot-blot ELISA which used 0.15, 0.3 and 0.6 μg of recombinant N-protein per dot, testing 1:100, 1:60 and 1:30 plasma dilutions, and incubation times of 5- and 10-minutes.

	0.6 μg	0.3 μg	0.15 μg	0.6 μg	0.3 μg	0.15 μg
1:100 Negative plasma						
1:100 Positive plasma						
1:60 Negative plasma						
1:60 Positive plasma						
1:30 Negative plasma						
1:30 Positive plasma						
	10-minute incubation			5-minute incubation		

Figure 3.8. Mean (\pm Std) signal intensities of dot-blot ELISA which used 0.15, 0.3 and 0.6 μ g of recombinant N-protein per dot, testing 1:100, 1:60 and 1:30 plasma dilutions, and incubation times of 5- and 10-minutes.

Notes: Different superscript letter within plasma dilution group indicates significant difference ($P < 0.05$) between recombinant N-protein amounts.



3.3.3.3. Study 3: Three different macaw plasma dilutions and three different recombinant N-protein amounts per dot used for dot-blot ELISA at an incubation times of 5-and 2-minutes

Dot-blot ELISAs, which used 0.3 and 0.6 µg of recombinant N-protein per dot, testing 1:60, 1:30 and 1:20 plasma dilutions, and incubation times of 2 and 5 minutes are shown in Figure 3.9. No signal was detected for ABV antibodies in the 1:60 and 1:30 negative plasma dilutions; a slight signal was observed with the 1:20 negative plasma dilution. For positive plasma, regardless of recombinant N-protein amount or plasma dilution, a stronger signal was detected with a 5-minute incubation than with a 2-minute incubation.

For positive plasma, signal intensity of the dot-blot ELISA using 0.6 and 0.3 µg recombinant N-protein, regardless of plasma dilution, was significantly higher ($P < 0.05$) for 5-minute than for 2-minute incubation (Figure 3.10). For positive plasma, there was no significant difference within or between plasma dilutions and recombinant N-protein per dot at 5-minute or at 2-minute incubations. There was a significant difference ($P < 0.05$) between positive and negative plasma tested under the same ELISA conditions and plasma dilutions.

Figure 3.9. Representative membranes of dot-blot ELISA which used 0.3 and 0.6 μg of recombinant N-protein per dot, testing 1:60, 1:30 and 1:20 plasma dilutions, and incubation times of 2- and 5-minutes.

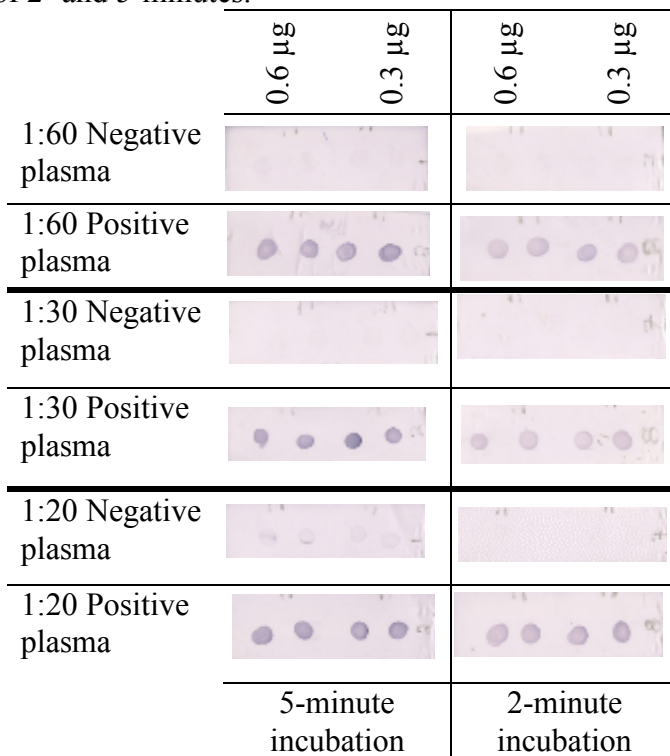
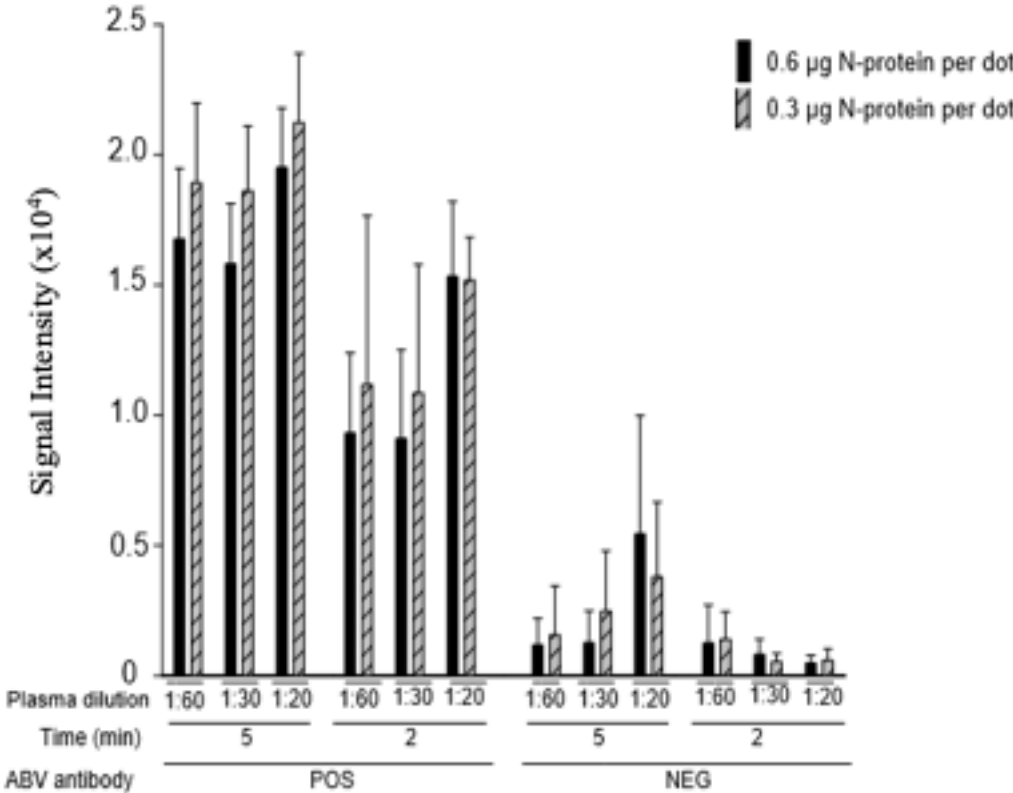


Figure 3.10. Mean (\pm Std) signal intensities of dot-blot ELISA which used 0.3 and 0.6 μ g of recombinant N-protein per dot, testing 1:60, 1:30 and 1:20 plasma dilutions, and incubation times of 2- and 5-minutes.



3.3.3.4. Study 4: Whole blood

Strong signals for ABV antibodies were detected using positive plasma at 1:60 dilution and whole blood at dilutions of 1:30 and 1:60 (Figure 3.11.). Positive whole blood at 1:100 had a distinct signal, but it was visibly less than the other positive samples. Negative samples had minimal to no signal and were visibly distinct from positive samples of the same dilution and sample matrix.

Signal intensities were not significantly different ($P < 0.05$) between positive 1:60 plasma dilution ($14,151 \pm 2,825$) and the positive whole blood dilution ($10,714 \pm 4,668$, $16,762 \pm 7,799$, and $16,046 \pm 185$ for the 1:100, 1:60 and 1:30 dilutions, respectively) (Fig. 3.12). There was a significant difference between positive 1:100 and 1:60 whole blood dilutions ($10,714 \pm 4,668$, $16,762 \pm 7,799$, respectively). There was no significant difference within the negative samples, but there was significant difference ($P < 0.05$) in the signal intensities between the positive and negative sample dilutions.

Figure 3.11. Representative membranes of dot-blot ELISA which used 0.3 μg of recombinant N-protein per dot, testing 1:60 plasma dilution and 1:100, 1:60 and 1:30 whole blood dilutions, and incubated for 5-minutes.

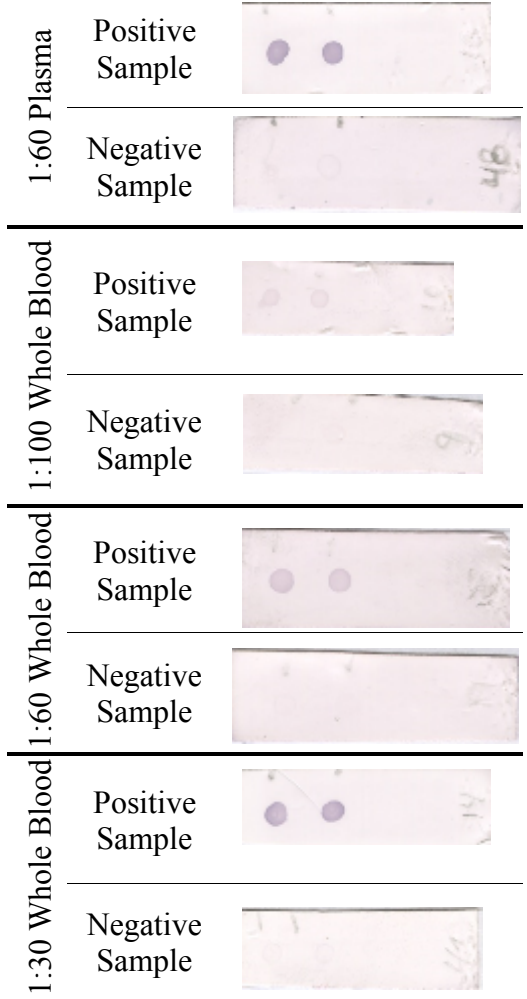
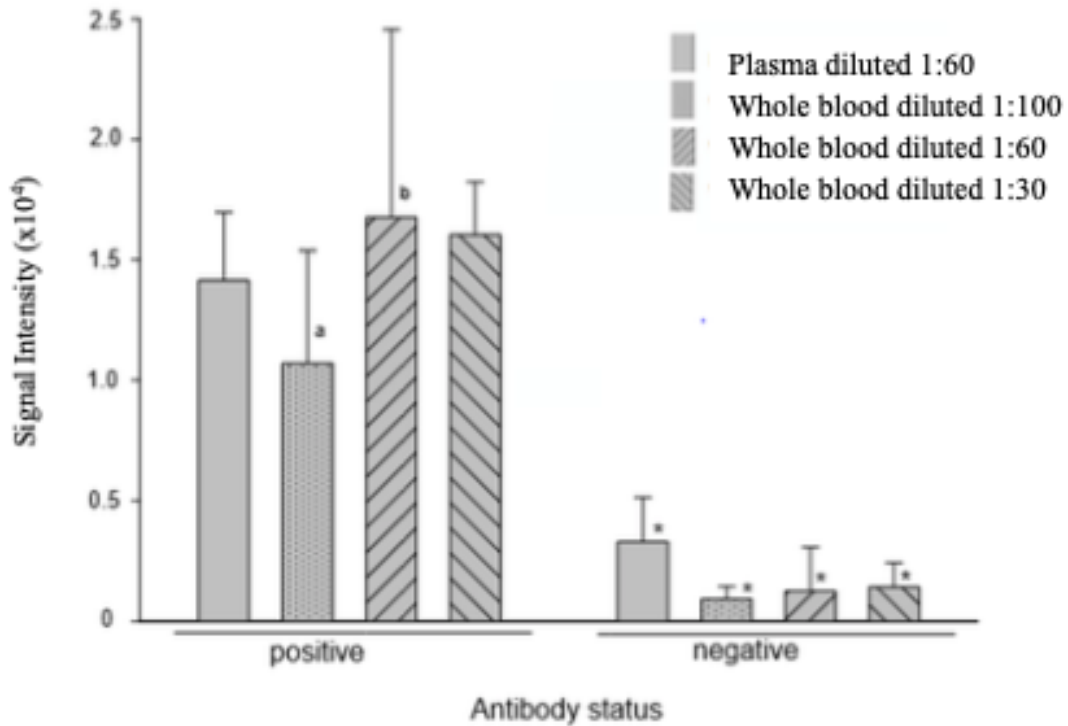


Figure 3.12. Mean (\pm Std) signal intensities of dot-blot ELISA which used 0.3 μ g of recombinant N-protein per dot, testing 1:60 plasma dilution and 1:100, 1:60 and 1:30 whole blood dilutions, and incubated for 5-minutes.

Notes: Different superscript letter indicated significant difference ($P < 0.05$) between whole blood dilutions.

An asterisk (*) indicates significant difference ($P < 0.05$) between positive and negative samples of the same matrix and dilution.



3.4. Discussion

The development of a rapid, dot-blot ELISA as a diagnostic assay for ABV would be useful for veterinary practitioners. This project developed a highly sensitive, rapid (<30 minutes run time) dot-blot ELISA to detect ABV antibodies in macaw blood or plasma. The dot-blot ELISA consisted of NC membrane dotted with 0.3 µg of recombinant N-protein and utilized a 1:50,000 dilution of an alkaline phosphatase conjugated anti-macaw IgY secondary antibody with two 5-minute incubations.

The target antigen amount, i.e. the recombinant N-protein dotted on the NC membrane, the sample dilution, and the incubation times were evaluated to optimize the dot-blot ELISA conditions. Dilution and type of secondary antibody remained constant: 1:50,000 of 1.0 mg/mL polyclonal IgG goat anti-macaw IgY-H+L conjugated with alkaline phosphatase. The use of the species-specific anti-IgY secondary antibody in a dot-blot ELISA performs better than commercial non-species specific secondary antibodies.²⁴ Anti-macaw IgY secondary antibody provides more accurate results in dot-blot ELISA than commercially available anti-chicken, anti-duck, and anti-bird IgY secondary antibodies.²⁴ The use of a species-specific anti-IgY secondary antibody was an important factor in optimizing the conditions of the dot-blot ELISA developed in this study because the assay was designed mainly for testing psittacines, which are the principle birds infected with ABV.

In our assay, recombinant N-protein was selected as the target antigen because N-protein is the immunodominant protein in ABV infections and the preferred antigen for use in microtiter plate ELISA.¹¹ Nucleoprotein use in immunologic assays has cross-

reactivity across ABV genotypes,²⁰ thus is a useful target antigen for immunological diagnostic assays like the ELISA. In determining the amount of recombinant N-protein to use for the dot-blot ELISA, signal intensity and visibility with positive and negative samples, background noise and specificity of reaction, and cost were considered. Recombinant N-protein amounts of ≤ 0.014 μg per dot resulted in minimal to no signal detection (Figure 3.6.). While 1.4 and 0.14 μg recombinant N-protein per dot gave strong visible signals and high signal intensity values with positive samples, the signal for the negative samples was greatest with 1.4 μg recombinant N-protein amounts. This could result in false positive reactions. Thus, recombinant N-protein amounts of 0.6, 0.3, and 0.15 μg were investigated. Recombinant N-protein 0.6 μg and 0.3 μg per dot had strong signal intensities with 10-, 5-, and 2-minute incubations, while signal intensity with 0.15 μg N-protein per dot was significantly less. With no significant difference in signal intensity nor visual reaction, 0.3 μg recombinant N-protein per dot was deemed optimal for the dot-blot ELISA because of the potential cost efficiency, dearth of false positives at plasma dilutions and incubation times used, and lack of background interference by *E. coli* protein.

Sampling volume is always a consideration in patients presented with clinical signs of PaBVs, especially in the lethargic bird.^{25,26} We evaluated different sample dilutions with the dot-blot ELISA to determine the minimal amount of sample volume that would give quality results. Signal intensity for plasma dilutions of 1:60 and 1:30 did not significantly differ from the higher dilution of 1:100 when used with 0.3 and 0.6 μg of recombinant N-protein (Figure 3.8), however the 1:100 dilution produced a visually

less intense signal (Figure 3.7). Conversely, the less dilute sample of 1:20 gave equivalent signal reaction with positive samples, but produced higher level of background noise that was deemed unacceptable (Figure 3.9 and 3.10). Plasma dilution 1:60 was chosen as standardized condition for dot-blot ELISA, which for the 3.0 mL of diluted plasma used in the assay would be 0.05 mL of plasma. The use of this minimal amount would provide adequate additional plasma to be used for other assays.

The use of whole blood in the dot-blot ELISA would be advantageous, as this would reduce sample processing and decrease the time to run the test. These are beneficial for rapid, point-of-care assays. Results using whole blood were not statistically different from plasma. Since the PCV of our birds was approximately 50%, the amount of antigen in the sample was approximately 50%, which made the whole blood dilutions of 1:30, 1:60, and 1:100 approximately equal to serum sample dilutions of 1:60, 1:120, and 1:200, respectively. Our results indicate that this difference in antibody levels would not be a factor and that either diluting a 0.05 or 0.1 mL sample of whole blood at a 1:60 dilution would give a similar sensitivity. Conversely, whole blood, in addition to plasma, also contains red blood cells, white blood cells, and thrombocytes, which could cause non-specific reactions or background staining of the NC membrane that could cause decreased specificity and increased false positive results. This is reported with ELISAs for feline leukemia virus (FeLV).^{27,28} In our study, there were no non-specific reactions or background staining for the negative samples. The numerous washes most likely reduced non-bound substances, such as hemoglobin and other cell constituents. Additionally, the FeLV ELISA is testing for FeLV antigens in the blood,

where our ELISA was testing for antibodies. In the FeLV ELISA a non-specific antigen in whole blood interacts with the anti-FeLV antibodies of the test.²⁷⁻²⁹

Results from a patient-side assay need to be obtained in a timely manner; the shorter the better. Our ELISA utilized two incubations; thus, the determination of the shortest incubation time is useful. Signal intensities with 5-minute incubations were significant less than 10-minute incubations (Figure 3.8), although visual signals for the 1:60 and 1:30 dilutions were difficult to differentiate (Figure 3.7). Visual signals for the 5-minute incubations were much stronger than those with a 2-minute incubation (Figure 3.10), making 5-minute incubations optimal for the dot-blot ELISA. Utilizing 5-minute incubations the dot-blot ELISA has a run-time of <30 minutes, making it applicable for a rapid point-of-care diagnostic assay. If a further reduction in run-time is need, modifications in the amount of recombinant N-protein amounts per dot and plasma dilutions can be evaluated.

Background noise in all tests also must be considered. In this study, faint signals were observed in the negative samples (Figure 3.2A and 3.3A). This background signal was likely due to *E. coli* proteins on the NC membrane interacting with antibodies in the samples. Whole cell lysates of *E. coli*, such as was done when producing the recombinant N-protein, have MW ranging from 25 – 500 kDa³⁰ and in our study, *E. coli* proteins of 38-41 kDa were identified by SDS-PAGE (Figure 3.1 lane 11). This MW, 38-41 kDa, is also the MW of the recombinant N-protein. Antibodies against *E. coli* are found in human serum and can cause background noise in serologic assays that use recombinant proteins.^{31,32} Similar studies in birds show non-specific signals due to *E.*

coli antibodies in plasma samples interacting with recombinant *E. coli* antigens in serologic tests.^{33,34} Affinity purification of the His-tagged recombinant N-protein with the Ni-NTA Agarose column did not remove all *E. coli* antigens from the recombinant *E. coli*/N-protein solution, as exhibited in Figure 3.3. *E.coli* proteins can have some histidine conformation or during the generation of the recombinant N-protein, some His-tagged *E.coli* proteins may have been generated with the insertion of the pET21a vector into the *E. coli*. Hence, some *E. coli* antigens were likely present in the recombinant N-protein solution blotted on the NC membrane strips and able to react with antibodies in the sample, consequently causing background noise in both the western blot and dot-blot ELISA.

To reduce non-specific signals and background noise in the assay, procedures that would adsorb or neutralize *E. coli* antibodies in plasma samples or that would increase the purity of the recombinant N-protein antigen could be investigated. However even without these additional procedures, optimizing the conditions for running the dot-blot ELISA readily decreases this non-specific background noise.

With the Western blot and SDS-PAGE, bands at approximately 17, 27, and 30 kDa were observed in addition to the recombinant N-protein band at 38-40 kDa (Figure 3.1, Figure 3.2 and Figure 3.3). These bands likely represent denatured recombinant N-protein or *E. coli* protein. In the dot-blot ELISA, all these denatured proteins are in the blotted dot along with the target antigen and available to react with the sample. Thus, the multiple antigen-antibody bindings with the many N-protein epitopes would impart a higher avidity for the ELISA producing a greater dot visibility and signal intensity

in an antibody positive sample.

3.5. Conclusion

A highly sensitive, rapid (<30 minutes run time) dot-blot ELISA was developed for the detection of ABV antibodies in macaws. Using 1:60 dilution of whole blood or plasma, the sample was incubated for 5-minutes with a NC membrane dotted with 0.3 µg of recombinant N-protein and then the NC membrane was incubated for 5-minutes with a 1:50,000 dilution of a alkaline phosphatase conjugated anti-macaw IgY secondary antibody. This dot-blot ELISA may be a useful rapid patient-side assay for assessing ABV exposure of birds, providing veterinarians and aviculturists information with which to develop appropriate biosecurity measures.

3.6. References

1. Kistler AL, Gancz A, Clubb S, et al. Recovery of divergent avian bornaviruses from cases of proventricular dilatation disease: Identification of a candidate etiologic agent. *J Virol.* 2008;5:88–102.
2. Honkavuori KS, Shivaprasad HL, Williams BL, et al. Novel borna virus in psittacine birds with proventricular dilatation disease. *Emerg Infect Dis.* 2008;14(12):1883–1886.
3. Gray P, Hoppes S, Suchodolski P, et al. Use of avian bornavirus isolated to induce proventricular dilatation disease in conures. *Emerg Infect Dis.* 2010;16(3):473–479.

4. Rinder M, Ackermann A, Kempf H, et al. Broad tissue and cell tropism of avian bornavirus in parrots with proventricular dilatation disease. *J Virol*. 2009;83(11):5401–5407.
5. Rubbenstroth D, Rinder M, Stein M, et al. Avian bornaviruses are widely distributed in canary birds (*Serinus canaria* f. domestica). *Vet Microbiol*. 2013;165(3-4):287–295.
6. Delnatte P, Mak M, Ojkic D, et al. Detection of avian bornavirus in multiple tissues of infected psittacine birds using real-time reverse transcription polymerase chain reaction. *J Vet Diagn Invest*. 2014;26(2):266–271.
7. Raghav R, Taylor M, Delay J, et al. Avian bornavirus is present in many tissues of psittacine birds with histopathologic evidence of proventricular dilatation disease. *J Vet Diagn Invest*. 2010;22(4):495–508.
8. Leal de Araujo J, Rech RR, Heatley JJ, et al. From nerves to brain to gastrointestinal tract: A time-based study of parrot bornavirus 2 (PaBV-2) pathogenesis in cockatiels (*Nymphicus hollandicus*). *PLoS One*. 2017;12(11):e0187797.
9. Fluck A, Enderlein D, Piepenbring A, et al. Correlation of avian bornavirus-specific antibodies and viral ribonucleic acid shedding with neurological signs and feather-damaging behavior in psittacine birds. *Vet Rec*. 2019;184(15):476–482.

10. de Kloet SR, Dorrestein GM. Presence of avian bornavirus RNA and anti-avian bornavirus antibodies in apparently healthy macaws. *Avian Dis.* 2009;53(4):568–573.
11. de Kloet AH, Kerski A, de Kloet SR. Diagnosis of avian bornavirus infection in psittaciformes by serum antibody detection and reverse transcription polymerase chain reaction assay using feather calami. *J Vet Diagn Invest.* 2011;23(3):421–429.
12. Weissenböck H, Fragner K, Nerdorost N, et al. Localization of avian bornavirus RNA by in situ hybridization in tissues of psittacine birds with proventricular dilatation disease. *Vet Microbiol.* 2010;145(1-2):9–16.
13. Delnatte P, Nagy E, Ojkic D, et al. Avian bornavirus in free-ranging waterfowl: prevalence of antibodies and cloacal shedding of viral RNA. *J Wildl Dis.* 2014;50(3):512–523.
14. Heatley JJ, Villalobos AR. Avian bornavirus in the urine of infected birds. *Vet Med Res Rep.* 2012;3:19–23.
15. Kistler AL, Smith JM, Alexander L, et al. Analysis of naturally occurring avian bornavirus infection and transmission during an outbreak of proventricular dilatation disease among captive psittacine birds. *J Virol.* 2010;84(4):2176–2179.
16. Rubbenstroth D, Schmidt V, Rinder M, et al. Phylogenetic analysis supports horizontal transmission as a driving force of the spread of avian bornavirus. *PLoS One.* 2016;11(8):e0160936.

17. Herzog S, Enderlein D, Heffels-Redmann U, et al. Indirect immunofluorescence assay for *Intra Vitam* diagnosis of avian bornavirus infected in psittacine birds. *J Clin Microbiol.* 2010;48(6):2282–2284.
18. Villanueva I, Grey P, Mirhosseini N, et al. The diagnosis of proventricular dilatation disease: Use of a Western blot assay to detect antibodies against avian Borna virus. *Vet Microbiol.* 2010;143(2-4):196–201.
19. Lierz M, Hafez HM, Honkavuori KS, et al. Anatomical distribution of avian bornavirus in parrots, its occurrence in clinically healthy birds and ABV-antibody detection. *Avian Pathol.* 2009;38(6):491–496.
20. Zimmermann V, Rinder M, Kaspers B, et al. Impact of antigenic diversity on laboratory diagnosis of avian bornavirus infections in birds. *J Vet Diagn Invest.* 2014;26(6):769–777.
21. Guo J, Payne S, Zhang S, et al. Avian bornaviruses: diagnosis, isolation, and genotyping. *Curr Protoc Microbiol.* 2014;34:15i.1.11.11–15i.1.11.33.
22. Wild D. The Immunoassay Handbook: Theory and Applications of Ligand Binding, ELISA and Related Techniques. *Elsevier Science Technol.* 2013. ProQuest. Ebook Central.
<http://ebookcentral.proquest.com/lib/tamumebooks/detail.action?docID=1117226>
23. Hameed SS, Guo J, Tizard I, et al. Studies on immunity and immunopathogenesis of parrot bornaviral disease in cockatiels. *Viol.* 2018;515:81-91.

24. Escandon P, Heatley JJ, Bergman LR, Tizard I, Musser JMB. Comparison of anti-avian IgY secondary antibodies used in western blot and dot-blot ELISA to select avian bornavirus antibodies in four different birds species. *Vet Med: Res and Rep.* 2019;10:141-150.
25. Rossi G, Dahlhausen RD, Galosi L, Orosz SE. Avian ganglioneuritis in clinical practice. *Vet Clin: Exot Anim Pract.* 2018;21(1):33–67.
26. Hoppes S, Tizard I, Shivaprasad HL. Avian Bornavirus and proventricular dilatation disease: diagnostics, pathology, prevalence, and control. *Vet Clin Exot Anim.* 2013;16(2):339–355.
27. Hawks DM, Legendre AM, Rohrbach BW. Comparison of four test kits for feline leukemia virus antigen. *J Am Vet Med Assoc.* 1991;199(10):1373–1377.
28. Westman ME, Malik R, Hail E, et al. Comparison of three feline leukemia virus (FeLV) point-of-care antigen test kits using blood and saliva. *Comp Immunol Microbiol Infect Dis.* 2017;50:88–96.
29. Hartmann K, Werner RM, Egberink H, et al. Comparison of six in-house tests for the rapid diagnosis of feline immunodeficiency and feline leukaemia virus infections. *Vet Rec.* 2001;149(11):317–320.
30. Chong BE, Wall DB, Lubman DM, Flynn SJ. Rapid profiling of *E. coli* proteins up to 500 kDa from whole cell lysates using matrix-assisted laser desorption/ionization time-of-flight mass spectrometry. *Rap Comm Mass Spectro.* 1997;11(17):1900–1908.

31. Yip CW, Hon CC, Zeng F, et al. Naturally occurring anti-*Escherichia coli* protein antibodies in the sera of healthy humans cause analytical interference in a recombinant nucleocapsid protein-based enzyme-linked immunosorbent assay for serodiagnosis of severe acute respiratory syndrome. *Clin Vaccine Immunol.* 2007;14:99–101.
32. Hernandez P, Heimann M, Riera C, et al. Highly effective serodiagnosis for Chagas' disease. *Clin Vaccine Immunol.* 2010;17:1598–1604.
33. Hadifar F, Ignjatovic J, Tarigan S, et al. Multimeric recombinant M2e protein-based ELISA: A significant improvement in differentiating avian influenza infected chickens from vaccinated ones. *PLoS One.* 2014;9:e108420.
34. Zhao S, Jin M, Li H, et al. Detection of antibodies to the nonstructural protein (NS1) of avian influenza viruses allows distinction between vaccinated and infected chickens. *Avian Dis.* 2005;49:488–493.

4. PROOF OF CONCEPT FOR A DOT-BLOT ENZYME IMMUNOSORBENT ASSAY TO DETECT AVIAN BORNAVIRUS IMMUNOGLOBULINS

4.1. Introduction

In 2008, avian bornavirus (ABV) was first determined as the causative agent of parrot bornavirus syndrome (PaBVs), with neurological and gastrointestinal involvement, in parrots.^{1,2} Parrot bornavirus syndrome clinical signs vary and likely depend on avian species and lesion distribution, however clinical signs generally include ataxia, seizures, blindness and gastrointestinal dysfunction, which leads to starvation and death.^{3,4} Necropsy, histology, reverse transcriptase polymerase chain reaction (RT-PCR) and immunodiagnostics are used to diagnose PaBVs post mortem. Histopathology findings in ABV infections include lymphoplasmacytic meningoencephalomyelitis and ganglioneuritis in the central, peripheral and/or autonomic nervous system.⁵⁻⁸ Avian bornavirus mRNA and antigens are detected in tissues and less invasive samples such as feather follicles, urofeces and cloacal swab by RT-PCR.^{6, 8-14}

Western blot, immunofluorescence and plate-based enzyme-linked immunosorbent assays (ELISA) are laboratory diagnostic assays used to detect antibody production against the ABV.^{12,14-20} A rapid point-of-care diagnostic assay to detect ABV antibodies is not commercially available but would be advantageous in early detection of infection before overt disease develops or to determine vaccination status.

An accurate and rapid diagnosis of ABV infection is important in making appropriate decisions on management, therapeutics and biosecurity practices for

veterinarians and pet owners. The purpose of this study is to evaluate a dot-blot ELISA performance and compare to the western blot, the current gold standard for antibody detection.

4.2. Material and methods

4.2.1. Animals and sample collection

The experimental protocol was reviewed and approved by the Texas A&M University Bio-safety and Animal Use Committees (IACUC 2016-0054), which complies with guidelines included in the National Research Council of the National Academies' publication *Guide for the Care and Use of Laboratory Animals*, 8th edition. Blood samples were collected from 18 Monk parakeets that were assigned into four groups: Group 1 (control) - three Monk parakeets unexposed to vaccine and not inoculated with Parrot Bornavirus-2 (PaBV-2); Group 2 (vaccinated) - five Monk parakeets vaccinated with recombinant nucleoprotein (N-protein); Group 3 (vaccinated/PaBV-2 inoculated) - four Monk parakeets vaccinated with recombinant N-protein and experimentally inoculated with PaBV-2; and, Group 4 (PaBV-2 inoculated) - six Monk parakeets experimentally inoculated with PaBV-2. Monk parakeets were housed with a light-dark cycle of 12-hours and a room temperature of 21°C (± 5.0), at the Schubot Exotic Bird Health Center aviary, College of Veterinary Medicine and Biomedical Sciences. Each bird was fed 1/6 cup per bird of premium daily FruitBlend (ZuPreem®, Shawnee, KS, USA), and had access to tap water ad libitum.

Blood samples in volume equivalent to 1% body weight were collected by jugular venipuncture. Blood was collected into lithium heparin tubes and stored at 4°C

prior to centrifugation at 5,000 x g for 10-minutes. Plasma was collected and stored at -20°C prior to analysis. Twelve blood samples were collected per bird; one sample at pre-vaccination time, four samples at post-vaccination time, and seven samples at post-inoculation time. All groups were sampled whether or not the group actually was being vaccinated or experimentally inoculated.

4.2.2. Recombinant nucleoprotein expression and purification

Recombinant N-protein, purified from *E. coli*, was produced following the method of Hameed et al (2018).²¹ Briefly, the procedure was as follows. Total RNA was extracted from frozen brain tissue of a Yellow-collared macaw (*Primolius auricollis*) infected with PaBV-4 using Qiagen RNeasy Mini kit (Qiagen, Hilden, Germany). The RNA was used to generate cDNA using reverse transcription kits (High Capacity Reverse Transcription Kit, Applied Biosystems, Foster City, CA, USA) and random hexamers. Subsequent PCR was performed to amplify the N-protein gene with primers Forward 5'-CATG CAT ATG CCA CCC AAG AGA CAA AGA AGC-3' and Reverse 5'-GTAC CTC GAG GTT TGC GAA TCC GGT TAC ACC-3'. The resulting PCR products were cloned, sequenced, and inserted into pET21a vector to generate a His-tagged fusion protein for expression in *E. coli* (Rosetta, Sigma-Aldrich, St. Louis, MO, USA). Recombinant *E. coli* was incubated for 12 hours in Luria broth fortified with ampicillin; the culture was continuously mixed at 150 rpm at room temperature. Recombinant *E. coli* was transferred to fresh media of Luria broth, ampicillin, and Isopropyl β -D-1-thiogalactopyranoside to induce protein expression and incubated for 6 hours, while being continuously stirred at 200 rpm at room temperature. The solution

was centrifuged at 3,500 x g for 30-minutes and the supernatant was removed. The bacterial pellet was resuspended in 40 mL of phosphate-buffered saline (PBS) and sonicated for 3 sets of 8-minutes to lyse the bacteria. The sonicated solution was then centrifuged at 12,000 x g for 20-minutes at 4°C. The supernatant was loaded on a Qiagen Ni-NTA Agarose column (Qiagen, Hilden, Germany), which had been pre-conditioned with 10 mL of binding buffer (20 mM sodium phosphate, 300 mM NaCl, pH 7.4, 10 mM imidazole); the Ni-NTA Agarose column has a high affinity for His-tagged proteins. Ten mL of wash buffer (20 mM sodium phosphate, 300 mM NaCl, pH 7.4, 20mM imidazole) was loaded on the column and allowed gravity flow. The column was then eluted by gravity flow with 10 mL of elution buffer (20 mM sodium phosphate, 300 mM NaCl, pH 7.4, 200 mM imidazole) and the elutant was collected in 1.0 mL fractions. The purity of each protein fraction was determined by sodium dodecyl sulfate polyacrylamide gel (SDS-PAGE) electrophoresis. Fractions containing the N-protein were combined and an Amicon Ultra 15 mL centrifugal filter (Millipore Sigma, Burlington, MA, USA) was used to concentrate the N-protein in 1.0 mL PBS. Finally, the protein concentration was measured using BCA™ Protein Assay Kit (Thermo Scientific™ PIERCE™, Waltham, MA, USA). Recombinant N-protein was stored at -20°C. Prior to use for vaccination or immunoassay, it was placed in a 37 °C waterbath until thawed.

4.2.3. Recombinant nucleoprotein vaccination

Recombinant N-protein vaccine was produced according to Hameed et al (2018).²¹ In brief, each recombinant N-protein vaccine dose was made 30-minutes prior to administering vaccine. Each 100 µL dose contained 25 µg recombinant N-protein and

0.5% alum (Invitrogen, Thermo Fisher Scientific™ PIERCE™, Waltham, MA, USA) in PBS.

Birds from Groups 2 and 3 were vaccinated with 100 µL dose of recombinant N-protein vaccine via left pectoral intramuscular injection. Vaccine boosters were administered by left pectoral intramuscular injection at 1 and 7 months after the initial vaccination.

4.2.4. Parrot bornavirus-2 inoculation

Parrot bornavirus-2 was isolated from the brain of experimentally infected Cockatiels (*Nymphicus hollandicus*).²² Virus for inoculation was grown as previously described.²³ Briefly, duck embryo fibroblast cell cultures were inoculated with stock virus and maintained in Dulbecco's modified eagle medium (Gibco®, Life Technologies Co., Thermo Fisher Scientific, Waltham, MA, USA) with 10% fetal bovine serum (Gibco®, Life Technologies Co.) at 37 °C in an atmosphere of 5% CO₂. After 3 days of incubation, cells were harvested, divided into 1.0 mL of aliquots and stored -80°C. Virus was confirmed as PaBV-2 by RNA extraction and RT-PCR analysis followed by sequence analysis of the PCR product, as described in Guo et al (2014) according to basic protocols 3 and 10.²³

Birds from Group 3 and 4 were inoculated by right pectoral intramuscular administration with 8×10^5 focus forming units (FFU) of PaBV-2 one month after the first vaccine booster. This method has previously induced PaBVs in cockatiels.^{8,22}

4.2.5. Western blot

Western blot assays were performed according to basic protocol 5, Guo et al (2014),²³ with the following modifications to detect N-protein antibodies. Briefly, 0.1 mg/mL of recombinant N-protein solution was mixed at a 1:1 ratio with gel loading buffer and boiled in a water bath for 3-minutes. Then 15 μ L of the boiled sample was loaded into each SDS-PAGE gel wells, separated using SDS-PAGE and electrophoretically transferred to a polyvinylidene difluoride (PVDF) membrane. The PVDF membrane was incubated in 5% dried skim milk/0.05% Tween/0.02M PBS overnight at room temperature. The membrane was then incubated for 2 hours with sample plasma that had been diluted 1:200 with 3.0 mL of 2% dried skim milk/0.05% Tween/0.02M PBS; this was followed with three 15-minute rinses of 0.05% Tween/0.02M PBS. The membrane was then incubated for 1 hour with 1:50,000 dilution of polyclonal IgG goat anti-macaw IgY-H+L conjugated with alkaline phosphatase, 1.0 mg/mL (anti-macaw IgY secondary antibody) (Bethyl A140-116AP, Bethyl Laboratories, Inc., Montgomery, TX, USA), in 3.0 mL of 2% dried skim milk/0.05% Tween/0.02M PBS. This was followed by three 15-minute rinses with 0.05% Tween/0.02M PBS. The membrane was then incubated for approximately 5-minutes, or until color change was observed, in a 5-bromo-4-chloro-3-indolyl phosphate (BCIP)/nitro blue tetrazolium (NBT) solution (SigmaFast BCIP/NBT substrate tablet, Sigma Aldrich, St. Louis, MO, USA) dissolved in 10 mL ultra-pure water. Finally, the membrane was rinsed with ultra-pure water.

Representative membranes of Western blot results for each of the Monk parakeet plasma samples are found in APPENDIX B.

4.2.6. Dot-blot enzyme-linked immunosorbent assay

The nitrocellulose (NC) membrane strip was blotted twice with 2.0 μ L of 0.15 mg/mL recombinant N-protein solution and allowed to air dry for 5-minutes. After air drying for 5-minutes, the NC membrane was incubated in 5% skim dried milk/ 0.05% Tween/0.02M PBS overnight at room temperature. The NC membrane strip was incubated for 5-minutes with plasma diluted 1:60 with 3.0 mL 2% dried skim milk/0.05% Tween/0.02M PBS solution, followed by three 1-minute rinses with 3.0 mL of 0.05% Tween/0.02M PBS. The membrane was then incubated for 5-minutes with 1:50,000 dilution of 1.0 mg/mL anti-macaw IgY secondary antibody conjugated with alkaline phosphatase in 3.0 mL of 2% dried skim milk/0.05% Tween/0.02M PBS. This was followed by three 1-minute rinses with 0.05% Tween/0.02M PBS. The membrane was then incubated for 5-minutes in a solution containing SigmaFast BCIP/NBT substrate tablet dissolved in 10 mL ultra-pure water. Finally, the membrane was rinsed with ultra-pure water.

The dot-blot ELISAs were scored as zero for no visual signal detected, one for a poor visual signal detected, two for a weak visual signal detected, three for a fair signal detected or four for a strong signal detected. To score all dot-blot ELISA membranes a reference membrane was chosen for each scoring digit (Figure 4.1.). Representative membranes of dot-blot ELISA results for each of the Monk parakeet plasma samples are found in APPENDIX B.

Figure 4.1. Dot-blot ELISA reference membranes scored zero to four.

Notes: 0 = no visual signal detected, 1 = poor visual signal detected, 2 = weak visual signal detected, 3 = fair visual signal detected and 4 = strong visual signal detected.



4.2.7. Digital images

Membranes were scanned using an Epson Expression 100000 XL flatbed scanner with 300 dpi resolution and saved in a.jpeg digital image format.

4.2.8. Statistical analysis

Performance parameters were determined for the dot-blot ELISA with 4 separate scenarios: all samples; samples from controls and vaccinated birds; samples from controls and inoculated birds; and, samples from controls and inoculated birds ≥ 3 weeks post-inoculation. Tables representing scenarios: samples from controls and vaccinated birds; samples from controls and inoculated birds; and, samples from controls and inoculated birds ≥ 3 weeks post-inoculation are found in APPENDIX B. For each scenario, a 2 X 2 table was constructed to determine sensitivity and specificity of the dot-blot ELISA, with true positives being both ELISA and western blot positive and true negatives being both ELISA and western blot negative, and 95% confidence intervals were calculated (MedCalc®, Oostende, Belgium).

Receiver operating characteristic (ROC) curves (true positive percentage against false positive percentage or sensitivity against 1-specificity) for each of the 4 scenarios were plotted and used to determine the sensitivity, specificity, and accuracy and area under the curve (AUC) at the optimal cut-off value for a positive dot-blot ELISA (Eng J. ROC analysis, Johns Hopkins University:, <http://www.jrocf.it.org>).²⁴ The AUC measurement identified the ability of the dot-blot ELISA, fail (AUC = 0.5), poor ($0.5 < \text{AUC} \leq 0.7$), good ($0.7 < \text{AUC} \leq 0.9$), and excellent ($0.9 < \text{AUC} < 1$), to discriminate truly uninfected from truly infected birds.²⁵ The accuracy of the dot-blot ELISA was

displayed in a dot diagram where data of the true negative and positive groups are dots on two vertical axes.

4.3. Results

4.3.1. Western blot

Western blot results using 216 Monk parakeet plasma samples grouped by: control, vaccinated, vaccinated/ PaBV-2 inoculated, and PaBV-2 inoculated are shown in Table 4.1. The recombinant N-protein signal was located at approximately 38-40kDa. Western blot results were positive if there was a strong visual signal detected at approximately 38-40kDa. No signal was detected one week prior to vaccination for all 18 Monk parakeets. No signal was observed for any of the samples collected from the Group 1, control Monk parakeets.

Following the first round of vaccination, a visual signal was observed two-weeks post-vaccination in 7 of 9 vaccinated Monk parakeets in Groups 2 and 3. A visual signal was detected in 9 of 9 vaccinated Monk parakeets in Groups 2 and 3 at four-weeks post-vaccination.

Prior to inoculation, no signal was observed for birds in Group 4, only PaBV-2 inoculated. One week following PaBV-2 inoculation, a visual signal was observed for all birds in Group 3, vaccinated/PaBV-2 inoculated and in Group 4, only PaBV-2 inoculated.

Table 4.1. Western blot results for the detection of viral antibodies from control, vaccinated, vaccinated/ PaBV-2 inoculated, and PaBV-2 inoculated Monk parakeets (*Myiopsitta monachus*).

Vaccination Timeline	Bird ID	Wk -1	Wk 2	Wk 4	Wk 6	Wk 8	Wk 10	Wk 12	Wk 15	Wk 17	Wk 23	Wk 27	Wk 34
Inoculation Timeline		Wk -10	Wk -7	Wk -5	Wk -3	Wk -1	Wk 1	Wk 3	Wk 6	Wk 8	Wk 14	Wk 18	Wk 25
Group 1: Control	409	-	-	-	-	-	-	-	-	-	-	-	-
	26	-	-	-	-	-	-	-	-	-	-	-	-
	264	-	-	-	-	-	-	-	-	-	-	-	-
Group 2: Vaccinated	424	-	+	+	+	+	+	+	+	+	-	+	+
	268	-	+	+	+	+	+	+	+	+	-	+	+
	428	-	+	+	+	+	+	+	+	+	+	+	+
	13	-	-	+	+	-	-	-	-	-	+	+	+
	51	-	-	+	+	+	+	-	-	-	+	+	+
Group 3: Vaccinated/ PaBV-2 inoculated	440	-	+	+	+	+	+	+	+	+	+	+	+
	888	-	+	+	+	+	+	+	+	+	+	+	+
	243	-	+	+	+	+	+	+	+	+	+	+	+
	4	-	+	+	-	+	+	+	+	+	+	+	+
Group 4: PaBV-2 inoculated	445	-	-	-	-	-	+	+	+	+	+	+	+
	427	-	-	-	-	-	+	+	+	+	+	+	+
	446	-	-	-	-	-	+	+	+	+	+	+	+
	405	-	-	-	-	-	+	+	+	+	+	+	+
	417	-	-	-	-	-	+	+	+	+	+	+	+
	48	-	-	-	-	-	+	+	+	+	+	+	+

4.3.2. Dot-blot ELISA scoring

Dot-blot ELISA scoring of all Monk parakeets (*Myiopsitta monachus*) samples grouped by control, vaccinated, vaccinated/ PaBV-2 inoculated, and PaBV-2 inoculated are shown in Table 4.2. A score of zero was given to all 18 samples collected one-week prior to vaccination. In Group 1 control, 32 of 36 samples scored zero; one, one, and two samples had a score of 1, 2, and 3, respectively.

After the initial vaccination, visual signal scores were not detected until four-weeks post-vaccination for most samples from vaccinated birds in Groups 2 and 3. One bird did not have a visual signal until 5-weeks after the first vaccine booster.

Following PaBV-2 inoculation, most birds in Group 3, vaccinated/PaBV-2 inoculated had a visual signal score at one-week post-inoculation, whereas for PaBV-2 inoculated only birds (Group 4), visual signal scores were not detected until three-weeks post-inoculation. Samples at ≥ 3 weeks post-inoculation from all inoculated birds had visual signals throughout the remainder of the study period.

Table 4.2. Dot-blot ELISA scoring of control, vaccinated, vaccinated/ PaBV-2 inoculated, and PaBV-2 inoculated Monk parakeets (*Myiopsitta monachus*).

Vaccination Timeline	Bird ID	Wk -1	Wk 2	Wk 4	Wk 6	Wk 8	Wk 10	Wk 12	Wk 15	Wk 17	Wk 23	Wk 27	Wk 34
Inoculation Timeline		Wk -10	Wk -7	Wk -5	Wk -3	Wk -1	Wk 1	Wk 3	Wk 6	Wk 8	Wk 14	Wk 18	Wk 25
Group 1: Control	409	0	0	0	0	0	0	0	3	0	1	2	0
	26	0	0	0	0	0	0	0	0	0	0	3	0
	264	0	0	0	0	0	0	0	0	0	0	0	0
Group 2: Vaccinated	424	0	1	2	1	3	4	1	4	1	4	4	4
	268	0	0	3	4	1	4	2	4	2	4	4	4
	428	0	0	4	4	4	0	4	4	4	4	4	4
	13	0	0	0	0	0	3	2	3	3	4	4	3
	51	0	0	3	3	0	0	2	4	3	4	4	4
Group 3: Vaccinated/ PaBV-2 inoculated	440	0	0	1	3	2	3	4	4	4	4	4	4
	888	0	0	3	3	3	4	4	4	4	4	4	4
	243	0	0	3	4	3	4	4	4	4	4	4	4
	4	0	0	0	3	3	0	4	4	4	4	4	4
Group 4: PaBV-2 inoculated	445	0	0	0	0	0	0	3	4	4	4	4	4
	427	0	0	0	0	0	0	2	4	4	4	4	4
	446	0	0	0	0	0	0	4	4	4	4	4	4
	405	0	0	0	0	0	1	4	4	4	4	4	4
	417	0	0	0	0	0	0	4	4	4	4	4	4
	48	0	0	0	0	0	3	3	4	4	4	4	4

4.3.3. Dot-blot ELISA performance

The receiver operating characteristic curves based on results of the dot-blot ELISA of the four separate scenarios, all samples, samples from controls and vaccinated birds, samples from controls and inoculated birds, and samples from controls and inoculated birds ≥ 3 weeks post-inoculation, are shown in Figure 4.2. Individual ROC analysis of the four separate scenarios are included in APPENDIX B. Using a score of ≥ 2 for a positive result, diagnostic sensitivities, specificities, 95% confidence intervals, accuracy and AUC for the four separate scenarios were calculated (Table 4.3). At a cut-off score of ≥ 2 , the dot-blot ELISA yielded the best test characteristics for a sample population containing birds ≥ 3 weeks after inoculation: sensitivity of 100 %, specificity of 96 %, accuracy of 98 % and AUC of 0.999.

The dot diagram displays the frequency distribution of the dot-blot ELISA samples against the known positive and negative western blot sample (Figure 4.3.). The cut-off (horizontal line) score of two, a score ≥ 2 for the ELISA was positive, showed the best division with minimal false negative and false positive results when the sample population were birds ≥ 3 weeks post-inoculation (Figure 4.3B).

Table 4.3. Sensitivity, specificity, 95% confidence intervals, accuracy and AUC for the dot-blot ELISA results with four separate scenarios.

	Sensitivity (%)	95% CI (%)	Specificity (%)	95% CI (%)	Accuracy (%)	AUC
All samples	81.9	74.1 to 88.2	85.4	76.3 to 92.0	83.3	0.933
After vaccination	70.4	58.4 to 80.7	96.0	88.8 to 99.2	83.6	0.956
After inoculation	91.4	82.3 to 96.8	96.0	88.8 to 99.2	93.8	0.971
3wks post-inoculation	100	94.0 to 100	96.0	88.8 to 99.2	98.1	0.999

Figure 4.2. ROC curves composed of results for the four separate scenarios

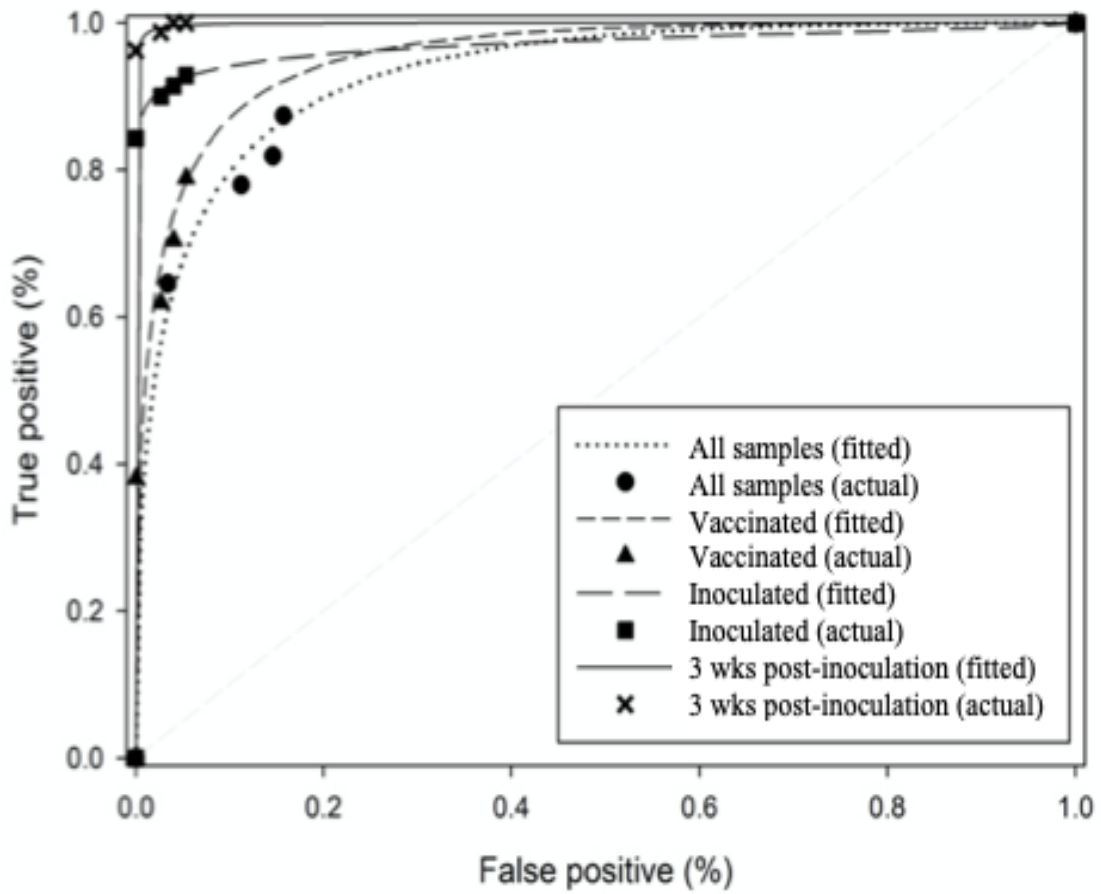
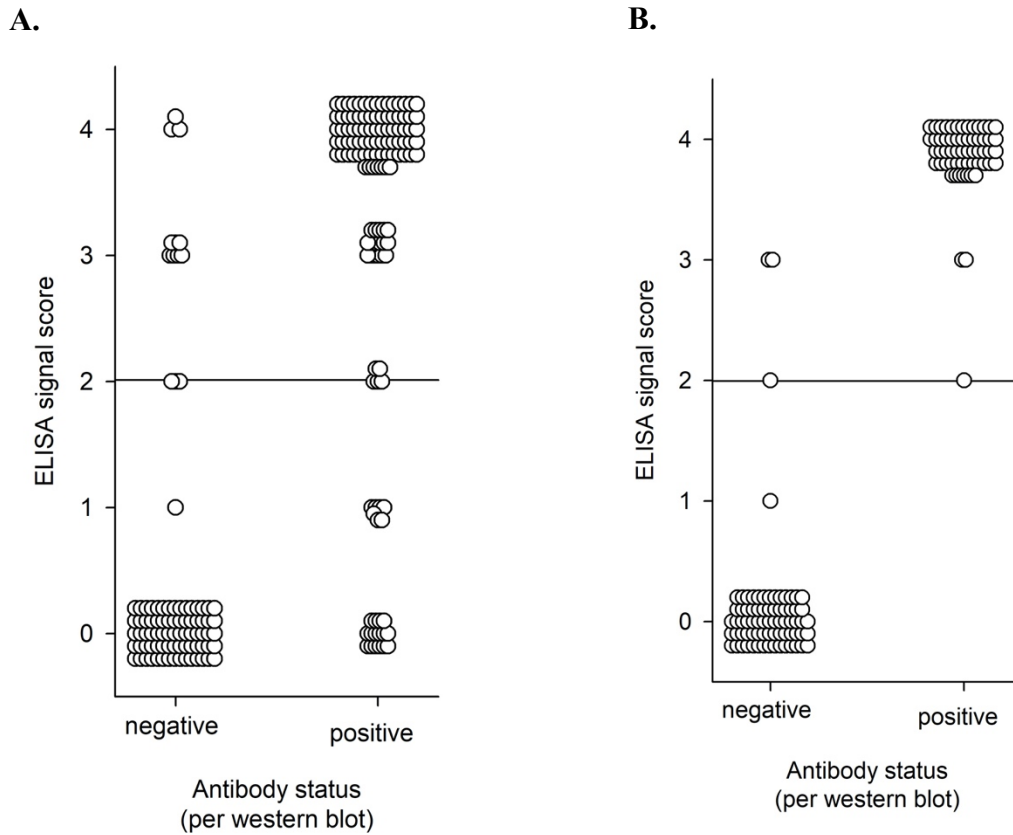


Figure 4.3. Dot diagrams of the known-positive and -negative samples displayed on two vertical axes.

Notes: The horizontal line indicates the cut-off point at score of two; a score ≥ 2 for the ELISA was positive. A. Dot diagram of overall ELISA signal scores. B. Dot diagram of three-weeks after inoculation for ELISA signal scores from controls and inoculated birds excluding dot-blot ELISA results from the first sampling after inoculation.



4.4. Discussion

Our study demonstrated that the dot-blot ELISA had excellent ability to discriminate true positive from true negative samples. Our results also suggest that the dot-blot ELISA could be used as a rapid serological assay for the detection of ABV-specific antibodies, obtaining results within minutes compared to other diagnostic immunoassays. Thus, it could be useful as a screening test or in birds with clinical signs of PaBVs, to confirm the diagnosis.

Using a cut-off score of ≥ 2 as a positive result, dot-blot ELISA had high sensitivity and specificity for all four scenarios: all samples; samples from controls and vaccinated birds; samples from controls and inoculated birds; and, samples from controls and inoculated birds ≥ 3 weeks post-inoculation. The dot-blot ELISA best sensitivity and specificity, 100% and 96% respectively, were achieved in a sample population that was ≥ 3 weeks post-inoculation. However, a difference in level of detection of the Western blot compared to the dot-blot ELISA was noted after experimental inoculation. The Western blot was able to detect antibodies one-week after inoculation, whereas the dot-blot ELISA did not detect antibodies until three-weeks after inoculation in Group 4 birds (Tables 4.1. and 4.2.). In Group 3, vaccinated/PaBV-2 inoculated birds, the primed immune system responded quicker to exposure to the pathogen; the dot-blot ELISA was able to detect antibodies one-week after experimental inoculation. Although, the dot-blot ELISA performance readily discriminated between ABV antibody positive and negative samples from experimentally infected birds, consideration of the time period between possible viral exposure and dot-blot ELISA testing is important.

Experimental inoculation with PaBV via intramuscular injection has shown to be a good mode of PaBV infection leading to classical PaBVs in Cockatiels (*Nymphicus hollandicus*).^{5,7,8,22,26-28} However, this mode of experimental inoculation does not represent the mode of transmission occurring in naturally infected birds, thus the timeline until antibodies could be detected may differ from that in our experimental model. The goal of our dot-blot ELISA is to be a rapid-patient side assay to detect naturally ABV infected birds. Therefore, assessment of the dot-blot ELISA performance should be further studied with samples from naturally infected birds comparing results with RT-PCR validation.

In serology assays such as Western blot and immunofluorescence, for ABV, N-protein is considered to be the immunodominant antigen.^{12,19,23} Thus, the use of recombinant N-protein in our study was two-fold: 1) used as the antigen of interest in our assay and 2) to safely produce viral antigen antibodies without exposing our birds to the virus which could lead to disease.

The poor sensitivity and specificity of the overall dot-blot ELISA results, 81.9% and 85.4% respectively, was most likely due to the lower level of detection of the Western blot as compared to the dot-blot ELISA. The Western blot was able to detect antibodies earlier after vaccination, two weeks after the first vaccination, whereas the dot-blot ELISA did not detect antibodies until four weeks after the first vaccination (Table 4.1 and 4.2). However, recombinant N-protein vaccination still produces antibodies within the limit of detection for both Western blot and dot-blot ELISA. Western blot and dot-blot ELISA will identify antibody production but will not identify

if the antibody production was from a viral or vaccine exposure. Therefore, vaccination with recombinant N-protein vaccination could cause an erroneous diagnosis in both assays and should be considered if a PaBV vaccine becomes commercially available. Diagnosis of ABV infection should not be solely based on serology testing for antibodies. ELISA positive birds should have additional diagnostic testing, RT-PCR or other immunological assays, to reinforce the diagnosis of a seropositive bird.

4.5. Conclusion

Our study shows that the dot-blot ELISA has good sensitivity and specificity, minimal to no background noise, and can produce results within 30 minutes. This suggests the possibility of further developing the dot-blot ELISA into a rapid patient-side diagnostic assay that will detect ABV antibodies in psittacine bird.

4.6. References

1. Kistler AL, Gancz A, Clubb S, et al. Recovery of divergent avian bornaviruses from cases of proventricular dilatation disease: identification of a candidate etiologic agent. *Virology*. 2008;5:88–102.
2. Honkavuori KS, Shivaprasad HL, Williams BL, et al. Novel bornavirus in psittacine birds with proventricular dilatation disease. *Emerg Infect Dis*. 2008;14(12):1883–1886.
3. Hoppes S, Tizard I, Shivaprasad HL. Avian Bornavirus and proventricular dilatation disease: diagnostics, pathology, prevalence, and control. *Vet Clin Exot Anim*. 2013;16(2):339–355.

4. Rossi G, Dahlhausen RD, Galosi L, Orosz SE. Avian ganglioneuritis in clinical practice. *Vet Clin: Exot Anim Pract.* 2018;21(1):33–67.
5. Piepenbring AK, Enderlein D, Herzog S, et al. Pathogenesis of avian bornavirus in experimentally infected Cockatiels. *Emerg Infect Dis.* 2012;18(2):234–241.
6. Raghav R, Taylor M, DeLay J, et al. Avian bornavirus is present in many tissues of psittacine birds with histopathologic evidence of proventricular dilatation disease. *J Vet Diagn Invest.* 2010;22(4):495–508.
7. Payne S, Shivaprasad HL, Mirhosseini N, et al. Unusual and severe lesions of proventricular dilatation disease in cockatiels (*Nymphicus hollandicus*) acting as healthy carriers of avian bornavirus (ABV) and subsequently infected with a virulent strain of ABV. *Avian Pathol* 2011;40(1):15–22.
8. Leal de Araujo J, Rech RR, Heatley JJ, et al. From nerves to brain to gastrointestinal tract: A time-based study of parrot bornavirus 2 (PaBV-2) pathogenesis in cockatiels (*Nymphicus hollandicus*). *PLoS One.* 2017;12(11):e0187797.
9. Rinder M, Ackermann A, Kempf H, et al. Broad tissue and cell tropism of avian bornavirus in parrots with proventricular dilatation disease. *J Virol.* 2009;83(11):755–756.
10. Rubbenstroth D, Rinder M, Stein M, et al. Avian bornaviruses are widely distributed in canary birds (*Serinus canaria* f. domestica). *Vet Microbiol.* 2013;165(3-4):287–295.

11. Delnatte P, Mak M, Ojkic D, et al. Detection of avian bornavirus in multiple tissues of infected psittacine birds using real-time reverse transcription polymerase chain reaction. *J Vet Diagn Invest.* 2014;26(2):266–271.
12. de Kloet AH, Kerski A, de Kloet SR. Diagnosis of avian bornavirus infection in psittaciformes by serum antibody detection and reverse transcription polymerase chain reaction assay using feather calami. *J Vet Diagn Invest.* 2011;23(3):421–429.
13. Weissenbock H, Fragner K, Nerdorost N, et al. Localization of avian bornavirus RNA by in situ hybridization in tissues of psittacine birds with proventricular dilatation disease. *Vet Microbiol.* 2010;145(1-2):9–16.
14. Fluck A, Enderlein D, Piepenbring A, et al. Correlation of avian bornavirus-specific antibodies and viral ribonucleic acid shedding with neurological signs and feather-damaging behavior in psittacine birds. *Vet Rec.* 2019;184(15):476–482.
15. Delnatte P, Nagy E, Ojkic D, et al. Avian bornavirus in free-ranging waterfowl: prevalence of antibodies and cloacal shedding of viral RNA. *J Wildl Dis.* 2014;50(3):512–523.
16. de Kloet SR, Dorrestein GM. Presence of avian bornavirus RNA and anti-avian bornavirus antibodies in apparently healthy macaws. *Avian Dis.* 2009;53(4):568–573.

17. Villanueva I, Grey P, Mirhosseini N, et al. The diagnosis of proventricular dilatation disease: Use of a Western blot assay to detect antibodies against avian Borna virus. *Vet Microbiol.* 2010;143(2-4):196–201.
18. Lierz M, Hafez HM, Honkavuori KS, et al. Anatomical distribution of avian bornavirus in parrots, its occurrence in clinically healthy birds and ABV-antibody detection. *Avian Pathol.* 2009;38(6):491–496.
19. Zimmermann V, Rinder M, Kaspers B, et al. Impact of antigenic diversity on laboratory diagnosis of avian bornavirus infections in birds. *J Vet Diagn Invest.* 2014;26(6):769–777.
20. Herzog S, Enderlein D, Heffels-Redmann U, et al. Indirect immunofluorescence assay for *Intra Vitam* diagnosis of avian bornavirus infected in psittacine birds. *J Clin Microbiol.* 2010;48(6):2282–2284.
21. Hameed SS, Guo J, Tizard I, et al. Studies on immunity and immunopathogenesis of parrot bornaviral disease in cockatiels. *Virology.* 2018;515:81-91.
22. Mirhosseini N, Gray PL, Hoppes S, et al. Proventricular dilatation disease in cockatiels (*Nymphicus hollandicus*) after infection with a genotype 2 avian bornavirus. *J Avian Med Surg.* 2011;25(3):199–204.
23. Guo J, Payne S, Zhang S, et al. Avian bornaviruses: diagnosis, isolation, and genotyping. *Curr Protoc Microbiol.* 2014;34:15i.1.11.11–15i.1.11.33.

24. Eng J. ROC analysis: web-based calculator for ROC curves. Baltimore: Johns Hopkins University [updated 2014 March 19; cited 2019 October 22]. Available from: <http://www.jrocfits.org>).
25. Swets JA. Measuring the accuracy of diagnostic systems. *Science*. 1988;240(4857):1285–1293.
26. Piepenbring AK, Enderlein D, Herzog S, et al. Parrot bornavirus (PaBV)-2 isolate cause different disease patterns in cockatiels than PaBV-4. *Avian Pathol*. 2016;45(2):156–168.
27. Heckmann J, Enderlein D, Piepenbring AK, et al. Investigation of Different Infection Routes of PaBV in Cockatiels. *Avian Dis*. 2017;61(1):90–95.
28. Rubbenstroth D, Brosinski K, Rinder M, et al. No contact transmission of avian bornavirus in experimental infected cockatiels (*Nymphicus hollandicus*) and domestic canaries (*Serinus canaria forma domestica*). *Vet. Microbiol*. 2014;172(1-2):146–156.

5. CONCLUSIONS ON INOCULATION OF VACCINATED AND UNVACCINATED MONK PARAKEETS (*Myiopsitta monachus*) WITH PARROT BORNAVIRUS-2

5.1. Introduction

In 2008, avian bornavirus (ABV) was discovered to be the causative agent of parrot bornavirus syndrome, formerly termed Proventricular Dilatation Disease or PDD, in psittacine.¹⁻³ Histopathology findings consistent with ABV lesions include lymphoplasmacytic meningoencephalomyelitis and ganglioneuritis in the central, peripheral and/or autonomic nervous system.⁴⁻⁷ Clinical signs of parrot bornavirus syndrome vary and likely depend on the avian species infected and lesion distribution, although clinical signs generally affect the neurological and gastrointestinal system. Neurologic signs include inability to perch, general weakness, ataxia, seizures and blindness.⁸⁻¹⁰ Gastrointestinal (GI) system signs include delayed crop emptying, regurgitation, dilatation of one or several parts of the GI tract and impaired GI system transit, all of which are caused by nerve damage in the enteric nervous system.⁸⁻¹⁰ Ultimately these lesions cause GI dysfunction leading to starvation and/or death. Parrot bornavirus syndrome diagnosis relies on clinical presentation, histopathological lesions, or viral antigen or mRNA detection, with more than one diagnostic test being positive providing greater probability in identifying infected birds.⁴⁻⁷

Cockatiels (*Nymphicus hollandicus*) are used as a psittacine model to study ABV infection and classical lesions of ABV pathogenesis after experimental inoculation with

the virus.^{4,6,7,11,12} Other psittacine species such as Budgerigars (*Melopsittacus undulatus*), Monk parakeets (*Myiopsitta monachus*) and Lovebirds (*Agapornis roseicollis*) have been experimentally infected with the virus but fail to develop clinical signs, gross abnormalities, or histological lesions.¹³⁻¹⁵ Recently, there has been a report of a single Monk parakeet naturally infected with PaBV-2 that had clinical signs before dying.¹⁶ This paper reports on Monk parakeets that developed histopathologic lesions after being inoculated with Parrot Bornavirus-2 (PaBV-2).

5.2. Materials and methods

5.2.1. Animals

This experimental protocol was reviewed and approved by the Texas A&M University Bio-safety and Animal Use Committees (IACUC 2016-0054), which complies with guidelines included in the National Research Council of the National Academies' publication Guide for the Care and Use of Laboratory Animals, 8th edition. Ten Monk parakeets were assessed as healthy based on their medical history and physical examination. Birds were then assigned to one of two groups: Group 1 (vaccinated) - four Monk parakeets were vaccinated with recombinant nucleoprotein (N-protein) and experimentally inoculated with PaBV-2; and, Group 2 (unvaccinated) - six Monk parakeets were experimentally inoculated with PaBV-2 and not vaccinated. Birds were housed with a light-dark cycle of 12 hours and a room temperature of 21°C (±5.0), at the Schubot Exotic Bird Health Center aviary, College of Veterinary Medicine and Biomedical Sciences. Each bird was fed 1/6 cup per bird of premium daily feed (FruitBlend®, ZuPreem, Shawnee, KS, USA), and had access to tap water ad libitum.

5.2.2. Recombinant nucleoprotein expression and purification

Recombinant N-protein, purified from *E. coli*, was produced following the method of Hameed et al (2018).¹⁷ Briefly, the procedure was as follows. Total RNA was extracted from frozen brain tissue of a Yellow-collared macaw (*Primolius auricollis*) infected with PaBV-4 using Qiagen RNeasy Mini kit (Qiagen, Hilden, Germany). The RNA was used to generate cDNA using reverse transcription kits (High Capacity Reverse Transcription Kit, Applied Biosystems, Foster City, CA, USA) and random hexamers. Subsequent PCR was performed to amplify the N-protein gene with primers Forward 5'-CATG CAT ATG CCA CCC AAG AGA CAA AGA AGC-3' and Reverse 5'-GTAC CTC GAG GTT TGC GAA TCC GGT TAC ACC-3'. The resulting PCR products were cloned, sequenced, and inserted into pET21a vector to generate a His-tagged fusion protein for expression in *E. coli* (Rosetta, Sigma-Aldrich, St. Louis, MO, USA). Recombinant *E. coli* was incubated for 12 hours in Luria broth fortified with ampicillin; the culture was continuously mixed at 150 rpm at room temperature. Recombinant *E. coli* was transferred to fresh media of Luria broth, ampicillin, and Isopropyl β -D-1-thiogalactopyranoside to induce protein expression and incubated for 6 hours, while being continuously stirred at 200 rpm at room temperature. The solution was centrifuged at 3,500 x g for 30-minutes and the supernatant was removed. The bacterial pellet was resuspended in 40 mL of phosphate-buffered saline (PBS) and sonicated for 3 sets of 8-minutes to lyse the bacteria. The sonicated solution was then centrifuged at 12,000 x g for 20-minutes at 4°C. The supernatant was loaded on a Qiagen Ni-NTA Agarose column (Qiagen, Hilden, Germany), which had been pre-conditioned

with 10 mL of binding buffer (20 mM sodium phosphate, 300 mM NaCl, pH 7.4, 10 mM imidazole); the Ni-NTA Agarose column has a high affinity for His-tagged proteins. Ten milliliters of wash buffer (20 mM sodium phosphate, 300 mM NaCl, pH 7.4, 20 mM imidazole) was loaded on the column and allowed gravity flow. The column was then eluted by gravity flow with 10 mL of elution buffer (20 mM sodium phosphate, 300 mM NaCl, pH 7.4, 200 mM imidazole) and the elutant was collected in 1.0 mL fractions. The purity of each protein fraction was determined by sodium dodecyl sulfate polyacrylamide gel (SDS-PAGE) electrophoresis. Fractions containing the N-protein were combined and an Amicon Ultra 15 mL centrifugal filter (MilliporeSigma, Burlington, MA, USA) was used to concentrate the N-protein in 1.0 mL PBS. Finally, the protein concentration was measured using BCA™ Protein Assay Kit (Thermo Scientific™ PIERCE™, Waltham, MA, USA). Recombinant N-protein was stored at -20°C and thawed out in 37 °C waterbath prior to use for vaccination or immunoassay.

5.2.3. Recombinant nucleoprotein vaccination

Recombinant N-protein vaccine was produced according to Hameed et al (2018).¹⁷ In brief, each recombinant N-protein vaccine dose was made 30-minutes prior to administering vaccine. Each 100 µL dose contained 25 µg recombinant N-protein and 0.5% alum (Invitrogen, Thermo Fisher Scientific™ PIERCE™, Waltham, MA, USA) in PBS.

Birds of Group 1 were vaccinated with 100 µL dose of recombinant N-protein vaccine via left pectoral intramuscular injection. Vaccine boosters were administered by left pectoral intramuscular injection at 1 and 7 months after the initial vaccination.

5.2.4. Parrot bornavirus-2 inoculation

Parrot bornavirus-2 (PaBV-2) was isolated from the brain of experimentally infected Cockatiels.¹¹ Virus for inoculation was grown as previously described.¹³ Briefly, duck embryo fibroblast cell cultures were inoculated with stock virus and maintained in Dulbecco's modified eagle medium (Gibco®, Life Technologies Co., Thermo Fisher Scientific, Waltham, MA, USA) with 10% fetal bovine serum (Gibco®, Life Technologies Co.) at 37 °C in an atmosphere of 5% CO₂. After 3 days of incubation, cells were harvested, divided into 1.0 mL of aliquots and stored -80°C. Virus was confirmed as PaBV-2 by RNA extraction and reverse transcriptase polymerase chain reaction (RT-PCR) analysis followed by sequence analysis of the PCR product, as described in Guo et al (2014) according to basic protocols 3 and 10.¹³

Birds were inoculated by right pectoral intramuscular administration 8×10^5 focus forming units (FFU) of PaBV-2 one month after the first vaccine booster. This method has previously induced parrot bornavirus syndrome in cockatiels.^{7,11}

5.2.5. Necropsy

After 7 (\pm 1) months following experimental inoculation, birds were humanely euthanized and necropsy was performed. Birds were initially anesthetized with 5% isoflurane in 95% oxygen via face mask and maintained anesthetized for collection of weight, body condition score (BCS), cloacal swab, and blood collection from the jugular vein. For euthanasia, chamber exposure to 100% carbon dioxide was performed immediately after sample collection while birds remained in a deep state of anesthesia. A complete necropsy was then performed and gross lesions were recorded. Paired samples

of forebrain, hindbrain, cerebellum, midbrain, spinal cord, sciatic nerve, optic nerve, brachial plexus, eye, proventriculus, and kidney were collected and stored at -80°C for later analyses by RT-PCR. The remainder of each organ was placed in 10% neutral buffered formalin for histological examination.

5.2.6 Western blot

Western blot assays were performed according to basic protocol 5, Guo et al (2014), with the following modifications to detect N-protein antibodies.¹³ Briefly, 0.1 mg/mL of recombinant N-protein solution was mixed at a 1:1 ratio with gel loading buffer and boiled in a water bath for 3-minutes. Then 15 µL of the boiled sample was loaded into each SDS-PAGE gel wells, separated using SDS-PAGE and electrophoretically transferred to a polyvinylidene difluoride (PVDF) membrane. The PVDF membrane was incubated in 5% dried skim milk/0.05% Tween/0.02M PBS overnight at room temperature. The membrane was then incubated for 2 hours with sample plasma that had been diluted 1:200 with 3.0 mL of 2% dried skim milk/0.05% Tween/0.02M PBS; this was followed with three 15-minute rinses of 0.05% Tween/0.02M PBS. The membrane was then incubated for 1 hour with 1:50,000 dilution of polyclonal IgG goat anti-macaw IgY-H+L conjugated with alkaline phosphatase, 1.0 mg/mL (Bethyl A140-116AP, Bethyl Laboratories, Inc., Montgomery, TX, USA), in 3.0 mL of 2% dried skim milk/0.05% Tween/0.02M PBS. This was followed by three 15-minute rinses with 0.05% Tween/0.02M PBS. The membrane was then incubated for approximately 5-minutes, or until color change was observed, in a 5-bromo-4-chloro-3-indolyl phosphate (BCIP)/nitro blue tetrazolium (NBT) solution

(SigmaFast BCIP/NBT substrate tablet, Sigma Aldrich, St. Louis, MO, USA) dissolved in 10 mL ultra-pure water. Finally, the membrane was rinsed with ultra-pure water.

5.2.7. Histology

Tissue samples were fixed in 10% neutral buffered formalin, embedded in paraffin, sectioned at 4 μm , stained with haematoxylin and eosin (H & E), and examined by light microscopy.

5.2.8. RT-PCR

Tissue and cloacal swabs were analyzed for the presence of viral mRNA by TaqMan-based one-step reverse transcriptase real-time PCR (TaqMan® Fast Virus 1-Step, Life Technologies Co.) according to Escandon et al., (2019).¹⁸ Total viral RNA was isolated from each sample using the QIAamp viral RNA mini kit (Qiagen, Valencia, CA, USA). Purified RNA was eluted in 60.0 μL elution buffer and stored at -80°C until use. RNA samples were then used in the TaqMan RT-PCR assay performed with TaqMan® Fast Virus 1-Step Master Mix (Invitrogen, Carlsbad, CA, USA) with PaBV phosphoprotein primers (5' AAGAAGAA[Y]CC[Y]TCCATGATCTC 3' and 5'-AA[Y]TGCCGAAT[B]A[R]GTCATC- 3') and TaqMan probe (5'-FAM-TCGATAACTG [Y]TCCCTTCCGGTC-BHQ-3') for the detection of PaBV phosphoprotein RNA. We also used PaBV matrix primers (5'-GGTAATTGTTCCCTGGATGG-3') and (5'-ACACCAATGTTCCGAAGACG-3'), and TaqMan probe. (5'-FAM-TCGATAACTG [Y]TCCCTTCCGGTC-BHQ-3'). Each reaction was carried out using 6.0 μL of TaqMan fast virus master mix, 5.0 μL of mRNA of sample, 0.4 μL ultrapure H₂O, 0.3 μM primers and 0.3 μM probe in a 12.0 μL

final reaction volume. All reactions were carried out using initial denaturing for 5 minutes at 48°C and 20 seconds at 95°C, then 45 amplification cycling parameters, and then reverse transcriptase inactivation and polymerase activation for 3 seconds at 95°C and 30 seconds at 56°C. Results were analyzed using the Sequence Detection System, Version 2.4.1 (SDS 2.4) software (Life Technologies Co.). All samples were tested in duplicate for both the matrix protein and phosphoprotein. Samples were considered negative at cycle threshold (CT) ≥ 37.0 . If a sample was positive for the matrix protein and negative for the phosphoprotein or vice versa, samples were retested.

5.2.9. Digital images

Membranes were scanned using an Epson Expression 100000 XL flatbed scanner with 300 dpi resolution and saved in a .jpeg digital image format.

5.2.10. Statistical analysis

Weights were analyzed using the t-test; body condition scores were analyzed using the Mann-Whitney Rank Sum Test. Proportion of gross abnormalities was analyzed using a z-test. SigmaPlot version 10.0.1 was used for performing all statistical analyses (Systat Software, Inc., San Jose, CA).

5.3. Results

5.3.1. Clinical and gross observations

At study end, body weights and body condition scores did not significantly differ ($P < 0.05$) between vaccinated and unvaccinated groups (Table 5.1.). Additionally, no birds had clinical signs consistent with parrot bornavirus syndrome. There was not a significant difference ($P=0.26$; 95% CI, -1.006 to 0.006) in the proportion of birds with gross lesions between the 2 groups. The predominant gross abnormalities at necropsy were discoloration of the distal portion of the proventriculus, dilation of the proventriculus and mottling of the liver. In the vaccinated group, two birds had dilation of the proventriculus, while two birds had no gross abnormalities. In the unvaccinated group, all birds had mild dilation of proventriculus and discoloration of the proventriculus and other abnormalities were found in individual birds (Table 5.1. and Figure 5.1.).

5.3.2. RT-PCR

Viral mRNA was detected in most tissue samples in all birds, regardless of study group (Table 5.2). In the unvaccinated group, viral mRNA was not detected in the kidney of one bird and the proventriculus of one bird.

Four of four vaccinated Monk parakeets had cloacal swabs positive for ABV mRNA at necropsy. In the unvaccinated group, 4 of 6 cloacal birds had cloacal swabs positive for ABV mRNA (Table 5.2).

Table 5.1. Body condition score, weight and necropsy finding of vaccinated and unvaccinated Monk parakeets (*Myiopsitta monachus*) inoculated with PaBV-2.

	Bird ID	BCS	Weight (g)	Necropsy findings
Vaccinated	440	3/5	110	Dilated proventriculus
	888	3/5	114	No abnormalities
	243	2/5	104	No abnormalities
	4	3/5	102	Dilated proventriculus
Unvaccinated	445	3/5	125	Mottling of the liver, discoloration of distal portion of proventriculus, and mild dilation
	427	3/5	100	Discoloration of distal portion of proventriculus and mild dilation
	446	2/5	98	Mottling of the liver, discoloration of distal portion of proventriculus, and mild dilation
	405	3/5	118	Mottling of the liver, crop full of feed, discoloration of distal portion of proventriculus, and mild dilation
	417	3/5	140	Mottling of the liver, discoloration of distal portion of proventriculus, and mild dilation
	48	3/5	125	Discoloration of distal portion of proventriculus and mild dilation

Figure 5.1. Mild dilation and discoloration of proventriculus in unvaccinated Monk parakeet (*Myiopsitta monachus*) inoculated with PaBV-2.

Notes: Green arrow denotes discoloration of distal portion of proventriculus.












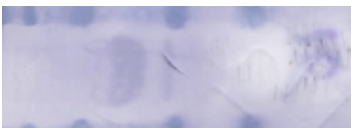
Table 5.2. RT-PCR results of the tissue and cloacal swabs from unvaccinated and vaccinated Monk parakeets (*Myiopsitta monachus*) inoculated with PaBV-2.

Bird ID	Forebrain	Hindbrain	Cerebellum	Midbrain	Spinal cord	Sciatic nerve	Optic Nerve	Brachial plexus	Eye	Proventriculus	Kidney	Cloacal swab
Vaccinated	440	+	+	+	+	+	+	+	+	+	+	+
	888	+	+	+	+	+	+	+	+	+	+	+
	243	+	+	+	+	+	+	+	+	+	+	+
	4	+	+	+	+	+	+	+	+	+	+	+
Unvaccinated	445	+	+	+	+	+	+	+	+	+	+	+
	427	+	+	+	+	+	+	+	+	+	+	+
	446	+	+	+	+	+	+	+	+	+	+	+
	405	+	+	+	+	+	+	+	+	-	+	-
	417	+	+	+	+	+	+	+	+	+	+	+
	48	+	+	+	+	+	+	+	+	+	-	-

5.3.3. Western blot

Western blot results detecting N-protein antibodies in plasma from Monk parakeets obtained prior to necropsy are shown in Figure 5.2. A strong N-protein signal of approximately 38-41kDa, was observed for all birds in the vaccinated and unvaccinated groups.

Figure 5.2. Western blot membranes detecting PaBV-2 antibodies from unvaccinated and vaccinated Monk parakeets (*Myiopsitta monachus*) inoculated with PaBV-2.

Bird	Vaccinated	Bird	Unvaccinated
440	MW 82 57 41 27 20 15 	445	MW 82 57 41 27 20 15 
888		427	
243		446	
4		405	
		417	
		48	

5.3.4. Histology

Histopathological lesions frequently observed were encephalitis in the brain, ganglioneuritis in the ventriculus, proventriculus and esophagus, and neuritis in the nerves (Table 5.3.). Additional, infrequent inflammatory lesions were seen in the adrenal glands, liver, crop, kidney, trachea, small intestine, and skeletal muscle. The lesions included lymphocytic and plasmacytic infiltration of the proventriculus, ventriculus, adrenal glands, liver, brain, and crop (Figure 5.3.-5.8.).

Table 5.3. Histological findings within the gastrointestinal tract, brain and nerve tissues from unvaccinated and vaccinated Monk parakeets (*Myiopsitta monachus*) inoculated with PaBV-2.

Tissue (changes)	Vaccinated	Unvaccinated
Brain (encephalitis)	3/4	2/6
Ventriculus (ganglioneuritis)	3/4	4/6
Proventriculus (ganglioneuritis)	2/4	4/6
Esophagus (ganglioneuritis)	2/4	5/6
Nerves (neuritis)	2/4	4/6

Figure 5.3. Lymphocytic and plasmacytic infiltration of the proventriculus of an unvaccinated Monk parakeet (*Myiopsitta monachus*) at 400x.

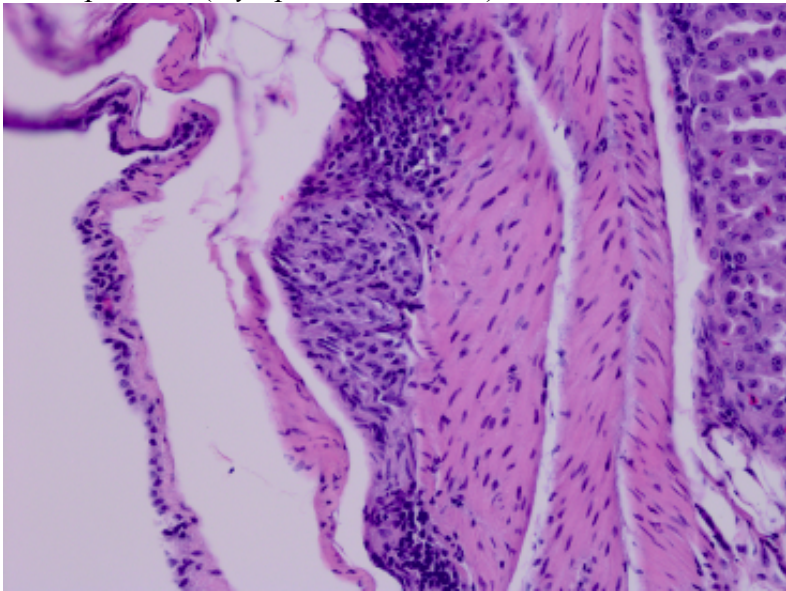


Figure 5.4. Lymphocytic and plasmacytic infiltration of the ventriculus of an unvaccinated Monk parakeet (*Myiopsitta monachus*) at 400x.

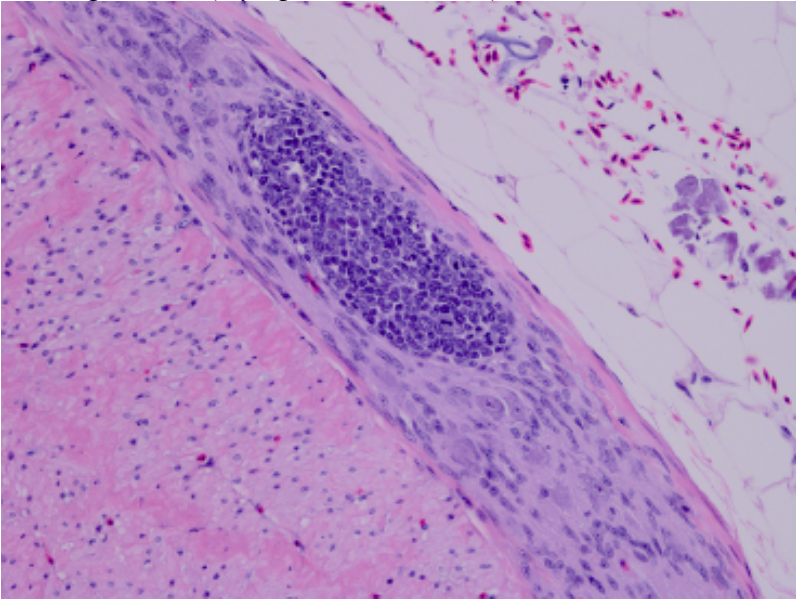


Figure 5.5. Lymphocytic and plasmacytic infiltration of the adrenal glands of an unvaccinated Monk parakeet (*Myiopsitta monachus*) at 100x.

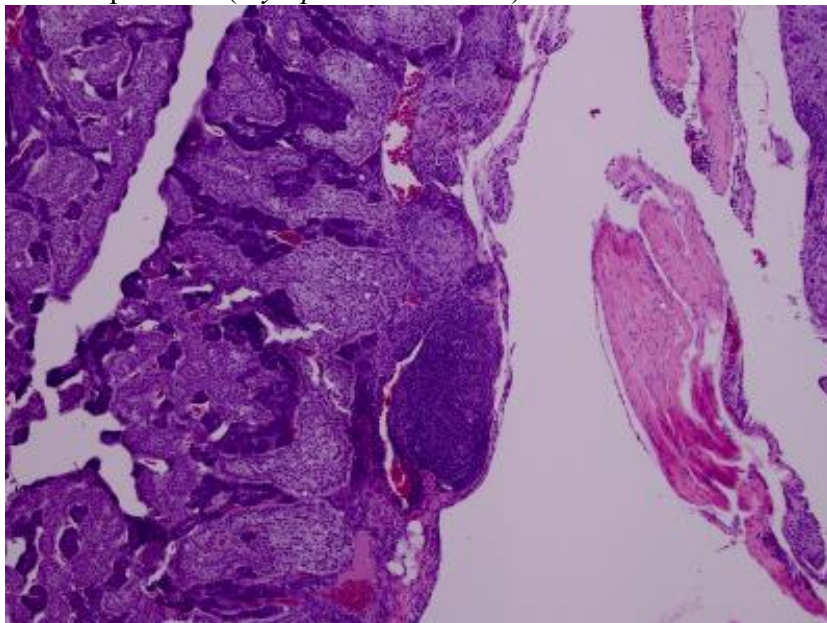


Figure 5.6. Lymphocytic and plasmacytic infiltration of the liver of an unvaccinated Monk parakeet (*Myiopsitta monachus*) at 400x.

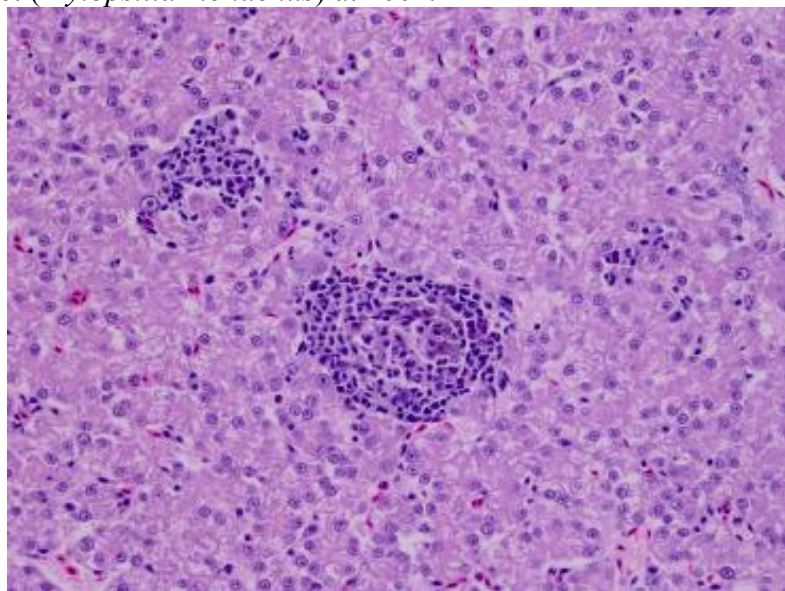


Figure 5.7. Lymphocytic and plasmacytic infiltration of the brain of an unvaccinated Monk parakeet (*Myiopsitta monachus*) at 400x.

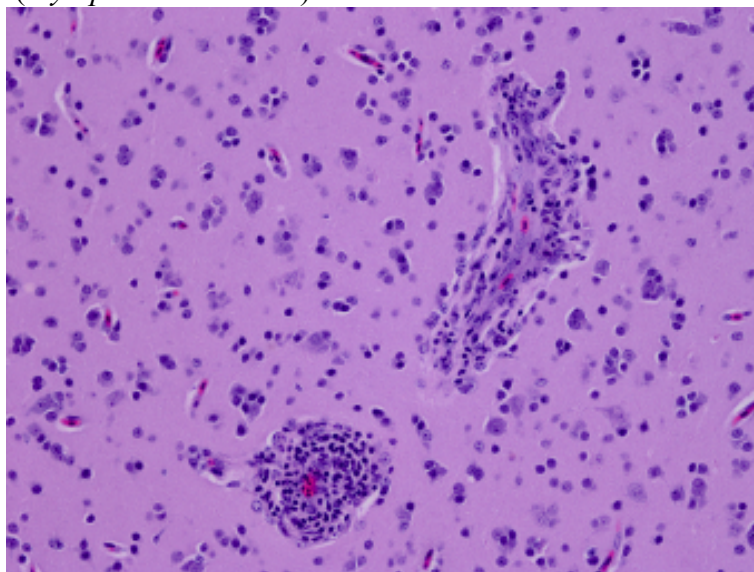
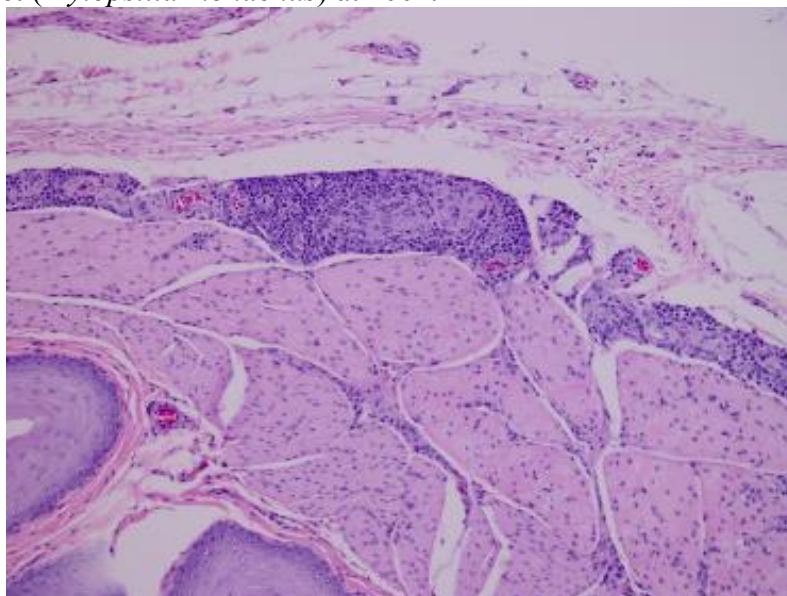


Figure 5.8. Lymphocytic and plasmacytic infiltration of the crop of an unvaccinated Monk parakeet (*Myiopsitta monachus*) at 200x.



5.4. Discussion

This is the first report of gross pathology, histopathological lesions, and viral distribution in Monk parakeets due to experimental inoculation with PaBV-2. Gross pathology was not significantly different between vaccinated and unvaccinated groups, even though only 2 of 4 birds in the vaccinated group had abnormalities noted, while the unvaccinated group had 6 of 6 birds with abnormalities. The statistical power was low due to the small sample size; thus, this statistical finding is inconclusive. Gross abnormalities noted were consistent with parrot bornavirus syndrome, a dilated proventriculus was identified in 8 of 10 birds (Table 5.1.).^{3,4,9,6,11,19} Gross pathology also revealed discoloration of the proventriculus in the unvaccinated group (Figure 5.1.), possibly due to the dilation of the proventriculus and thinning of the proventricular wall. Previous studies have shown gross changes of transparent walls with visible undigested food and dilated, thin-walled gastrointestinal tract.^{10,20} These findings suggest that Monk parakeets could succumb to fatal parrot bornavirus syndrome over time, as has been reported in a naturally infected Monk parakeet.¹⁶

Parrot bornavirus-2 mRNA and PaBV-2 antibodies were found in all PaBV-2 inoculated birds (Table 5.2. and Figure 5.2.), a finding that is similar in other experimental and naturally infected psittacines.^{2,5,7 21-27}

Vaccination of Monk parakeets did not abate infection, virus replication, viral distribution, and immunological response to the infection, similar to other bird species vaccinated with the recombinant N-protein.^{17,28,29} Histopathological lesions of lymphoplasmacytic meningoencephalomyelitis and ganglioneuritis, similar to those

described in other bird species, were seen in both groups of PaBV infected birds (Table 5.3.).^{5-7,12} Though this was not a study on the protective value of the recombinant N-protein vaccine, 2 of 4 vaccinated birds, compared to 0 of 6 unvaccinated birds, did not have gross abnormalities at necropsy, a trend towards the possible protective value of vaccination against gross abnormalities that is reported for the vaccine.¹⁷

Vaccinated and unvaccinated groups did not have the weight loss, reduction in body condition score, nor other clinical signs as seen in previous experimental inoculation studies (Table 5.1.).^{6,9,11,19} No Monk parakeets were removed early from the study due to clinical signs; in cockatiels, clinical signs and mortality of cockatiels are seen between 30-80 days post-inoculation of PaBV-2.¹¹

5.5. Conclusion

This is the first report of Monk parakeets experimentally inoculated with PaBV-2 developing histopathological lesions consistent of PaBV infection. Monk parakeets of this study did not develop clinical signs consistent with parrot bornavirus syndrome for the period of the study, 7 (\pm 1) months after inoculation. Vaccination with recombinant N-protein did not alter the severity of gross necropsy abnormalities, viral shedding, viral mRNA distribution nor histopathological changes in Monk parakeets experimentally inoculated with PaBV-2.

5.6. References

1. Kistler AL, Gancz A, Clubb S, et al. Recovery of divergent avian bornaviruses from cases of proventricular dilatation disease: identification of a candidate etiologic agent. *Virology*. 2008;5:88–102.
2. Honkavuori KS, Shivaprasad HL, Williams BL, et al. Novel bornavirus in psittacine birds with proventricular dilatation disease. *Emerg Infect Dis*. 2008;14(12):1883–1886.
3. Gray P, Hoppes S, Suchodolski P, et al. Use of avian bornavirus isolated to induce proventricular dilatation disease in conures. *Emerg Infect Dis*. 2010;16(3):473–479.
4. Piepenbring AK, Enderlein D, Herzog S, et al. Pathogenesis of avian bornavirus in experimentally infected Cockatiels. *Emerg Infect Dis*. 2012;18(2):234–241.
5. Raghav R, Taylor M, DeLay J, et al. Avian bornavirus is present in many tissues of psittacine birds with histopathologic evidence of proventricular dilatation disease. *J Vet Diagn Invest*. 2010;22(4):495–508.
6. Payne S, Shivaprasad HL, Mirhosseini N, et al. Unusual and severe lesions of proventricular dilatation disease in cockatiels (*Nymphicus hollandicus*) acting as healthy carriers of avian bornavirus (ABV) and subsequently infected with a virulent strain of ABV. *Avian Pathol: J of The W.V.P.A.* 2011;40(1):15–22.
7. Leal de Araujo J, Rech RR, Heatley JJ, et al. From nerves to brain to gastrointestinal tract: A time-based study of parrot bornavirus 2 (PaBV-2)

- pathogenesis in cockatiels (*Nymphicus hollandicus*). *PLoS One*. 2017;12(11):e0187797.
8. Hoppes S, Gray PL, Payne S, Shivaprasad HL, Tizard I. The isolation, pathogenesis, diagnosis, transmission, and control of avian bornavirus and proventricular dilatation disease. *Vet Clin North Am Exot Anim Pract*. 2010;13(3):495–508.
 9. Hoppes S, Tizard I, Shivaprasad HL. Avian Bornavirus and proventricular dilatation disease: diagnostics, pathology, prevalence, and control. *Vet Clin Exot Anim*. 2013;16(2):339–355.
 10. Rossi G, Dahlhausen RD, Galosi L, Orosz SE. Avian ganglioneuritis in clinical practice. *Vet Clin: Exot Anim Pract*. 2018;21(1):33–67.
 11. Mirhosseini N, Gray PL, Hoppes S, et al. Proventricular dilatation disease in cockatiels (*Nymphicus hollandicus*) after infection with a genotype 2 avian bornavirus. *J Avian Med Surg*. 2011;25(3):199–204.
 12. Piepenbring AK, Enderlein D, Herzog S, et al. Parrot bornavirus (PaBV)-2 isolate cause different disease patterns in cockatiels than PaBV-4. *Avian Pathol*. 2016;45(2):156–168.
 13. Guo J, Payne S, Zhang S, et al. Avian bornaviruses: diagnosis, isolation, and genotyping. *Curr Protoc Microbiol*. 2014;34:15i.1.11.11–15i.1.11.33.
 14. Tizard I, Shivaprasad HL, Guo J, Hameed S. The pathogenesis of proventricular dilatation disease. *Anim Health Res Rev*. 2017;17(2):110-126.

15. Leal de Araujo J, Tizard I, Guo J, et al. Are anti-ganglioside antibodies associated with proventricular dilatation disease in birds? *PeerJ*. 2017;5:e3144.
16. Sa-Ardta P, Rinder M, Sanyathitiseree P, et al. First detection and characterization of Psittaciform bornaviruses in naturally infected and diseased birds in Thailand. *Vet Microbiol*. 2019;230:62-71.
17. Hameed SS, Guo J, Tizard I, et al. Studies on immunity and immunopathogenesis of parrot bornaviral disease in cockatiels. *Viol*. 2018;515:81-91.
18. Escandon P, Heatley JJ, Tizard I, et al. Treatment with nonsteroidal anti-inflammatory drugs fails to ameliorate pathology in cockatiels experimental infected with Parrot bornavirus-2. *Vet Med: Res and Rep* 2019;10:185-195.
19. Gancz AY, Kistler AL, Greninger AL, et al., Experimental induction of proventricular dilatation disease in cockatiels (*Nymphicus hollandicus*) inoculated with brain homogenates containing avian bornavirus 4. *J Virol*. 2009;6:100.
20. Berthane Y, Smith DA, Newman S, et al. Peripheral neuritis in psittacine birds with proventricular dilatation disease. *Avian Pathol*. 2001;30(5):563–570.
21. Rinder M, Ackermann A, Kempf H, et al. Broad tissue and cell tropism of avian bornavirus in parrots with proventricular dilatation disease. *J Virol*. 2009;83(11):755–756.

22. Rubbenstroth D, Rinder M, Stein M, et al. Avian bornaviruses are widely distributed in canary birds (*Serinus canaria* f. domestica). *Vet Microbiol.* 2013;165(3-4):287–295.
23. Delnatte P, Mak M, Ojkic D, et al. Detection of avian bornavirus in multiple tissues of infected psittacine birds using real-time reverse transcription polymerase chain reaction. *J Vet Diagn Invest.* 2014;26(2):266–271.
24. de Kloet SR, Dorrestein GM. Presence of avian bornavirus RNA and anti-avian bornavirus antibodies in apparently healthy macaws. *Avian Dis.* 2009;53(4):568–573.
25. Lierz M, Hafez HM, Honkavuori KS, et al. Anatomical distribution of avian bornavirus in parrots, its occurrence in clinically healthy birds and ABV-antibody detection. *Avian Pathol.* 2009;38(6):491–496.
26. Weissenbock H, Fragner K, Nerdorst N, et al. Localization of avian bornavirus RNA by in situ hybridization in tissues of psittacine birds with proventricular dilatation disease. *Vet Microbiol.* 2010;145(1-2):9–16.
27. Fluck A, Enderlein D, Piepenbring A, et al. Correlation of avian bornavirus-specific antibodies and viral ribonucleic acid shedding with neurological signs and feather-damaging behavior in psittacine birds. *Vet Rec.* 2019;184(15):476–482.
28. Runge S, Olbert M, Herden C, et al. Viral vector vaccines protect cockatiels from inflammatory lesions after heterologous parrot bornavirus 2 challenge infection. *Vaccine.* 2017;23(4):557–563.

29. Olbert M, Romer-Oberdorfer A, Herden C, et al. Viral vector vaccines expressing nucleoprotein and phosphoprotein genes of avian bornavirus ameliorate homologous challenge infections in cockatiels and common canaries. *Sci Rep.* 2016;10:36840.


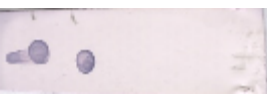


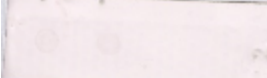
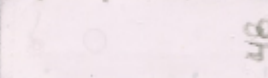






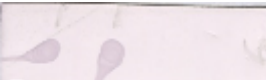

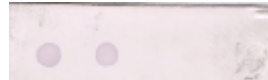

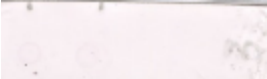
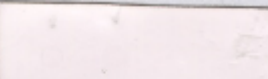
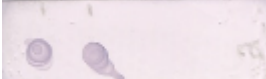
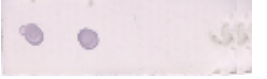
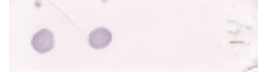
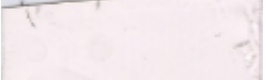

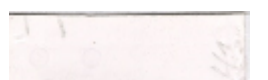
APPENDIX A

CHAPTER 3 DIGITAL IMAGES

	Study 1.A	Study 1.B	Study 1.C
1:100 Positive plasma	<p>1.4µg 0.14µg 0.014µg 0.0014µg 0.00014µg</p>	<p>1.4µg 0.14µg 0.014µg 0.0014µg 0.00014µg</p>	<p>1.4µg 0.14µg 0.014µg 0.0014µg 0.00014µg</p>
1:100 Negative plasma			
1:60 Positive plasma			
1:60 Negative plasma			
1:30 Positive plasma			
1:30 Negative plasma			



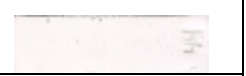



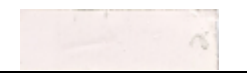
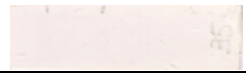
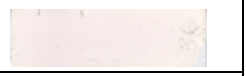
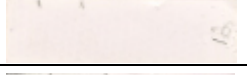
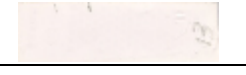


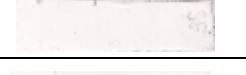
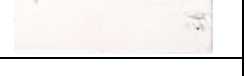
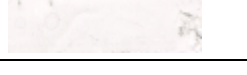

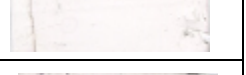
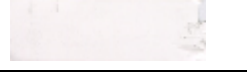


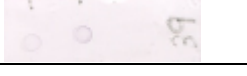


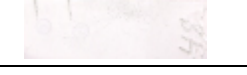



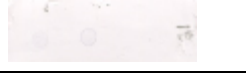
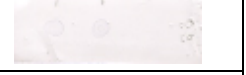
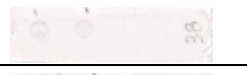
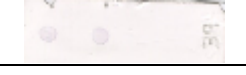


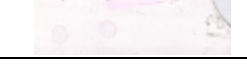

	Study 2.A						Study 2.B						Study 2.C					
	0.6 μ g	0.3 μ g	0.15 μ g	0.6 μ g	0.3 μ g	0.15 μ g	0.6 μ g	0.3 μ g	0.15 μ g	0.6 μ g	0.3 μ g	0.15 μ g	0.6 μ g	0.3 μ g	0.15 μ g	0.6 μ g	0.3 μ g	0.15 μ g
1:100 Negative plasma																		
1:100 Positive plasma																		
1:60 Negative plasma																		
1:60 Positive plasma																		
1:30 Negative plasma																		
1:30 Positive plasma																		
	10-minute incubation			5-minute incubation			10-minute incubation			5-minute incubation			10-minute incubation			5 minute incubation		

	Study 3.A				Study 3.B				Study 3.C			
	0.6 μ g	0.3 μ g	0.6 μ g	0.3 μ g	0.6 μ g	0.3 μ g	0.6 μ g	0.3 μ g	0.6 μ g	0.3 μ g	0.6 μ g	0.3 μ g
1:60 Negative plasma												
1:60 Positive plasma												
1:30 Negative plasma												
1:30 Positive plasma												
1:20 Negative plasma												
1:20 Positive plasma												
	5-minute incubation		2-minute incubation		5-minute incubation		2-minute incubation		5-minute incubation		2-minute incubation	

		Study 4.A	Study 4.B	Study 4.C
1:60 Plasma	Positive Sample			
	Negative Sample			
1:100 Whole Blood	Positive Sample			
	Negative Sample			
1:60 Whole Blood	Positive Sample			
	Negative Sample			
1:30 Whole Blood	Positive Sample			
	Negative Sample			

APPENDIX B



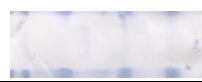



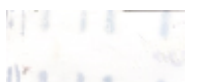

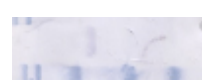
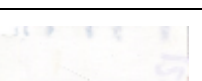
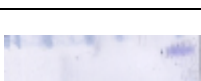

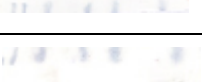
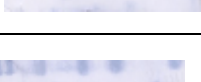
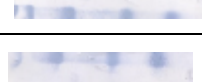
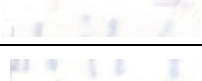
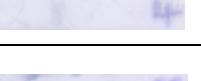
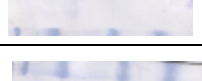

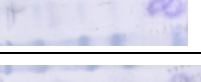
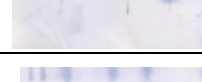

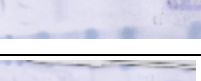
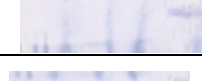
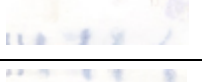
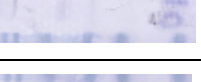










CHAPTER 4 DIGITAL IMAGES AND ROCS

Control sample for dot-blot ELISA			
	445	427	446
Wk -10			
Wk -8			
Wk -6			
Wk -3			
Wk -1			
Wk 1			
Wk 3			
Wk 6			
Wk 8			
Wk 14			
Wk 18			
Wk 25			

	Vaccinated samples for dot-blot ELISA				
	424	268	428	13	51
Wk -10					
Vaccination					
Wk -8					
Wk -6					
Vaccine Booster #1					
Wk -3					
Wk -1					
Wk 1					
Wk 3					
Wk 6					
Wk 8					
Wk 14					
Vaccine booster #2					
Wk 18					
Wk 25					

Vaccinated /PaBV-2 inoculated sample for dot-blot ELISA				
	440	888	243	4
Wk -10				
Vaccination				
Wk -8				
Wk -6				
Vaccine Booster #1				
Wk -3				
Wk -1				
PaBV-2 inoculation				
Wk 1				
Wk 3				
Wk 6				
Wk 8				
Wk 14				
Vaccine booster #2				
Wk 18				
Wk 25				

PaBV-2 inoculated samples for dot-blot ELISA						
	445	427	446	405	417	48
Wk -10						
Wk -8						
Wk -6						
Wk -3						
Wk -1						
PaBV-2 inoculation						
Wk 1						
Wk 3						
Wk 6						
Wk 8						
Wk 14						
Wk 18						
Wk 25						

Control samples for western blot			
	445	427	446
Wk -10			
Wk -8			
Wk-6			
Wk -3			
Wk -1			
Wk 1			
Wk 3			
Wk 6			
Wk 8			
Wk 14			
Wk 18			
Wk 25			

	Vaccinated samples for western blot				
	424	268	428	13	51
Wk -10					
Vaccination					
Wk -8					
Wk -6					
Vaccine Booster #1					
Wk -3					
Wk -1					
Wk 1					
Wk 3					
Wk 6					
Wk 8					
Wk 14					
Vaccine booster #2					
Wk 18					
Wk 25					

	Vaccinated/PaBV-2 inoculated samples for western blot			
	440	888	243	4
Wk -10				
Vaccination				
Wk -8				
Wk-6				
Vaccine Booster #1				
Wk -3				
Wk -1				
PaBV-2 inoculation				
Wk 1				
Wk 3				
Wk 6				
Wk 8				
Wk 14				
Vaccine booster #2				
Wk 18				
Wk 25				

PaBV-2 inoculated samples for western blot						
	445	427	446	405	417	48
Wk -10						
Wk -8						
Wk -6						
Wk -3						
Wk -1						
PaBV-2 inoculation						
Wk 1						
Wk 3						
Wk 6						
Wk 8						
Wk 14						
Wk 18						
Wk 25						

OVERALL ROC ANALYSIS

10/15/2019

ROC Analysis: Web-based Calculator for ROC Curves

ROC Analysis

Web-based Calculator for ROC Curves

John Eng, M.D. (jeng@jhmi.edu)
Russell H. Morgan Department of Radiology and Radiological Science
Johns Hopkins University School of Medicine, Baltimore, Maryland, USA



To access this page, you may use the link www.jrocfiit.org.

Instructions: This web page calculates a receiver operating characteristic (ROC) curve from data pasted into the input data field below. To analyze your data, use the following steps to fill out the data form on this page.

1. Select the data format. (See [explanation of data formats](#).)
2. Paste or enter your data into the "Input Data" field or click the "Paste Example Data" button. Data may be pasted from programs such as Microsoft Excel or Word.
3. Enter the number of rating categories. (See [explanation of data formats](#).) This is not needed for the example data or Format 5.
4. Click the "Run Program" button.
5. To export the ROC plot to Microsoft Word or Excel, see [instructions below](#).

Computer requirements: A reasonably up-to-date version of a web browser that supports HTML5 is required. Unlike previous versions of this page, installation of Java is not required. Please send any bugs, questions, comments, or suggestions to jeng@jhmi.edu. All email will be answered.

Suggested citation: The citations below conform to the styles used by the [National Library of Medicine](#) and the [American Psychological Association](#), respectively.

1. Eng J. ROC analysis: web-based calculator for ROC curves. Baltimore: Johns Hopkins University [updated 2014 March 19; cited <date>]. Available from: <http://www.jrocfiit.org>.
2. Eng, J. (n.d.). ROC analysis: web-based calculator for ROC curves. Retrieved <date>, from <http://www.jrocfiit.org>.

Acknowledgment: This web page contains JROCFIT and JLABROC4, JavaScript programs for calculating receiver operating characteristic (ROC) curves. JROCFIT performs calculations for discrete ratings data, and JLABROC4 performs calculations for continuously distributed data. JROCFIT and JLABROC4 are direct translations of the ROCFIT and LABROC4 programs, respectively. The latter two were Fortran programs developed by the late Charles Metz and colleagues at the University of Chicago. JROCFIT and JLABROC4 reproduce all output of the original programs. See below for [program translation details](#).

Data Format: Format 1 Format 2 Format 3 Format 4 Format 5
Number of Rating Categories: (Not needed for example data or for Format 5.)

Input Data: (paste or enter)

```
1 5  
1 5  
1 5  
1 5  
1 5  
1 5  
1 5  
1 5  
1 5  
1 5  
1 5  
1 5  
1 5  
1 5  
1 5  
1 5  
1 5  
1 5  
1 5  
1 5  
1 5
```

ROC Curve

Program Output: (may be copied and pasted into other programs)

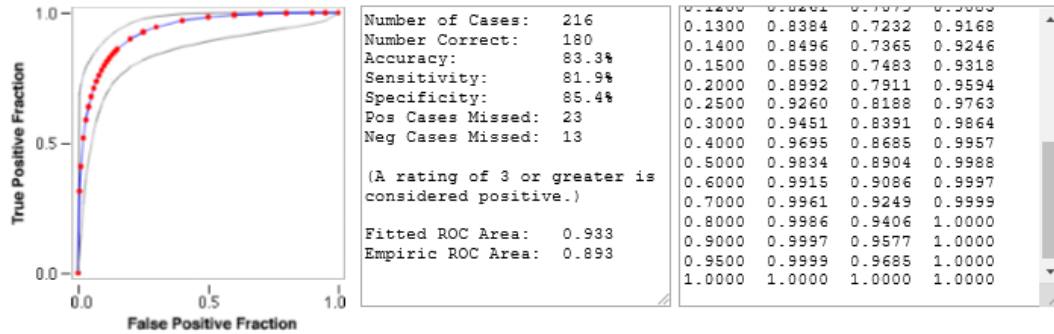
```
0.600 0.9915 (0.9086, 0.9997)  
0.700 0.9961 (0.9249, 0.9999)  
0.800 0.9986 (0.9406, 1.0000)  
0.900 0.9997 (0.9677, 1.0000)  
0.950 0.9999 (0.9685, 1.0000)  
  
ESTIMATES OF EXPECTED OPERATING POINTS ON FITTED ROC CURVE:  
Expected 95% C.I. of 95% C.I. of  
Operating Point Lower Bound Upper Bound  
( FPF , TPF ) ( FPF , TPF ) ( FPF , TPF )  
(0.0412, 0.6437) (0.0141, 0.4619) (0.1003, 0.7974)  
(0.0967, 0.7915) (0.0514, 0.6831) (0.1661, 0.8743)  
(0.1243, 0.8315) (0.0708, 0.7388) (0.2010, 0.8998)  
(0.1593, 0.8684) (0.0950, 0.7885) (0.2469, 0.9246)  
  
WARNINGS AND ERROR MESSAGES:  
Chi-square goodness of fit not calculated because  
some expected cell frequencies are less than 5.  
Chi-square goodness of fit not calculated because  
some expected cell frequencies are less than 5.
```

Summary Statistics:

Points for Plotting: (copy & paste to Excel)

10/15/2019

ROC Analysis: Web-based Calculator for ROC Curves



ROC Curve Type: Fitted Empirical

Key for the ROC Plot

RED symbols and BLUE line: Fitted ROC curve.

GRAY lines: 95% confidence interval of the fitted ROC curve.

BLACK symbols ± GREEN line: Points making up the empirical ROC curve (does not apply to Format 5).

Exporting the ROC plot to Word or Excel: Due to limitations of web technology, there is no one-step method for exporting the ROC plot to Microsoft Word or Excel. However, two methods are available for exporting:

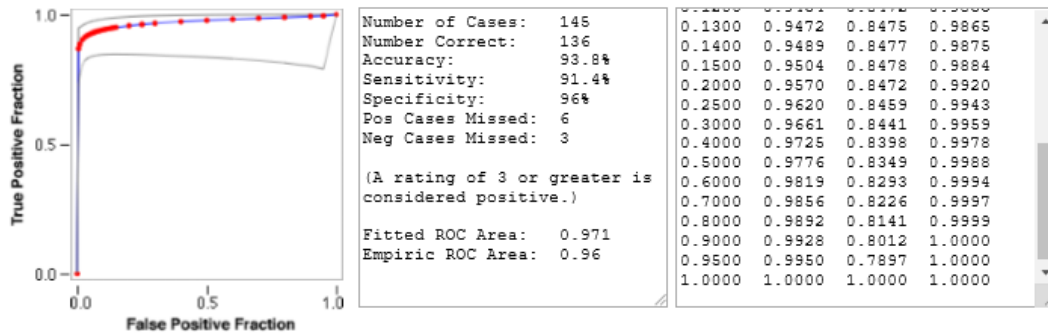
1. Select all of the text in the "Points for Plotting" field, which is located to the right of the graph above. Copy and paste this text into Microsoft Excel. In Excel, create a graph from the data by usual methods. This is a good way to obtain a publication-quality graph of the ROC curve.
2. Copy a snapshot of the browser window by pressing Alt-PrintScreen, switch to the Microsoft Word window, and paste the image by pressing Control-V. In Word, you need to use Format...Picture (or the cropping tool from the Picture toolbar) to crop and scale the image as needed.

Program translation details: This page contains JROCFIT and JLABROC4, programs for fitting receiver operating characteristic (ROC) curves using the maximum likelihood fit of a binormal model. JROCFIT and JLABROC4 are literal JavaScript translations of the Fortran source code for ROCFIT and LABROC4, programs developed and maintained by the late Dr. Charles Metz and his colleagues at the University of Chicago. During translation, data input routines were added to JROCFIT and JLABROC4 in order to provide a more convenient user interface. The translation was performed with kind permission from Dr. Metz, but neither he nor his colleagues were otherwise involved in the translation, nor do they share any responsibility for the translation's accuracy. While the translation was performed as carefully as possible, the author and Johns Hopkins University assume no responsibility for the accuracy of the programs' operation, regardless of cause.

(Page last updated: 23 March 2017)

10/15/2019

ROC Analysis: Web-based Calculator for ROC Curves



ROC Curve Type: Fitted Empirical

Key for the ROC Plot

RED symbols and BLUE line: Fitted ROC curve.

GRAY lines: 95% confidence interval of the fitted ROC curve.

BLACK symbols ± GREEN line: Points making up the empirical ROC curve (does not apply to Format 5).

Exporting the ROC plot to Word or Excel: Due to limitations of web technology, there is no one-step method for exporting the ROC plot to Microsoft Word or Excel. However, two methods are available for exporting:

1. Select all of the text in the "Points for Plotting" field, which is located to the right of the graph above. Copy and paste this text into Microsoft Excel. In Excel, create a graph from the data by usual methods. This is a good way to obtain a publication-quality graph of the ROC curve.
2. Copy a snapshot of the browser window by pressing Alt-PrintScreen, switch to the Microsoft Word window, and paste the image by pressing Control-V. In Word, you need to use Format...Picture (or the cropping tool from the Picture toolbar) to crop and scale the image as needed.

Program translation details: This page contains JROCFIT and JLABROC4, programs for fitting receiver operating characteristic (ROC) curves using the maximum likelihood fit of a binormal model. JROCFIT and JLABROC4 are literal JavaScript translations of the Fortran source code for ROCFIT and LABROC4, programs developed and maintained by the late Dr. Charles Metz and his colleagues at the University of Chicago. During translation, data input routines were added to JROCFIT and JLABROC4 in order to provide a more convenient user interface. The translation was performed with kind permission from Dr. Metz, but neither he nor his colleagues were otherwise involved in the translation, nor do they share any responsibility for the translation's accuracy. While the translation was performed as carefully as possible, the author and Johns Hopkins University assume no responsibility for the accuracy of the programs' operation, regardless of cause.

(Page last updated: 23 March 2017)

VACCINATED ROC ANALYSIS

10/15/2019

ROC Analysis: Web-based Calculator for ROC Curves

ROC Analysis

Web-based Calculator for ROC Curves

John Eng, M.D. (jeng@jhmi.edu)
Russell H. Morgan Department of Radiology and Radiological Science
Johns Hopkins University School of Medicine, Baltimore, Maryland, USA



To access this page, you may use the link www.jrocfiit.org.

Instructions: This web page calculates a receiver operating characteristic (ROC) curve from data pasted into the input data field below. To analyze your data, use the following steps to fill out the data form on this page.

1. Select the data format. (See [explanation of data formats.](#))
2. Paste or enter your data into the "Input Data" field or click the "Paste Example Data" button. Data may be pasted from programs such as Microsoft Excel or Word.
3. Enter the number of rating categories. (See [explanation of data formats.](#)) This is not needed for the example data or Format 5.
4. Click the "Run Program" button.
5. To export the ROC plot to Microsoft Word or Excel, see [instructions below.](#)

Computer requirements: A reasonably up-to-date version of a web browser that supports HTML5 is required. Unlike previous versions of this page, installation of Java is not required. Please send any bugs, questions, comments, or suggestions to jeng@jhmi.edu. All email will be answered.

Suggested citation: The citations below conform to the styles used by the [National Library of Medicine](#) and the [American Psychological Association](#), respectively.

1. Eng J. ROC analysis: web-based calculator for ROC curves. Baltimore: Johns Hopkins University [updated 2014 March 19; cited <date>]. Available from: <http://www.jrocfiit.org>.
2. Eng, J. (n.d.). ROC analysis: web-based calculator for ROC curves. Retrieved <date>, from <http://www.jrocfiit.org>.

Acknowledgment: This web page contains JROCFIT and JLABROC4, JavaScript programs for calculating receiver operating characteristic (ROC) curves. JROCFIT performs calculations for discrete ratings data, and JLABROC4 performs calculations for continuously distributed data. JROCFIT and JLABROC4 are direct translations of the ROCFIT and LABROC4 programs, respectively. The latter two were Fortran programs developed by the late Charles Metz and colleagues at the University of Chicago. JROCFIT and JLABROC4 reproduce all output of the original programs. See below for [program translation details.](#)

Data Format: Format 1 Format 2 Format 3 Format 4 Format 5

Number of Rating Categories: (Not needed for example data or for Format 5.)

Input Data: (paste or enter)

```
0 1
0 1
0 1
0 1
0 1
0 1
0 1
0 1
0 1
0 1
0 1
0 1
0 1
0 1
0 1
0 1
0 1
0 1
0 1
0 1
0 1
0 1
0 1
0 1
```

Program Output: (may be copied and pasted into other programs)

```
0.600 0.9968 (0.7029, 1.0000)
0.700 0.9987 (0.7040, 1.0000)
0.800 0.9996 (0.7045, 1.0000)
0.900 0.9999 (0.7044, 1.0000)
0.950 1.0000 (0.7037, 1.0000)
```

ESTIMATES OF EXPECTED OPERATING POINTS ON FITTED ROC CURVE:

Expected Operating Point	95% C.I. of Lower Bound	95% C.I. of Upper Bound
(FPF , TPF)	(FPF , TPF)	(FPF , TPF)
(0.0038, 0.3779)	(0.0001, 0.0797)	(0.0535, 0.7837)
(0.0201, 0.6283)	(0.0042, 0.3906)	(0.0708, 0.8244)
(0.0332, 0.7097)	(0.0099, 0.5159)	(0.0897, 0.8566)
(0.0540, 0.7851)	(0.0190, 0.6197)	(0.1270, 0.8988)

WARNINGS AND ERROR MESSAGES:

Chi-square goodness of fit not calculated because some expected cell frequencies are less than 5.
Chi-square goodness of fit not calculated because some expected cell frequencies are less than 5.

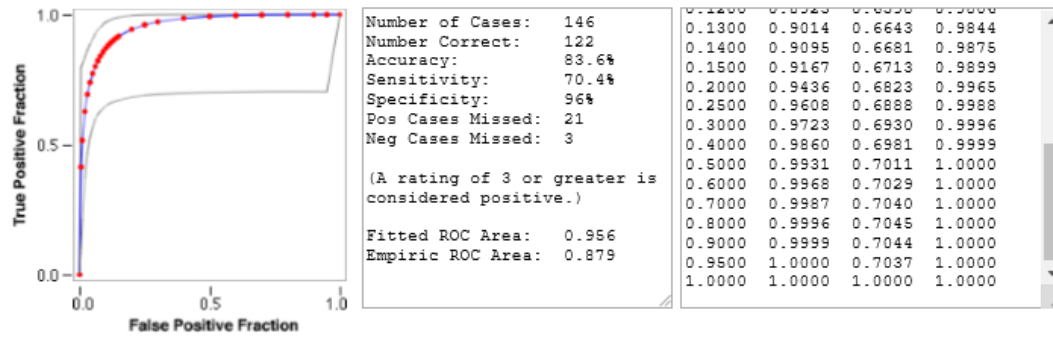
ROC Curve

Summary Statistics:

Points for Plotting: (copy & paste to Excel)

10/15/2019

ROC Analysis: Web-based Calculator for ROC Curves



ROC Curve Type: Fitted Empirical

Key for the ROC Plot
RED symbols and BLUE line: Fitted ROC curve.
GRAY lines: 95% confidence interval of the fitted ROC curve.
BLACK symbols ± GREEN line: Points making up the empirical ROC curve (does not apply to Format 5).

Exporting the ROC plot to Word or Excel: Due to limitations of web technology, there is no one-step method for exporting the ROC plot to Microsoft Word or Excel. However, two methods are available for exporting:

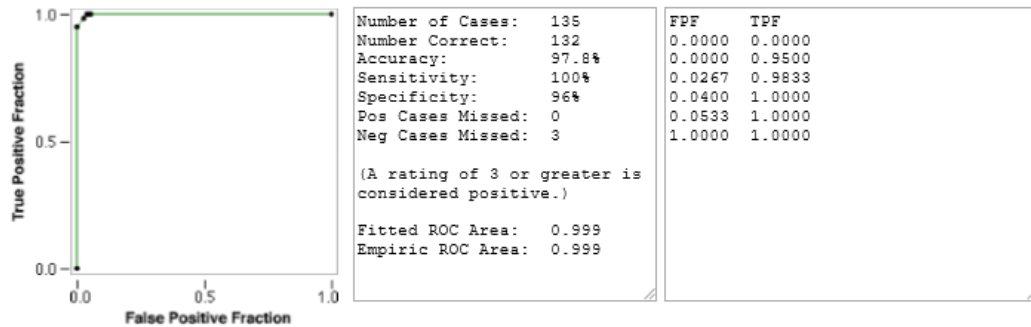
1. Select all of the text in the "Points for Plotting" field, which is located to the right of the graph above. Copy and paste this text into Microsoft Excel. In Excel, create a graph from the data by usual methods. This is a good way to obtain a publication-quality graph of the ROC curve.
2. Copy a snapshot of the browser window by pressing Alt-PrintScreen, switch to the Microsoft Word window, and paste the image by pressing Control-V. In Word, you need to use Format..Picture (or the cropping tool from the Picture toolbar) to crop and scale the image as needed.

Program translation details: This page contains JROCFIT and JLABROC4, programs for fitting receiver operating characteristic (ROC) curves using the maximum likelihood fit of a binormal model. JROCFIT and JLABROC4 are literal JavaScript translations of the Fortran source code for ROCFIT and LABROC4, programs developed and maintained by the late Dr. Charles Metz and his colleagues at the University of Chicago. During translation, data input routines were added to JROCFIT and JLABROC4 in order to provide a more convenient user interface. The translation was performed with kind permission from Dr. Metz, but neither he nor his colleagues were otherwise involved in the translation, nor do they share any responsibility for the translation's accuracy. While the translation was performed as carefully as possible, the author and Johns Hopkins University assume no responsibility for the accuracy of the programs' operation, regardless of cause.

(Page last updated: 23 March 2017)

10/29/2019

ROC Analysis: Web-based Calculator for ROC Curves



ROC Curve Type: Fitted Empirical

Key for the ROC Plot

RED symbols and BLUE line: Fitted ROC curve.

GRAY lines: 95% confidence interval of the fitted ROC curve.

BLACK symbols ± GREEN line: Points making up the empirical ROC curve (does not apply to Format 5).

Exporting the ROC plot to Word or Excel: Due to limitations of web technology, there is no one-step method for exporting the ROC plot to Microsoft Word or Excel. However, two methods are available for exporting:

1. Select all of the text in the "Points for Plotting" field, which is located to the right of the graph above. Copy and paste this text into Microsoft Excel. In Excel, create a graph from the data by usual methods. This is a good way to obtain a publication-quality graph of the ROC curve.
2. Copy a snapshot of the browser window by pressing Alt-PrintScreen, switch to the Microsoft Word window, and paste the image by pressing Control-V. In Word, you need to use Format...Picture (or the cropping tool from the Picture toolbar) to crop and scale the image as needed.

Program translation details: This page contains JROCFIT and JLABROC4, programs for fitting receiver operating characteristic (ROC) curves using the maximum likelihood fit of a binormal model. JROCFIT and JLABROC4 are literal JavaScript translations of the Fortran source code for ROCFIT and LABROC4, programs developed and maintained by the late Dr. Charles Metz and his colleagues at the University of Chicago. During translation, data input routines were added to JROCFIT and JLABROC4 in order to provide a more convenient user interface. The translation was performed with kind permission from Dr. Metz, but neither he nor his colleagues were otherwise involved in the translation, nor do they share any responsibility for the translation's accuracy. While the translation was performed as carefully as possible, the author and Johns Hopkins University assume no responsibility for the accuracy of the programs' operation, regardless of cause.

(Page last updated: 23 March 2017)

Table representing scenario: samples from controls and vaccinated birds used are highlight in orange.

Vaccination Timeline	Bird ID	Wk -1	Wk 2	Wk 4	Wk 6	Wk 8	Wk 10	Wk 12	Wk 15	Wk 17	Wk 23	Wk 27	Wk 34
Inoculation Timeline		Wk -10	Wk -7	Wk -5	Wk -3	Wk -1	Wk 1	Wk 3	Wk 6	Wk 8	Wk 14	Wk 18	Wk 25
Group 1: Control	409												
	26												
	264												
Group 2: Vaccinated	424												
	268												
	428												
	13												
	51												
Group 3: Vaccinated/ PaBV-2 inoculated	440												
	888												
	243												
	4												
Group 4: PaBV-2 inoculated	445												
	427												
	446												
	405												
	417												
	48												

Table representing scenario: samples from controls and inoculated birds used are highlight in orange.

Vaccination Timeline	Bird ID	Wk -1	Wk 2	Wk 4	Wk 6	Wk 8	Wk 10	Wk 12	Wk 15	Wk 17	Wk 23	Wk 27	Wk 34
Inoculation Timeline		Wk -10	Wk -7	Wk -5	Wk -3	Wk -1	Wk 1	Wk 3	Wk 6	Wk 8	Wk 14	Wk 18	Wk 25
Group 1: Control	409												
	26												
	264												
Group 2: Vaccinated	424												
	268												
	428												
	13												
	51												
Group 3: Vaccinated/ PaBV-2 inoculated	440												
	888												
	243												
	4												
Group 4: PaBV-2 inoculated	445												
	427												
	446												
	405												
	417												
	48												

Table representing scenario: samples from controls and inoculated birds ≥ 3 weeks post-inoculation used are highlight in orange.

Vaccination Timeline	Bird ID	Wk -1	Wk 2	Wk 4	Wk 6	Wk 8	Wk 10	Wk 12	Wk 15	Wk 17	Wk 23	Wk 27	Wk 34
Inoculation Timeline		Wk -10	Wk -7	Wk -5	Wk -3	Wk -1	Wk 1	Wk 3	Wk 6	Wk 8	Wk 14	Wk 18	Wk 25
Group 1: Control	409												
	26												
	264												
Group 2: Vaccinated	424												
	268												
	428												
	13												
	51												
Group 3: Vaccinated/ PaBV-2 inoculated	440												
	888												
	243												
	4												
Group 4: PaBV-2 inoculated	445												
	427												
	446												
	405												
	417												
	48												